TMR4520 - Master's Thesis in Marine Hydrodynamics

Forces on a net panel

by

Håkon Ådnanes

Trondheim, 2011

NTNU
Faculty of Engineering Science
and Technology
Department of Marine Technology

Abstract

Four different methods for calculating forces on and deformation of a net suspended in current have been compared.

The four methods are: 1) The method presented by Løland in his PhD thesis. Uses drag and lift coefficients based on experimental values. A zero moment requirement, and iteration is used to find the deformation and forces on net elements. 2) The solution of the catenary equation adapted to a net problem. 3) FhSim, a simulation software under development by SINTEF. Finds forces by adding contributions on single twines, based on coefficients from the modified cross flow principle. 4) AquaSim by Aquastructures, a commercial analysis software package. Forces on nets found from single twine contribution. A brief presentation of the different methods is given, with a more detailed discussion of the catenary equation method.

The drag and lift coefficients are compared to experimental data. The Løland and catenary equation methods are generally closest to the experimental data. An error analysis of the catenary equation for four different solidity ratios showed decreasing relative error on drag force, lift force and end point angle with increasing current velocity. At current velocity above $0.6\mathrm{m/s}$, all these gave a relative error of 16% or less. The relative error of maximum tension increase with increasing current velocity.

The four methods are compared with respect to drag force, lift force, and deformation. This is done with gradual increase of current velocity (case 1), and gradual increase of solidity ratio (case 2). The catenary equation and Løland method gives consistently almost equal lift force. FhSim and AquaSim also give very similar results for lift force, but the values are considerable lower than those from the other two methods. In FhSim, the low lift force is supported by relative small net deformations. Deformations according to AquaSim are larger, but still lower than those given from Løland and the catenary equation.

The drag force from Løland, the catenary equation and FhSim are generally in the same range, with some partial exceptions. At relative high current velocity or solidity ratio, the drag force from AquaSim is found to be many times larger than those calculated from the other methods. Due to the drag force being calculated as contributions from every single twine, the proportionality with the projected area is reduced, leading to a significant overestimation at large deformations.

Drag coefficients in FhSim should be larger for net panels with a angle relative to the current less than 60°. The lift coefficients for panels with an angle above 45° should also be larger. The solidity and angle independent factor in Lølands drag formula should be reduced or neglected.

Some sort of shielding effect due to twines upstream should be implemented in AquaSim to reduce the overestimation of drag force at large net deformation.

The lift coefficients for the catenary equation are likely high. The method seems to be viable for aquaculture application.

Preface

This text is the master's thesis and conclusion of the undersigned's master degree (siv.ing) in Marine Hydrodynamics.

The final project text has very much been a process. At the start of the semester, some work was done with respect to the possibility of analysis of full scale models in regular or irregular waves, relating to offshore fish farming. The global 3D flow profile related to analysis of the impact a complete system will have, was also discussed as a possibility. Considering the number of parameters, it was thought best to simplify the problem. With time, this developed to a very simplified case, which was considered in more detail, and compared across several methods. Due to the time used on these "detours", the final project description had to be limited. A fresh start at the same project with given assignment text would likely give a more substantial thesis. With hindsight, the work done in the beginning, relating to offshore fish farming, although very interesting, was unfortunately not very relevant to the finished thesis. Obtaining the relevant software also took some time.

Several people have contributed in varying degree with help and encouragement during the work with this assignment. First my supervisor, professor Odd Magnus Faltinsen has during more or less weekly meetings contributed continuously with ideas and guidance. The work with the the catenary equation in relation to a net is based on work by Trygve Kristiansen, and he has been very helpful on this, and other related topics. Thanks also to Are Berstad at Aquastructures for information about AquaSim, encouragement and interest in the work. Jørgen Walaunet at Aquastructures was helpful with technical support for AquaSim. Egil Lien at SINTEF contributed with ideas to the problem to be addressed.

A special thanks to Martin Føre who has, very graciously, done every FhSim analysis. He has also contributed with a text explaining the governing equations in FhSim, and been more then willing to answer many questions.

Trondheim, June 13, 2011

Håkon Ådnanes

Contents

List of Figures

List of Tables

Nomenclature

α	End point angle.
α_i	Angle relative to current flow for net element i. From water surface to net panel.
α_i	Partial derivative of normal force coefficient.
ρ_s	Density of seawater.
ρ_{net}	Density of net.
θ_i	Angle relative to current flow for net element i. From vertical line to net panel.
B	Width of net in x direction (Norwegian: “Bredde”).
C_D	Drag coefficient
C_D^{CC}	Drag coefficient on a single cylinder
C_L	Lift coefficient
C_N	Normal coefficient
C_T	Tangential coefficient
d	Twine diameter.
F_C^{sink}	Current force on bottom weights sinker tube.
F_D	Drag force
F_L	Lift force
F_N	Normal force
F_T	Tangential force
F_y^i	Reaction force in y - direction on node i
F_z^i	Reaction force in z - direction on node i
L	Length of undisturbed net in negative z direction (depth).
l_{st}	Length of twine cable (Norwegian: “stolpelengde”).
r	Current reduction factor due to nets upstream.
Re	Reynolds number
Sn	Netting solidity. Projected twine area/Circumscribed net area.
T_i	Tension in net element i.

U	Current velocity through net.
U_∞	Undisturbed far field current velocity.
W_{sink}	Weight of sinker (bottom weights).

Chapter 1

Introduction

1.1 Motivation

The Norwegian salmon farming industry is booming. It experience record profit (E24.no, 2010), and have produced around 1 million ton in 2010. 2.5 million tons in 2020 might be realistic (Almås, 2010). The human population continues to grow, thus the food production must increase. Aquaculture is an efficient way to produce food, both in terms of needed area, CO_2 emission, and fresh water usage (Edvardsen, 2010). The industry is also faced with challenges. Escaping fish damages wild fish stock, and leads to public outcry. Louse travels easily from location to location unless certain precautions are taken. Biologic waste from the fish can also damage local environment. Salmon are carnivores, and feed must presently come from other fish. This means catching fish to feed fish, which is not the most efficient solution.

It is very important to ensure good knowledge of every aspect tied to safe operation and production of fish in aquaculture farms. Large aquaculture plants can hold huge amounts of fish. Single net cages with circumference $157\ \mathrm{m}$ and a depth of $15 - 30\ \mathrm{m}$ are quite common. With a typical upper fish density of $20 - 25\ \mathrm{kg/m^3}$ one cage can hold 700 tons of fish ready for slaughter. One location will often consist of around $5 - 12$ cages which make up one mooring system. Every part of the plant need to be sufficiently strong and dimensioned for all conditions. This implies being able to calculate and/or approximate the size of the environmental maximum load cases. Forces from both waves and current are of importance when dimensioning a fish farm (Berstad & Tronstad, 2005). The Norwegian Standard for fish farming, NS9415 (2009) gives requirements to dimensioning and procedures. Considerations must be given to the increase in solidity due to biofouling. The largest amount of biofouling occurs typically around summer. Maximum current forces is thought generally small around summer, and larger around spring and winter. As shown in the pre-work to this thesis, (Ådnanes, 2010), that might not necessarily be the case. This support the general statement given by Fredheim et al. (2010) about the need for more knowledge about force models related to aquaculture.

1.2 Some previous relevant work

Generally, deformation of and force on freely hanging net screens in infinite flow is a fairly new scientific undertaking, and not much extensive work exist easily available. The most thorough work treat screens spanning the entire cross area of the flow channel (netting in wind tunnel and air ducts etc). As salmon export continued to grow during the 1980's, little or no research attention had been paid to the analysis

of current forces on net cages. In 1987 a research program entitled "Current forces on and flow through fish farming structures" was started. As a part of this program a series of model test, such as Rudi et al. (1988) aimed at current force calculation was carried out (Løland, 1991, p11-12). Much of the later work regarding force on and deformation of net structures are to some degree directly or indirectly based upon these model tests.

Vikestad & Lien (2005) investigated a non-dimensional weight and velocity parameter able to estimate the drag force and net deformation on a net to be used in aquaculture application. This analytic approach showed good agreement with a FEM approach done in RIFLEX for deformation on a relative small, rigid net panel ($1\mathrm{m} \times 1\mathrm{m}$). They introduced a drag force reduction factor based on the net panel deformation and reduced velocity, $V_{red} = U(\rho/2w)$. w is the net weight in water pr unit length. The work was based on the Morison force formulation,

$$F_D = \frac{1}{2}\rho U^2 C_D dA,\ F_L = \frac{1}{2}\rho U^2 C_L dA \tag{1.1}$$

with drag and lift coefficients from Aarsnes & Løland (1990).

$$C_D(\alpha, Sn) = 0.04 + (Sn - 1.24Sn^2 + 13.7Sn^3 - 0.04)\cos\alpha \tag{1.2}$$

$$C_D(\alpha, Sn) = (0.57Sn - 3.54Sn^2 + 10.1Sn^3)\sin 2\alpha \tag{1.3}$$

Løland (1991) used much of the same approach as Vikestad & Lien (2005) based their work on, but used a slightly different formulation for C_D and C_L. Lølands approach is given in more detail in chapter 2.1. Tronstad (2000) developed a model for nonlinear hydroelastic analysis of net structures. The hydrodynamic load model for net membranes will be explored related to the application in AquaSim in chapter 2.4.

Lader & Enerhaug (2005) investigated forces on and deformation of a flexible circular net cage in uniform flow. A 1:7.1 scaled net cage with ring diameter $1.435\mathrm{m}$ and depth about $1.44\mathrm{m}$ was suspended in a flume tank, and attached to load cells. Full scale nets were used. 16 bottom weights was distributed around the net. The experiment was done for three different weight sets, with bottom weights of $400\mathrm{g}$, $600\mathrm{g}$ or $800\mathrm{g}$ each. The current had a uniform profile, and varied from $0.04\mathrm{m/s}$ to $\sim 0.50\mathrm{m/s}$. Important findings showed that the forces on and deformation of the net structure were highly dependent of each other. Estimates of *global* forces on the structure based on stiff element approximation gave large errors compared to the experimental data. Forces on the net structure was dependent of Reynolds number.

Berstad & Tronstad (2005) looked at the response from current and regular or irregular waves on a typical polyethylene fish farm. A system wide approach is used, and a 10 cage fish farm was investigated with respect to maximum force in different components in the system. Findings showed that both current and waves influenced the maximum mooring forces on a fish farm. Design loads will likely be reduced by using irregular, as opposed to regular waves in the analysis.

In a study by Lader et al. (2007) interactions between net panels and waves was discussed based on a series of experiments. The damping effect of nets with different solidity was measured by running a set of waves through a net panel spanning the width and depth of a wave flume tank. The findings showed increased net solidity gave increased wave force both normal and tangential to the net. The damping effect did not show the same positive solidity dependency. For shorter waves, nets with higher solidity ratio did not necessarily give the highest damping effects on the waves.

Biofouling can cause big problems for the fish farmer. Growth will increase the net solidity, and thus increase the drag force and decrease the available oxygen for the fish. Regular net cleaning is required where this is a problem. The Norwegian standard for fish farming, NS9415 (2009) states that a factor

of 50% must be added to the solidity ratio when analysisng to account for the increased forces due to biofouling. Swift et al. (2006) measured the increase in drag force due to biofouling on net panels. Net panels experienced different types and amounts of marine growth, resuling in some scatter in the results. There was found a increase in the drag coefficient of $6 - 240\%$, and only two of nine net panels showed an C_D increase less then 80%. The solidity of the biofouled nets was found to have increased $414 - 670\%$(!).

Fredheim et al. (2010) collects several contributions related to a research program dedicated to reducing the probability of fish escape. Three accredited certification companies was asked to calculate forces on different components in a fish farm. The calculations were to be based on measured environmental data. There was considerable difference between the three companies, and also compared to the measured data. This showed the need for better understanding of what and how forces act upon these kinds of structures. There was also expressed the need for better models to calculate forces due to current and waves.

1.3 The assignment

The objective of this thesis, is to compare different methods for calculating force on and deformation of a net panel.

Four methods are chosen. The first is Lølands suggested method given in his thesis, (Løland, 1991). The second is use of a modified catenary equation. This method should also be examined in greater detail. Thirdly, FhSim is a software in development. An early version of this program is part of the comparison. Lastly, AquaSim, a commercial software, which is widely used for calculating dimensioning forces of aquaculture plants.

The thesis aims to give insight in the validity of different methods, and where possible the validity of different assumptions the methods might employ. On this basis, the following points should be done:

- Give a short overview of some of the relevant work relating to calculating forces on and deformation of net panels.
- Present the four different methods to be used in the thesis. Where possible, give insight in governing equations and structure of program/method.
- Give a more in depth presentation of the solution of the catenary equation as a method for calculating forces and deformation on a net panel.
- Develop a script to use the catenary solution (and the Løland method) on a net panel.
- Verify the methods by comparing drag and lift coefficient for a given combination of solidity ratio, current speed and net panel inclination with coefficient from experiments.
- Carry out an error analysis on the catenary equation solution.
- Present results for all methods with varying current speed and solidity ratio. Drag force, lift force and net deformation from the different methods should be compared and commented.
- Give conclusions and recommendations for further work.

1.4 Structure of the report

Since the assignment is comparison of four methods, much of the text will consists of answering the same problem or question four times, one for each of the methods. Many results are also presented, and compared between the four methods. Abbreviations are then often used in tables and figures, they should be fairly logical. LO - Loland is Lølands method. CE - CatEq is the soluiton of the catenary equation. FH - FhSim is FhSim by SINTEF. AS - AquaSim is AquaSim by Aquastructures. In each chapter, figure legend and table the methods should be presented is the same order of succession (LO, CE, FH and AS).

The thesis contains 6 chapters in addition to appendices. The first is a an introduction chapter. In chapter 2, the four methods are presented. The catenary equation method is examined in more detail. The Løland and catenary equations are implemented in a basic Matlab script, and the procedure is given. Chapter 3 consists of two major parts. First, the validation of the four methods by comparing drag and lift coefficients with those given in the experiment done by Rudi et al. (1988). The second part is an error analysis performed on the catenary equation, determining the level of influence different parameters will have on the results. The error analysis is done for four solidity rations. The results for the first is given in the text, while the results for the three last is given in appendix A.1 - A.3. In chapter 4 the results from parameter variation is given for the four methods. This chapter is split in four parts. First, the models and input data that are to be used are presented for all four methods. The parameter variation is split in two major cases. The second part of chapter 4 is the first case, with variation in current velocity. The last part of chapter 4 is the second case, varying solidity ratio. Chapter 5 deals with the comparison of the four methods. Lastly, chapter 6 includes conclusions and recommendations for further work.

Some figures might be somewhat small. This is due to a desire of keeping the report as compact as possible. The figures should be explained in the text, so the general shape will often times be of most interest. For some plots (net shape plots 5.2 - 5.5) only some of the subplots are selected to save space. Every plot and figure is given in high resolution electronically in appendix C.

Much of the work was done in Matlab. The solutions of Lølands method and the catenary equation are done in several scripts and functions in appendix B. The results from FhSim and AquaSim had to be extracted, and compared to the other results. FhSim gave the results in different comma separated files (csv-files), which cloud do some degree be read by Matlab. The results from AquaSim had to be extracted manually, and pasted into a Matlab script. This became a rather large “m-file”, and it is not included with the other Matlab files. To run this file, the values from Løland and the catenary equation for each case must be run in “main.m” (see appendix B.1).

1.5 Simplifications, limitations and definitions

Since the methods primarily was compared with each other, and not directly with a set of experiments, the direct validity of the results will be limited. The net have only been suspended perpendicular to the incoming flow. An obvious extension of the problem would be to include an angle on the net relative to the current direction (twist around the z-axis). The effect of waves have not been studied here. Wave will induce a water flow, which might be significant on the upper part of the net. The inertia forces in the structure from the wave induced motions, will give cyclic load patterns in any bearing point or mooring cables. The effect of (regular) waves on a complete system is significant (Berstad & Tronstad, 2005), and must be included in a complete model.

Current in this thesis is uniform. Varying current in depth or width will probably influence a fish farm

differently then a uniform current profile.

Unless otherwise stated, all net panel use the same directions and coordinate system. y is the positive current direction normal to the net. x runs parallel to the net. z is positive up. The origo is in the middle at the top of the net. Drag force, F_D act in the positive current direction (y), lift force acts normal to this, positive z direction. The normal force, F_N acts normal to the net panel direction, and tangential force, F_T tangential to the net panel. See figure 1.1.

When analyzing, a simple, slim two dimensional net is considered. The net is suspended from the water surface, and free to rotate. It hangs loose, free to deform, with bottom weight at the lower end. No bending stiffness is assumed.

At some points in the text, measurements such as twine diameter are given with great accuracy. This is purely an academic exercise. In real life you can not give a twine diameter down to $0.001\mathrm{mm}$ accuracy.

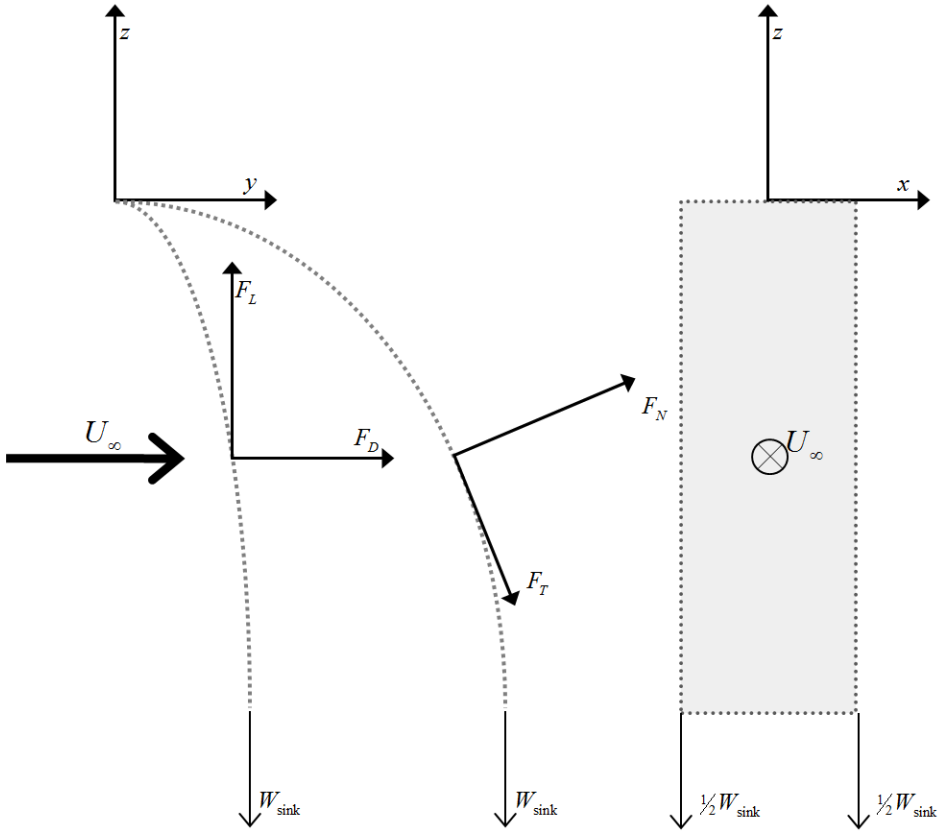

Figure 1.1: Definitions of force direction and coordinate system. First part of the figure shows two nets with different deformation.

Chapter 2

Presentation of the four methods

The four methods which are to be compared, will be presented. The amount of relevant information related to the four methods is very different. One is based on a PhD, and another is based on own calculations. One method is is basically a project in development, and lastly there is a comersial software. A relative brief introduction will be given for three of the four methods. The presentation of the solution of the catenary equation should be somewhat more substantial.

2.1 Løland

2.1.1 Presentation of the original experiment and analysis

Lølands thesis aimed at finding a model for current force calculation, primarily for use on fish farms. This was done by investigating results from several model tests done by Rudi et al. (1988). Rudi et al. investigated the drag and lift on a rigid net panel to establish relations between the nets solidity, angle and drag and lift coefficients. Lølands main assumption was that a net cage can be modeled as a sum of single net panels. Lølands goal was to more accurately calculate the forces on complete system. An important factor in this aspect is the reduction factor, r. As the flow passes through a net panel, the velocity will decrease some percentage based on the characteristic of the net. Løland presented this as a geometric series based on the drag coefficient of the previous net panel. The current velocity for a net number i ($i-1$ nets upstream) is given as $U_i = U_\infty \cdot r^i$, where r is given as

$$r = 1.0 - 0.46 \cdot C_D \tag{2.1}$$

The thesis focus on complete fish farm system, and contains less information about the correct force on and deformation of a single net panel.

"The current force model is constructed in such a way that it takes into account the most important effects such as the net solidity, weights of sinkers, shielding, initial geometry and deformation of the net cages." (Løland, 1991, p86)

2.1.2 Conclusions and developed formulas

It is assumed the mean drag and lift force on a net can be split up into the sum of the mean force on smaller net panels. On a small section, dA the drag force, dF_D and lift force, dF_L can be expressed as

$$dF_D = \frac{1}{2}\rho\, C_D(\theta, Sn)\, U^2\, dA \tag{2.2}$$

$$dF_L = \frac{1}{2}\rho\, C_L(\theta, Sn)\, U^2\, dA \tag{2.3}$$

where A is the net panel area ($B \cdot L$), U is the relevant current velocity and ρ the density of water. C_D and C_L are based on data from the experiments done by Rudi et al. (1988). During several test with different solidity, velocity, net angle and bottom weights the drag and lift force was measured, plotted and the following relations was derived by curve fitting.

$$C_D = 0.04 + \left(-0.04 + 0.33Sn + 6.54Sn^2 - 4.88Sn^3\right)\cos\theta \tag{2.4}$$

$$C_L = \left(-0.05Sn + 2.3Sn^2 - 1.76Sn^3\right)\sin 2\theta \tag{2.5}$$

Where Sn is the solidity ratio, defined by the twine dimater, d, and mesh size l_{st} [1]. See section 2.1.3 for more details about solidity. θ is the angle between a net section and a vertical line, as given in figure 2.1. The factor 0.04 was introduced to take into account the drag force on the net parallel to the flow, and assumed independent of net panel angle. Faltinsen (2011) shows the value of this factor is to large. 0.04 is used in this thesis, as this is most widespread.

Considering a small section of the net panel, dA and zero moment requirements at each node the following equilibrium is found (See figure 2.1):

$$dF_D^i \cdot \frac{dL}{2} cos(\theta_i) + dF_L^i \cdot \frac{dL}{2} sin(\theta_i) + F_y^{i-1} \cdot\, dL cos(\theta_i) - F_z^{i-1} \cdot\, dL sin(\theta_i) = 0 \tag{2.6}$$

This gives an expression for θ_i which must be solved numerically since C_D and C_L is dependent of the unknown, θ_i.

$$\theta_i = tan^{-1}\left[-\frac{\frac{1}{2}\rho C_D(\theta_i, Sn)U^2 dA + 2F_x^{i-1}}{\frac{1}{2}\rho C_L(\theta_i, Sn)U^2 dA - 2F_z^{i-1}}\right] \tag{2.7}$$

The reaction forces at node i are then found:

$$F_y^i = dF_D^i + F_y^{i-1}$$

$$F_z^i = dF_L^i - F_z^{i-1}$$

Beginning at the lower end where F_z^0 and F_y^0 are known the net deformation and total force can be found.

2.1.3 A note about solidity

Løland uses in his thesis the following formula for the solidity ratio, which will represent a net with rather large knots:

$$Sn = \frac{2d}{l_{st}} + \frac{1}{2}\left(\frac{d}{l_{st}}\right)^2 \tag{2.8}$$

[1] l_{st} is defined according to NS9415 (2009) chapter 3.71.1. Use l_{st} instead of mesh size or equivalent due to habit from previous work related to fishing gear in Norwegian. (Norwegian: “stolpelengde” or “halvmaske”)

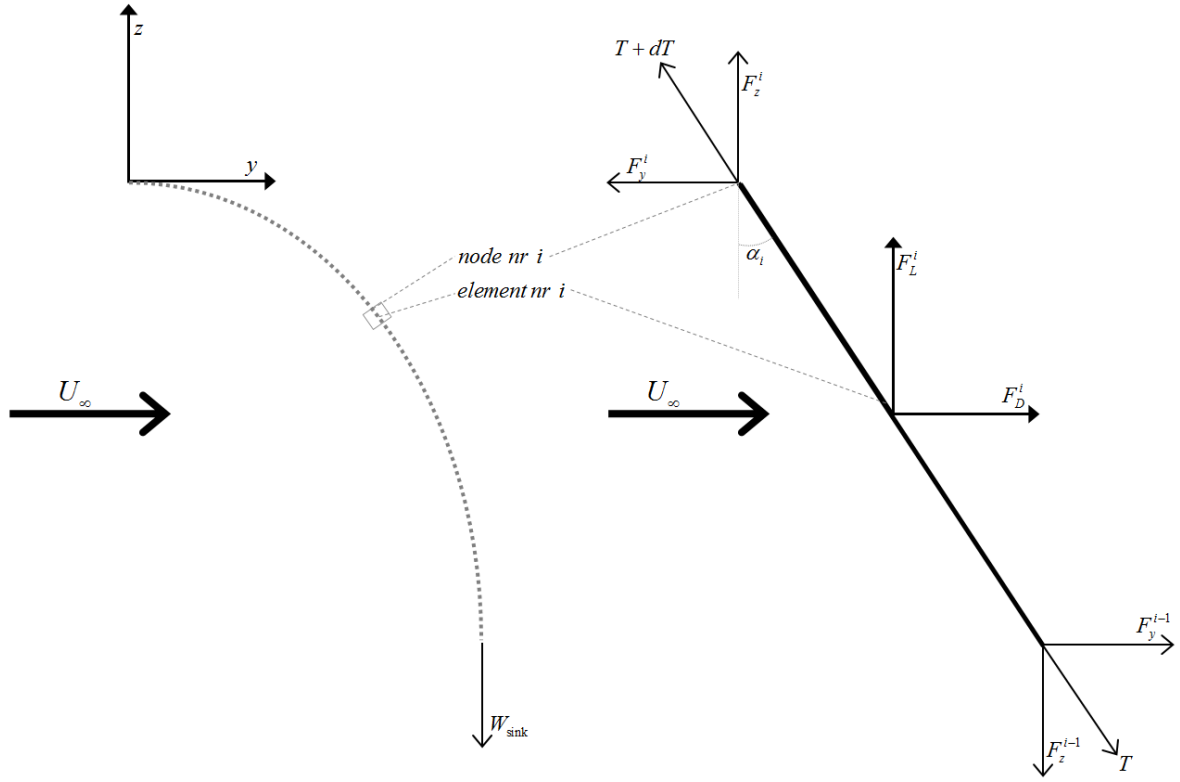

Figure 2.1: A deformed net element with angle θ_i indicated. No weight in water assumed

Assuming a knotless net the following expression is found.

$$Sn = \frac{2d}{l_{st}} - \left(\frac{d}{l_{st}}\right)^2 \tag{2.9}$$

A third variation is also used (see Vikestad & Lien, 2005; Tronstad, 2000, p73). This is correct if a small knot is assumed. This is the simplest variation, and often used as an estimate.

$$Sn = \frac{2d}{l_{st}} \tag{2.10}$$

The three formulas for Sn will represent a net panel with a large knot, no knot and a medium knot, respectively. Equation 2.9 is used in the calculation done in this assignment, and in several other publications (Kristiansen, 2010; Lader et al., 2007).

In Lølands thesis the solidity is given along with values for d and l_{st}, but there is an error between the given formula, the values for d, l_{st} and Sn. See table 2.1, the values for Lølands data is taken from (Løland, 1991, p135). Sn^{LO} denotes the caculated value based on equation 2.8, Sn^{GIVEN} is the value Løland uses, Sn^{NOKNOT} is the value based on equation 2.9, l_{st}^{new} is the value used to get the value of Sn^{GIVEN} from equation 2.9.

2.1.4 Matlab

A simple Matlab function was made to calculate the forces on and deformation of a net suspended in current accordin to Løland. The function takes in solidity Sn, net length L, net width B, sea water

l_{st}[mm]	d[mm]	Sn^{GIVEN}	Sn^{LO} (eq 2.8)	Sn^{NOKNOT} (eq 2.9)	l_{st}^{new}[mm]
29.0	1.83	0.130	0.128	0.122	27.200
19.5	1.38	0.144	0.144	0.137	18.450
12.0	1.03	0.184	0.175	0.164	10.655
15.5	1.83	0.234	0.243	0.222	10.545

Table 2.1: Comparison between different solidity ratios formulas.

density ρ_s, incident current velocity U, number of elements the net is to be divided into N_{el}, and the weight of sinkers W_{sink}.

Start values are given for $F_y^{i=1} = 0$ and $F_z^{i=1} = W_{sink}$. θ_i is found from iteration with start value $\theta_{TEMP} = 90°$.

Drag and lift force are found from

$$F_D = \sum_{i=1}^{N_{el}} = dF_D^i \quad F_L = \sum_{i=1}^{N_{el}} = dF_L^i \tag{2.11}$$

where dF_D^i and dF_L^i are found from equation 2.2 and 2.3.

The deformation is found for each element, from the end and up, from $dy(i) = ds \sin\theta_i$ and $dz(i) = ds \cos\theta_i$. The net shape in y and z direction is then given by adding the displacement contributions from the top ($i = N_{el}$), and down ($i = 1$).

For the Matlab code, see appendix B.14.

2.1.5 Test of the implementation of Lølands formula

To check if the implementation of the formulas are done correctly, a reproduction of the results given in Lølands thesis was undertaken. Lølands results are taken from p101 in his thesis (Løland, 1991). Calculations are done with solidity ratio $Sn = 0.130$. The drag force values from the solution of the catenary equation (see chapter 2.2) are also given for comparison.

U [m/s]	W_{sink} [N]	Angle $[deg]$	Drag Force [N]
0.159	2	27(19)	1.8(1.3) [1.4]
0.159	5	12(8)	2.0(1.4) [1.6]
0.316	2	59(53)	4.4(3.9) [3.7]
0.316	5	33(29)	6.1(5.0) [5.3]
0.490	2	72(71)	7.6(6.8) [5.0]
0.490	5	56(52)	10.7(9.5) [8.9]

Table 2.2: Comparison between Lølands given results and implementation of the formula in Matlab (numbers in parenthesis). For information; drag values from the catenary equation are given, [numbers in square brackets]. Number of elements used, $N_{el} = 1$.

There is some difference in the results, where ideally none should be present. Løland uses a weight, G, of the net in water, but since the size of this weight was not clearly stated in the thesis, it is assumed to be zero. The calculation in this assignment is done with $\rho_s = 1025\ \mathrm{kg/m^3}$. This can account for some of the difference in results. If Løland used a different density some small deviance could ensue, but not

nearly enough to explain the differences seen in table 2.2. The different equations used in determining the solidity may also influence the results.

Assuming a rigid net panel, and using the equations from Løland directly, the drag force can be computed by hand using the input from Lølands given results. Taking the angle $\theta = 27°$, solidity ratio $Sn = 0.130$, and the current speed of $U = 0.159\mathrm{m/s}$ the drag coefficient according to equation 2.4 is $C_D = 0.1315$, giving the drag force of $F_D = 1.3\mathrm{N}$, equal to what the Matlab script gets.

The relevant drag coefficient from the experiments by Rudi, for a net panel with inclination $30°$ is $C_D = 0.19$ (see table 3.3). Using this value, the drag force becoemes $F_D = 1.8\mathrm{N}$, which is what Løland gives as the drag force. It is likely Løland used coefficient directly from the experiments, and not from the formula.

"Throughout this dr.ing thesis the drag coefficients used are taken directly from the model tests, or from following estimated functional relationship:" (equations 2.4 and 2.5) (Løland, 1991, p87)

This is probably the major cause of the deviation.

2.2 Catenary equation

2.2.1 Theory and procedure

The catenary equation can be used to calculate the deformation of and tension in mooring chains, towing cables and generally hanging lines with little or none bending stiffness that are influenced by different forces. These equations will be adjusted and used on a net segment. Some of the work is based on the note by Faltinsen (2011), and in particular that which is done by T. Kristiansen. This method treats the panel as a single line, or rather as a sheet, and can not account for local "buckling" of the net. A thin strip should be used to avoid issues with this.

Neglecting nets weight in water and elasticity

First the weight of the net and the elasticity will be neglected to simplify the solution. In Faltinsen, (1990,p258) the equations for change in tension and angle on a mooring line are given. This will be used as an approximation of a narrow two dimensional net panel. By evaluating a sufficiently small element, i, with width B and length ds, assuming neutral buoyancy, no bending stiffness and no elasticity we get the changes in tension dT_i and angle, $d\theta_i$ for each element.

$$dT_i = \frac{1}{2}\rho U_\infty^2 C_T(\theta_i) B ds \tag{2.12a}$$

$$T_i d\theta_i = \frac{1}{2}\rho U_\infty^2 C_N(\theta_i) B ds \tag{2.12b}$$

where C_T is the tangential force coefficient, C_N is the normal force coefficient, and U_∞ the far field flow velocity. The position change of elements is found by $dy_i = -sin(\theta_m)ds$, $dz_i = cos(\theta_m)ds$. For element i the lower position is denoted (y_i, z_i) and the upper is denoted (y_{i+1}, z_{i+1}). Likewise for lower and upper values of θ. The angle for each element is defined at the midpoint $\theta_m = 1/2(\theta_i + \theta_{i+1})$.

The normal force coefficient, C_N, is made dependent of the prior element by using Taylor expansion. Expanding and taking only the first part:

$$C_N(\theta_{i+1}) \simeq C_N(\theta_i) + d\theta_i \underbrace{\left.\frac{\partial C_N(\theta)}{\partial \theta}\right|_{\theta=\theta_i}}_{\alpha_i} \tag{2.13}$$

$C_N(\theta_{i+1})$ is then dependent on $C_N(\theta_i)$ and $d\theta_i$. Beginning at the lowest part of the net, $i = 1$, θ_1 and T_1 is given from the weight of the sinker and possible current load on the sinker tube or equivalent. Need to find an expression for $d\theta_i$, which is the unknown. Can then solve for the next element by using $\theta_{i+1} = \theta_i + d\theta_i$ and $T_{i+1} = T_i + dT_i$. Evaluating at mid-point for each element $(i + 1/2)$ a expression balancing the change in external forces is found. Using equations 2.12a and 2.12b. The change in tension, must be balanced by a corresponding change in the normal force coefficient.

$$T_{i+\frac{1}{2}}\, d\theta_i = \frac{1}{2}\rho\, U_\infty^2 C_N(\theta_{i+\frac{1}{2}}) B\, ds \tag{2.14}$$

The change in tension is only due to half an element. Defining $T_{i+\frac{1}{2}} = T_i + \frac{1}{2}\, dT_i$ and $C_N(\theta_{i+\frac{1}{2}}) = C_N(\theta_i) + \frac{1}{2} d\theta_i \alpha_i$.

$$(T_i + \frac{1}{2} dT_i) d\theta_i = \frac{1}{2}\rho\, U_\infty^2 \left[C_N(\theta_i) + \frac{1}{2} d\theta_i \left.\frac{\partial C_N(\theta)}{\partial \theta}\right|_{\theta=\theta_i} \right] B\, ds \tag{2.15}$$

extracting, and using the definition for α_i from equation 2.13, the following expression for $d\theta_i$ is found:

$$d\theta_i = \frac{\frac{1}{2}\rho\, U_\infty^2 C_N(\theta_i) B\, ds}{T_i + \frac{1}{2} dT_i - \frac{1}{4}\rho U_\infty^2 B\, ds\, \alpha_i} \tag{2.16}$$

Introducing κ the expression can be simplified a bit.

$$\kappa = \frac{\frac{1}{2}\rho U_\infty^2 B\, ds}{T_i + \frac{1}{2} dT_i}$$

$$d\theta_i = \frac{\frac{1}{2}\rho\, U_\infty^2 B\, ds\, C_N(\theta_i)}{T_i + \frac{1}{2} dT_i \left(1 - \frac{\frac{1}{2}\rho\, U_\infty^2 B\, ds}{T_i + \frac{1}{2} dT_i} \frac{1}{2}\alpha_i\right)} = \frac{\kappa C_N(\theta_i)}{1 - \frac{1}{2}\alpha_i \kappa} \tag{2.17}$$

Introducing net weight in water and elasticity

Still neglecting bending stiffness and only considering membrane forces the same procedure can be used to take into account a relative net weight in water and elasticity of the net. The equations then becomes (from Faltinsen, 1990, p258):

$$dT_i = \left(w \cdot cos(\theta_i) - \frac{1}{2}\rho U_\infty^2 C_T(\theta_i) B \left(1 + \frac{T_i}{AE}\right)\right) ds \tag{2.18a}$$

$$T_i d\theta_i = \left(w \cdot sin(\theta_i) + \frac{1}{2}\rho U_\infty^2 C_N(\theta_i) B \left(1 + \frac{T_i}{AE}\right)\right) ds \tag{2.18b}$$

where w is the weight per unit length of the net in water ($w = \rho_{net} \cdot A_t \cdot (B/l_{st})$), A_t is the cross-sectional area of a single twine, T_i the tension of element i, E the elastic modulus of the net twines.

Using the same definitions for α_i as above, the following expression for $d\theta_i$ is found

$$d\theta_i = \frac{w\ sin(\theta_i)ds + \frac{1}{2}\rho U_\infty^2\ C_N(\theta_i)B\left(1 + \frac{T_i}{A_t E}\right)ds}{T_i + \frac{1}{2}dT_i - \frac{1}{2}\rho U_\infty^2 \frac{1}{2}\alpha_i B\left(1 + \frac{T_i}{A_t E}\right)ds} \tag{2.19}$$

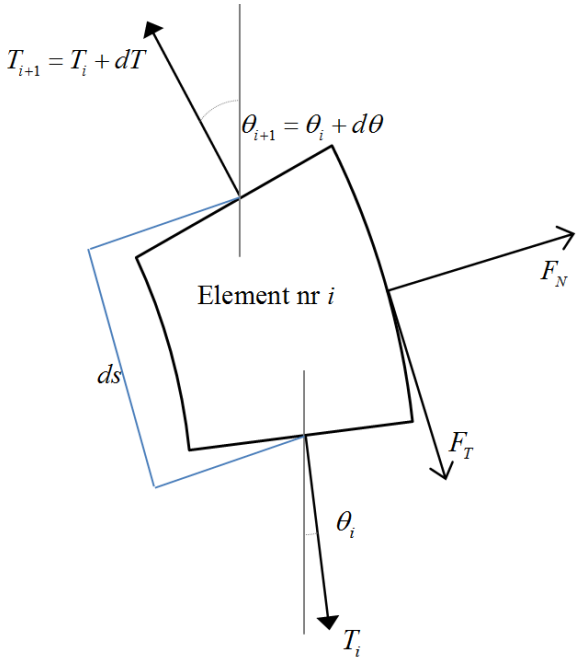

Figure 2.2: A deformed net element, i, with indicated tension, T and angle θ.

2.2.2 Coefficients

The catenary equation solution uses normal and tangential force on a net (twine) to find the net deformation. Drag and lift coefficients are used to give the total drag and lift force on the net. The normal and tangential force on a net plane can be expressed as a function of drag and lift force:

$$F_N = F_D cos(\theta) + F_L sin(\theta) \tag{2.20a}$$

$$F_T = F_D sin(\theta) - F_L cos(\theta) \tag{2.20b}$$

C_D, C_L, C_N and C_T are then found from the given relations

$$C_D = \frac{F_D}{\frac{1}{2}\rho A U_\infty^2},\ C_L = \frac{F_L}{\frac{1}{2}\rho A U_\infty^2},\ C_N = \frac{F_N}{\frac{1}{2}\rho A U_\infty^2},\ C_T = \frac{F_T}{\frac{1}{2}\rho A U_\infty^2} \tag{2.21}$$

where A is the outlined area ($A = L \cdot B$). The projected net area is in some cases also used where the solidity dependence is expressed directly in the coefficient ($A = L \cdot B \cdot Sn$). (Swift et al., 2006)

$$C_N = C_D cos(\theta) + C_L sin(\theta) \tag{2.22a}$$

$$C_T = C_D sin(\theta) - C_L cos(\theta) \tag{2.22b}$$

This is general, and valid in the range $-\pi/2 \leq \theta \leq \pi/2$. The force on a net (or section of a net) should not be calculated independent of the angle between net and incoming current. A net section

standing (close to) vertical in the water column must be treated different than a net section lying (close to) horizontal. Different approaches should be used for different angles. Here, the expressions are split in two parts. 1) For small angles defined, up to $45°$ ($0 \leq \theta \leq \pi/4$) and 2) for larger angles, up to $90°$ ($\pi/4 \leq \theta \leq \pi/2$).

For $0 \leq \theta \leq \pi/4$

When water passes through the net, the flow velocity increases. Using conservation of mass the current speed over the twines is defined as $U_{av} = U_\infty cos(\theta)/(1 - Sn)$. C_N can be expressed as the drag component of the decomposed part of the current normal to the net. The current velocity should be adjusted for the speed up through the net. This is assumed valid up to a net angle of $45°$. The solid part of the net is built up by twines. One twine can be expressed as cylinder. The drag coefficient on a single cylinder, C_D^{CC} is known. In Morison's formula for drag on a cylinder, $F_D = \frac{1}{2}\rho C_D^{CC} U^2 A$, A is the total (solid) area. On a net, this solid area is equal to $A \times Sn$.

The normal force on a net segment is then expressed as:

$$F_N = \frac{1}{2}\rho \left(\frac{U_\infty \cos\theta}{(1 - Sn)} \right)^2 C_D^{CC} A \cdot Sn \tag{2.23}$$

Using the definition in 2.21, the coefficient for normal force on an inclined net can be expressed as a a function of the total net solidity, the angle of the net, θ, and the Reynolds number dependent drag coefficient for a single cylinder.

$$C_N(\theta) = C_D^{CC} cos^2(\theta) \frac{Sn}{(1 - Sn)^2} \ , \ 0 \leq \theta \leq \pi/4 \tag{2.24}$$

The drag coefficient on single circular cylinder, C_D^{CC}, is found from a equation curve fitted to experimental values from from Goldstein(1965)(via Faltinsen, 2011), valid for Reynolds numbers in the range $10^{3/2} < Re < 10^4$. Se figure 2.3

$$\begin{aligned} C_D^{CC} = A + B_1 \log_{10}(Re) + B_2(\log_{10}(Re))^2 + B_3(\log_{10}(Re))^3 + B_4(\log_{10}(Re))^4 \\ + B_5(\log_{10}(Re))^5 + B_6(\log_{10}(Re))^6 + B_7(\log_{10}(Re))^7 \end{aligned} \tag{2.25}$$

$A = -78.46675, B_1 = 254.73873, B_2 = -327.8864, B_3 = 223.64577, B_4 = -87.92234, B_5 = 20.00769, B_6 = -2.44894, B_7 = 0.12479$

Where $Re = Re^{AV} = U_\infty cos(\theta) d / [\nu(1 - Sn)]$, d is the twine diameter, ν the kinematic viscosity, θ the net section inclination relative to the direction of the incident flow, U_∞.

C_T is found from the following relation from Schubauer et al. (1950):

$$\frac{C_T(\theta)}{\theta} = \frac{4C_N(\theta)}{8 + C_N(\theta)} \ , \ 0 \leq \theta \leq \pi/4 \tag{2.26}$$

which yields the following expressions for C_L and C_D by combining equations 2.22a and 2.22b.

$$C_L(\theta) = C_N \sin(\theta) - C_T \cos(\theta) \tag{2.27}$$

$$C_D(\theta) = C_N \cos(\theta) + C_T \sin(\theta) \tag{2.28}$$

This gives us values for C_T, C_N, C_L and C_D for a given solidity, ambient flow velocity, twine diameter and net angle. This is valid for Reynolds numbers in the range $10^{3/2} < Rn < 10^4$, and net screen angle $0 \leq \theta \leq \pi/4$. Values for C_D and C_L can now be calculated and compared with other methods for net plane inclined up to $45°$. Using formulas and principles valid only up to $45°$, a different procedure is needed for larger angles.

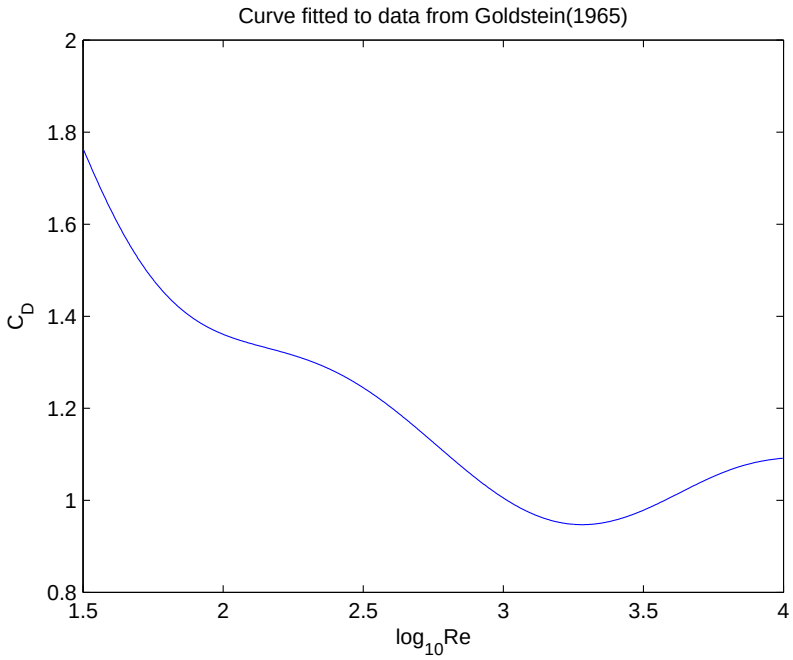

Figure 2.3: Drag coefficient on circular cylinder. (Plot of equation 2.25.)

For $\pi/4 < \theta \leq \pi/2$

Rudi et al. (1988) proposed the following procedure for the range $\pi/4 < \theta \leq \pi/2$.

$$C_D(\theta) = C_D(0)cos(\theta) \tag{2.29a}$$

$$C_L(\theta) = C_L(\pi/4)sin(2\theta) \tag{2.29b}$$

Substituting equations 2.29a and 2.29b into equations 2.22a and 2.22b the following expression is found:

$$C_N(\theta) = C_D(0)cos^2(\theta) + C_L(\pi/4)sin(2\theta)sin(\theta) \tag{2.30}$$

$$C_T(\theta) = \frac{1}{2}C_D(0)sin(2\theta) - C_L(\pi/4)sin(2\theta)cos(\theta) \tag{2.31}$$

$C_D(0)$ and $C_L(\pi/4)$ is dependent on Reynolds number and solidity, and found from:
$C_D(0) = C_N(0) = C_D^{CC} \cdot (Sn/(1-Sn)^2)$ and $C_L(\pi/4) = C_N(\pi/4)sin(\pi/4) - C_T(\pi/4)cos(\pi/4)$, where $C_N(\pi/4)$ is found from: $C_N = C_D^{CC}(Re)\frac{1}{2}\frac{Sn}{(1-Sn)^2}$ and C_T from: $C_T = \frac{\pi C_N}{8+CN}$.

The theoretical drag and lift coefficients can now be calculated and compared with the experimental values from Rudi et al. (1988). The normal and tangential force coefficient are also given for $\theta = 0-90°$. Put together, this can be used in a method for finding the forces on and deformation of a net panel in uniform current by solving the catenary equation.

Solving the problem

To solve the problem, with or without accounting for net weight and elasticity, an expression for α_i is needed. Two expressions for α_i are found by differentiate the expressions for C_N in equations 2.24 and 2.30.

$$\alpha_i = \begin{cases} -2C_D^{CC}sin(\theta_i)cos(\theta_i)\frac{Sn}{(1-Sn)^2}, & 0 \leq \theta \leq \pi/4 \\ C_D(0)sin(\theta_i)cos(\theta_i) + \frac{1}{2}C_L(\pi/4)(2sin(3\theta_i) - sin(\theta_i)), & \pi/4 < \theta \leq \pi/2 \end{cases} \tag{2.32}$$

The equations presented makes it possible to plot the net position, and integrate the overall drag and lift force. If every net panel has a inclination larger then 45° the drag force can be expressed as

$$F_D = \int_L \frac{1}{2}\rho U_\infty^2 B C_D ds\Big|_{\theta \geq \pi/4} = \frac{1}{2}\rho U_\infty^2 B \int_{\theta_1}^{\theta_e} C_D(0)\cos\theta ds \tag{2.33}$$

Where θ_1 is the angle at the end point, and θ_e at the top. Since $\int_{\theta_1}^{\theta_e} \cos\theta ds = -z_{bot}$, the drag force will be proportional with the projected area. z_{bot} is the z-coordinate of the end point of the net. $z_{bot} \times B = A_{projected}$. This corresponds to a rigid panel approximation (such as (Løland, 1991, p100)). As seen in the end of chapter 3.1, this approximation would lead to an under prediction of drag force relative to the method where the drag coefficient is dependent on the angle of the net panel. This also corresponds to the findings of Lader & Enerhaug (2005). If the lift force is considered the same way, the total lift force will be under predicted relative to the method where the calculation procedure for the coefficients is dependent on the net angle.

Notice also, in the catenary equation, the deformation of the net is not directly dependent on the drag and lift force on each panel, but rather on $C_D(0)$, $C_L(\pi/4)$ and C_D^{CC}.

The presented drag and lift force are found by adding together the contribution of each element.

$$F_D = \sum_{i=1}^{N_{el}} dF_D^i = \sum_{i=1}^{N_{el}} \frac{1}{2}\rho U_\infty^2 B C_D^i ds \tag{2.34a}$$

$$F_L = \sum_{i=1}^{N_{el}} dF_L^i = \sum_{i=1}^{N_{el}} \frac{1}{2}\rho U_\infty^2 B C_L^i ds \tag{2.34b}$$

where C_D^i and C_L^i is dependent on the angle of the net element.

2.2.3 Matlab

To solve the catenary equation a Matlab script has been made. The code is found in appendix B, and electronic in appendix C. The emphasize was not primarly on user friendliness, so the format requirements to the input values is not very obvious. The script also handles the Løland method presented in chapter 2.1.

A net panel with width B and length, L is divided into N_{el} elements with a constant length $ds = L/N_{el}$. It is suspended from the origin of a coordinate system, Oyz, and is free to rotate around $(0, 0)$. No bending stiffness in the net is assumed. At the end the tension is known to be equal to the bottom weight $T = T_1 = W_{sink}$, and the angle is known to be $\theta = 0$. If lateral current load on the sinker, F_C^{sink} is incorporated, the tension becomes $T = T_1 = \sqrt{W_{sink}^2 + F_C^{sink}}$, and the angle $\theta_1 = tan^{-1}(F_C^{sink}/W_{sink})$. Density and elasticity of the net and density of the water is given, and the whether or not net weight and elasticity is accounted for is decided independent of those values.

The implementation of net weight and elasticity seems to be correct as using a very high stiffness ($E = 1.0 \cdot 10^{99}$ MPa) and net density of $\rho_{net} = 1025\ \mathrm{kg/m^3}$ (same as water density) gives the same results as not accounting for net weight and elasticity.

Since the known start values are in the lower end of the net, the deformation of the net if found by summing the change in y and z from the top down after the change for each element is found.

2.3 FhSim

FhSim is a software package developed at SINTEF Fisheries and Aquaculture. The program is suitable to simulate and visualize systems describable by ordinary differential equation (ODE). As of now, calculation models exists for trawling and mooring/anchoring operations.

A project goal is to be able to preserve code used in earlier project in the same framework, and utilize this when new projects touch the same or similar problems. This should reduce the tendency to make new code for existing solutions and increase efficiency when programming new scenarios and models. This requires strict conventions and programming rules to ensure compatibility. Different models can then be combined to simulate increasingly complex scenarios. (Føre, 2011)

Efforts to implement functionality to enable calculation for fish farms are currently being made. A comparison with an established solution, like AquaSim, is desirable for the developer. By studying results for a simplified case, strengths, weaknesses and restrictions should be discussed and addressed.

This is a work in progress, and the presentation and analysis is based on a version from February 2011. The available source material was somewhat sparse. Mostly based on a note by Føre (2011) and an article by Ersdal & Faltinsen (2006).

2.3.1 Theory: Presentation of program and governing equations

The net elements are described as triangle or square shaped surface elements. Structurally, net elements are built up by triangular Priour elements. One elements goes over several twine lengths (l_{st}), and follows the local twine orientation, horizontal and vertical with two of its three sides. The elements are affected by three main forces: 1) Tension in the twines, 2) Gravity forces such as weight of net and sinkers and 3) Hydrodynamic forces. (Føre, 2011)

The hydrodynamic forces are computed as the normal and tangential forces on the twine. The model uses the relative current velocity (current velocity - element velocity), and finds the normal force coefficient from the work done by Ersdal & Faltinsen (2006), as will be described later. It does not affect this work, but it should be noted that the net elements does not affect the water flow. The water will have the same velocity before, as they pass through and after the net panel. (Føre, 2011)

The modified cross flow principle

Ersdal & Faltinsen (2006) investigated the normal force on a cylinder when the water flow angle of attack is smaller then what is usually accepted as the valid region for the cross flow principle. They presented the modified cross flow principle. Small meaning from 0 to 20° from the surface on a stationary cylinder, and from 4° to 50° on an oscillating. Normal force meaning skin friction, but since the the flow at some point will be separated from the cylinder (on the leeward side) the pressure gradient will create some drag force which will have a component normal to the cylinder. Since this thesis simplifies by looking at a single net panel perpendicular to the incoming flow, the angle of attack will only be sufficiently small to use the modified cross flow principle at some places with extreme deformation. For a complete fish farm it will be relevant for larger parts of the system. Since the principle seems to be at the core of the governing equations in FhSim, it will be presented here.

The normal force on a cylinder with constant angle of attack relative to the ambient flow, α, and with

constant velocity, U_∞ can be expressed as

$$F_N = \frac{1}{2}\rho U_\infty^2 C_N(\alpha) L d \tag{2.35}$$

where L is the length of the cylinder, and d the diameter. The modified cross flow principle is presented by expressing C_N as a function of current velocity U_∞, the angle between flow and cylinder (or twine cable), α, and different coefficients which are dependent on the flow characteristics of the boundary layer. α is defined as the angle between the cylinder and the surface. $\alpha = 0$ will correspond to a net panel parallel to the flow direction, $\alpha = 90^\circ$ when the net panel is perpendicular to the current flow direction. The notation C_N^{mod} will be used for the coefficient presented in Ersdal & Faltinsen (2006).

$$C_N^{mod} = [C_{nt} + f(\alpha, U)(C_{nl} - C_{nt})] \sin\alpha |\sin\alpha| \tag{2.36}$$

C_{nl} is the normal force coefficient for laminar boundary layer, C_{nt} for turbulent. The values are set to $C_{nl} = 1.15$ and $C_{nt} = 0.8$. From inspection it was chosen a linear transition model for the coefficient from laminar to turbulent boundary layer; $f(\alpha, U)$.

$$f(\alpha, U) = \begin{cases} 0 & = \text{ if } \alpha < \alpha_t, \\ \frac{\alpha - \alpha_t}{\alpha_l - \alpha_t} & = \text{ if } \alpha_t \leq \alpha \leq \alpha_l, \\ 1 & = \text{ if } \alpha > \alpha_l, \end{cases} \tag{2.37}$$

where α_t is the upper limit for the turbulent boundary layer, α_l the lower limit for the laminar boundary layer. Observing where in the Reynolds number range the transitions occur, the values can be found from the equations:

$$\frac{Ud}{\nu \sin\alpha_t} = 3.4 \cdot 10^5 \tag{2.38a}$$

$$\frac{Ud}{\nu \sin\alpha_l} = 2.0 \cdot 10^5 \tag{2.38b}$$

$d/\sin\alpha = l$, where l is the actual length over the inclined cylinder parallel to the water flow. Using this will produce results with the same accuracy as the measurements.

Normal force in FhSim

In addition to the modified cross flow principle for relevant parts of the net, FhSim uses the linear model for normal drag on angles less then 4°, and a fixed value $C_{nt} = 1.15$ in accordance to the cross flow principle with corrections from Ersdal & Faltinsen (2006) when the angle is large enough. The value is not specifically stated in the documentation, but the documentation infers to the article, so it is assumed the value of C_{nt} is the same in the program as in the article. The following is used to express the normal force on the twines in an element (F_{N_u} and F_{N_v}), going in a horizontal (u) and vertical (v) direction:

$$F_{N_u} = k_u \cdot |V_{hd}|^2 \cdot C_{N_u}^{mod} \tag{2.39a}$$

$$F_{N_v} = k_v \cdot |V_{hd}|^2 \cdot C_{N_v}^{mod} \tag{2.39b}$$

where V_{hd} is the relative velocity of the current. Since waves are neglected, and only steady state solutions is relevant in this thesis, the velocity is here equal to U_∞. k_u and k_v is given as

$$k_u = \frac{1}{2}\,\rho_s d_{twine} \cdot l_{st} N_{twines_u} \tag{2.40a}$$

$$k_v = \frac{1}{2}\,\rho_s d_{twine} \cdot l_{st} N_{twines_v} \tag{2.40b}$$

where N_{twines_u} and N_{twines_v} is number of twines in u and v direction. The reason for dividing into horizontal (u) and vertical (v) twines is to enable different lengths on the sides of the Priour elements. The normal force coefficients, C_{N_u} and C_{N_v}, are expressed in the same way, as C_N:

$$C_N^{mod} = C_{nlin} \sin\alpha \quad \text{for } \alpha < \alpha_{lin}, \tag{2.41a}$$

$$C_N^{mod} = C_{nt} \sin^2\alpha \quad \text{for } \alpha_{lin} \leq \alpha < \alpha_t, \tag{2.41b}$$

$$C_N^{mod} = \left(C_{nt} + \frac{\alpha - \alpha_t}{\alpha_l - \alpha_t} \left(C_{nl} - C_{nt} \right) \right) \sin^2\alpha \quad \text{for } \alpha_t \leq \alpha < \alpha_l, \tag{2.41c}$$

$$C_N^{mod} = C_{nl} \sin\alpha \quad \text{for } \alpha_l < \alpha, \tag{2.41d}$$

$$C_N^{mod} = C_{nt} \quad \text{for rest} \tag{2.41e}$$

C_{nl} and C_{nt} same as above. $C_{nlin} = 0.068$ (value from Ersdal & Faltinsen, 2006) is based on the linear model for normal force on a cylinder. This performs best and is valid at values of α less than $\alpha_{lin} = 4°$. For the cases investigated in this thesis, the value of C_N^{mod} will for the most part be within the turbulent boundary layer, $C_N^{mod} = C_{nt} = 1.15$.

Tangential force in FhSim

The expression for tangential forces on the horizontal (u) and vertical (v) twines is similar to the expression of normal force in equations 2.39, with the same definitions for k_u and k_v as in equation 2.40.

$$F_{T_u} = k_u \cdot |V_{hd}|^2 \cdot C_T \tag{2.42a}$$

$$F_{T_v} = k_v \cdot |V_{hd}|^2 \cdot C_T \tag{2.42b}$$

C_T is here only approximated from $C_T = C_{T_{nom}} \cdot \pi$, where the coefficient $C_{T_{nom}} = 0.01$. Both the tangential and normal forces on the twines are summed up and equally distributed between the nodes in the Priour elements.

Discussion of the method

The modified cross flow principle in Ersdal & Faltinsen (2006) is based on experiments on a smooth cylinder without any disturbance on its length. Summation of force on single twines does not take into account the fact that the cross section is often not circular, and the surface not smooth. Since the majority of the normal force is assumed to be skin friction this might increase if a less smooth surface is considered. With angle of attack small enough to utilize the modified cross flow principle, the projected area will be quite small, resulting in a small drag force. Any potential error in this part will thus have a small effect on the overall results. Sections of a circular net cage will always have the current at an angle close to zero.

Not accounting for a reduction in current velocity after a net panel will not affect this work, but if larger system should be analyzed using the same current over several net panels in succession this assumption will lead to an over predication. A simple way to counter this is by using a reduction factor, which reduces the current speed every time a net is passed. Løland (1991) reduces the speed as a geometric series, see equation 2.1. The drag and lift forces are practically not dependent on the current velocity before the net panel angle becomes small.

2.4 AquaSim

AquaSim is a finite element (FEM) software for simulation and analysis of reactions forces in marine constructions exposed to loads such as current, waves, wind, impulse loads, pre-described displacements and other operational loads. It will cope with slender, coupled, flexible system of a relative high degree of complexity. Operating in the time domain, AquaSim can account for non-linear and hydroelastic effects. AquaSim is often used for dynamic analysis of fish farms in order to meet the dimensioning requirement of the Norwegian Standard for marine fish farms, NS9415 (2009).

The software is able to model a complete fish farming system, and can include nets, floaters, bridles, mooring frames, mooring cables and bottom chain. This system-wide approach and visualized results makes it fairly intuitive to use.

The software package consists of several programs. Superdraw is used to give global geometry to the system. The model is exported to AquaBase, where local geometry and material properties are added to the components. Parameters such as net twine cross section area, mesh size, rope diameter, elasticity and more is set and varied here. Several load cases can also be defined and managed here. The defined cases are then read and calculated by the main "equation engine", AquaSim (aquasim_2_6.exe), and result files are generated. These can be read by AquaView [2].

2.4.1 Theory: Presentation of program and governing equations

The hydrodynamic load model in AquaSim is, according to Berstad (2011), largely based on the work by Tronstad (2000). Tronstad based his model on the following prinsiples:

- The incoming flow is uniform, and the individual cable elements does no influence the flow.
- Shedding effect or influence on the flow due to the presence of the net is not accounted for.
- Hydrodynamic load on or effects of knots are not included.
- Drag force act along the velocity component, lift force act normal to the velocity component.
- The drag and lift coefficient are based on a flow independence principle where drag and friction coefficients are constant.
- Single rod summation and linear mesh geometry description over the width and length of the plane net cable structure.

(From Tronstad, 2000, p74)

The forces on a single twine is derived on a local orthogonal coordinate system with x-axis in the twine direction. Using notation from this thesis the force on a single twine is found as:

$$F_i = \frac{1}{2}\rho U_\infty^2 C_i \; l_{st} \; d \tag{2.43}$$

where the hydrodynamic coefficients in the different directions is given as a sum of the decomposed lift and drag coefficients

$$C_i = C_D(\alpha)e_{Ui} + C_L(\alpha)e_{Li} \tag{2.44}$$

e_L is the unit vector in the direction of the lift force, e_U is the unit vector along the incident flow direction and $i = \{x, y, z\}$. C_D and C_L are the drag and lift coefficients on a single twine cable, defined from the

[2] A beta version of AVS Explorer was used in addition to AquaView 2

normal and tangential coefficients on a cylinder:

$$C_D(\alpha) = C_N \sin^3 \alpha + \pi C_T \cos^3 \alpha \tag{2.45}$$

$$C_L(\alpha) = C_N \sin^2 \alpha \cos \alpha + \pi C_T \cos^2 \alpha \sin \alpha \tag{2.46}$$

According to the code from Berstad (2011) the following is used, $C_N = 1.20$ and $C_T = 0.02 \cdot C_N = 0.024$. Tronstad states the Reynolds number dependency is known to only be significant for $Re \leq 500$, and is thus neglected. The equations and methods from Tronstad (2000) seems to be in accordance with the short extract from the AquaSim program code in Berstad (2011).

It should also be noted that Tronstad defines the angle, α, as the angle between the incoming flow, and the tangential vector to the net. In other words, $\alpha = 90^\circ$ is a net panel normal to the flow, while $\alpha = 0^\circ$ is a net panel parallel to the flow direction.

The net is modeled as a membrane, consisting of meshes. One single mesh consists of four rods [3]. The total force (F_T), on one mesh m, is given as the sum of lift and drag forces in the x, y and z direction.

$$\left(F_{Tm} = \sum_{i=4}^{4} \left(F_{L_{ij}} + F_{D_{ij}} \right) \right), j = \{x, y, z\} \tag{2.47}$$

The membrane is modeled as a set of membrane elements. The total drag and lift force are distributed to the element corner nodes from the mesh nodes. (Tronstad, 2000, pp 74-81)

[3] Nets with hexagonal shaped meshes with six rods also exists, and AquaSim does have a method for dealing with this, but the norm is usually square nets.

Chapter 3

Validation of methods and error analysis using catenary equation

3.1 Validation of methods by comparison to experimental coefficients

One way to verify a model, is to compare it with experimental results. There are not very many useful experimental series available for this purpose. Løland (1991) based his thesis, calculations and equations on a series of experiments from Rudi et al. (1988). Since this is an available, and well known set of experiments, the results from the theoretical approaches will be compared with data from these experiments. The drag and lift coefficient for all four methods will be calculated and compared to the ones from Rudi.

From Rudi et al. (1988) the drag and lift coefficients from the flow velocity $U = 0.159\mathrm{m/s}$, $U = 0.316\mathrm{m/s}$ and $U = 0.966\mathrm{m/s}$ and solidity ratio $Sn = 0.130$, $Sn = 0.144$, $Sn = 0.184$ and $Sn = 0.317$ are used.

There is a dependence on the twine diameter, d, in catenary equation and FhSim. The relationship between d and Sn is not always clearly given in the source material. Løland does not use this direct dependence of twine diameter, but uses solidity ratio as variable. It is assumed the source material (Løland, 1991; Rudi et al., 1988) is consistent, and uses the same values for twine diameter through the work. The values for d used here are given in table 3.1.

$d[\mathrm{mm}]$	$l_{st}[\mathrm{mm}]$	$A_{twine}[\mathrm{mm}^2]$	Sn
1.830	27.200	2.629	0.130
1.380	18.450	1.495	0.144
1.030	10.655	0.833	0.184
1.830	10.545	2.629	0.317

Table 3.1: Diameter, mesh size and solidity ratio used for the validation in in chapter 3.1.

The coefficients are based on drag and lift forces on a rigid net panel in a frame with length $L = 1.5\mathrm{m}$, and width $B = 1.5\mathrm{m}$. The frame should not affect the results in any other way than keeping the panel rigid. For the Løland and catenary equation methods, the drag and lift coefficients were calculated based on the formula presented in the previous chapter. In FhSim, the lift and drag force was picked directly from the four bearing points supporting the system and summed. In AquaSim ropes, a frame and weights had to be modeled to be able to read the forces. The frame beam was modeled stiff, but any influence

on the flow and forces was minimized or removed by setting any weight, hydrodynamic coefficient etc to very low or zero. Simulations at very low speeds showed a slight buoyancy, and most of this was compensated for in the calculation. Drag and lift coefficients from equation 2.21.

θ is in the catenary equation and this chapter defined as the angle between a vertical line and the orientation of the rigid net panel. $\theta = 0$ corresponds to the panel standing vertical, normal to the flow direction.

In the rest of the chapter the following abbreviation are used when drag and lift coefficients from different methods are compared. LO is results from Lølands method. CE is the catenary equation solution for net panels. FH is results from FhSim. AS from AquaSim, and Rudi is based on the results from the experiments by Rudi et al. (1988).

3.1.1 Net inclination, $\theta = 0°, 30°, 45°$

At net inclination $\theta = 0$ the data from AquaSim is missing. For some reason the program was not able to give a result for this angle. The same procedure was used for every angle both in Superdraw, AquaBase and AquaView. There were no problems with any of the other angles.

Notice Lølands method does not account for the flow velocity, so the drag and lift coefficients will be equal across the three speeds. The same seems almost to hold for results from FhSim, also. The flow speed dependence in FhSim is very small in this region. Only drag force is presented for $\theta = 0$, since the lift force will be very close to, or ideally, exactly zero.

In the results from $\theta = 0$ (table 3.2), the drag coefficient from CE seems to be closest to Rudi. These two sets have a clearly decreasing C_D-value with increasing current velocity. This is consistent with the Reynolds number dependent decrease in C_D^{CC} is this region (See figure 2.3). Values from Rudi are clearly speed dependent, and since LO is not, the curve fitted values cannot follow Rudi at all speeds. LO-values are closest to Rudi at high current speeds. FH is generally far from Rudi, and also far from LO at high Sn-values.

At net inclination $\theta = 30$ (table 3.3) the drag coefficients shows the same pattern as for $\theta = 0$. This is especially evident in the relationships CE - Rudi and LO - FH. AS is quite close to Rudi except at top current speed, where the drag is lower. The lift coefficients are generally low, and more difficult to spot major differences in, but for all three speeds, the C_L of Rudi more then doubles from $Sn = 0.184$ to $Sn = 0.317$. This "jump" is also found in LO, and to slightly lower degree in CE. It is not found in FH or AS. FH has a consistently low lift coefficients. The drag force from AS is close to Rudi, except at $Sn = 0.317$. AS gives high C_L-values except for at high current speed and solidity ratios, where it is low compared to Rudi.

At net inclination $\theta = 45$ (table 3.4) much of the same general ratios as for lower inclinations, are still predominant. LO and CE are still closest to Rudi, both for the drag and lift coefficients. AS is very close to Rudi's drag coefficients for low solidity ratio, but to low at $Sn = 0.317$. FH has got consistently the lowest lift and drag coefficients.

3.1.2 Net inclination, $\theta = 60°, 80°, 90°$

As the net panel angel increases, the assumption of the load on a single twine being independent of other twines becomes increasingly problematic. In the catenary solution different methods for determining force coefficients are used on net panels with more or less inclination than $\theta = 45°$. For CE the equation used here is $C_D(\theta) = C_D(0)\cos\theta$.

Sn	U_∞	C_D[N]				
[−]	[m/s]	LO	CE	FH	AS	Rudi
0.130	0.159	0.14	0.21	0.13	–	0.21
0.144	0.159	0.17	0.25	0.15	–	0.24
0.184	0.159	0.25	0.36	0.18	–	0.35
0.317	0.159	0.61	0.81	0.26	–	0.92
0.130	0.316	0.14	0.19	0.13	–	0.19
0.144	0.316	0.17	0.23	0.15	–	0.20
0.184	0.316	0.25	0.33	0.18	–	0.30
0.317	0.316	0.61	0.70	0.26	–	0.71
0.130	0.966	0.14	0.16	0.13	–	0.18
0.144	0.966	0.17	0.19	0.15	–	0.19
0.184	0.966	0.25	0.27	0.18	–	0.26
0.317	0.966	0.61	0.65	0.26	–	0.58

Table 3.2: Drag coefficient for $\theta = 0$

Sn	U_∞	Net angle	C_D[N]					C_L[N]				
[−]	[m/s]	[deg]	LO	CE	FH	AS	Rudi	LO	CE	FH	AS	Rudi
0.130	0.159	30	0.13	0.16	0.11	0.20	0.19	0.02	0.05	0.02	0.09	0.04
0.144	0.159	30	0.15	0.19	0.12	0.21	0.18	0.03	0.05	0.02	0.10	0.05
0.184	0.159	30	0.22	0.27	0.15	0.26	0.24	0.05	0.08	0.03	0.11	0.08
0.317	0.159	30	0.53	0.61	0.22	0.42	0.71	0.14	0.18	0.04	0.14	0.23
0.130	0.316	30	0.13	0.14	0.11	0.15	0.15	0.02	0.04	0.02	0.05	0.04
0.144	0.316	30	0.15	0.17	0.12	0.17	0.16	0.03	0.05	0.03	0.05	0.04
0.184	0.316	30	0.22	0.25	0.15	0.21	0.22	0.05	0.07	0.03	0.06	0.07
0.317	0.316	30	0.53	0.54	0.22	0.36	0.55	0.14	0.16	0.04	0.09	0.18
0.130	0.966	30	0.13	0.12	0.11	0.13	0.15	0.02	0.03	0.02	0.03	0.03
0.144	0.966	30	0.15	0.14	0.12	0.15	0.15	0.03	0.04	0.03	0.03	0.03
0.184	0.966	30	0.22	0.20	0.15	0.19	0.21	0.05	0.06	0.03	0.04	0.05
0.317	0.966	30	0.53	0.48	0.22	0.34	0.49	0.14	0.14	0.05	0.07	0.12

Table 3.3: Drag and lift coefficient for $\theta = 30°$.

Sn	U_∞	Net angle	C_D[N]					C_L[N]				
[−]	[m/s]	[deg]	LO	CE	FH	AS	Rudi	LO	CE	FH	AS	Rudi
0.130	0.159	45	0.11	0.11	0.09	0.15	0.16	0.03	0.05	0.02	0.09	0.04
0.144	0.159	45	0.13	0.13	0.10	0.17	0.16	0.04	0.05	0.02	0.10	0.04
0.184	0.159	45	0.19	0.18	0.12	0.20	0.22	0.06	0.08	0.03	0.10	0.08
0.317	0.159	45	0.44	0.41	0.18	0.33	0.49	0.16	0.18	0.04	0.13	0.22
0.130	0.316	45	0.11	0.10	0.09	0.12	0.11	0.03	0.04	0.02	0.04	0.04
0.144	0.316	45	0.13	0.12	0.10	0.14	0.12	0.04	0.05	0.02	0.05	0.04
0.184	0.316	45	0.19	0.17	0.12	0.17	0.18	0.06	0.07	0.03	0.05	0.07
0.317	0.316	45	0.44	0.37	0.18	0.30	0.39	0.16	0.16	0.04	0.08	0.17
0.130	0.966	45	0.11	0.08	0.09	0.11	0.11	0.03	0.03	0.02	0.03	0.03
0.144	0.966	45	0.13	0.10	0.10	0.13	0.12	0.04	0.04	0.02	0.03	0.03
0.184	0.966	45	0.19	0.14	0.12	0.16	0.17	0.06	0.06	0.03	0.04	0.05
0.317	0.966	45	0.44	0.31	0.18	0.29	0.39	0.16	0.14	0.04	0.07	0.13

Table 3.4: Drag and lift coefficient for $\theta = 45°$.

The general trend for drag coefficients at $\theta = 60°$ (in table 3.5) is similar to earlier sets. The "jump" from $Sn = 0.184$ to $Sn = 0.317$ is less evident, especially for Rudi. CE over predicts the C_D values relative to Rudi, but comes closer at increasingly higher current speed, while LO is closest at low current speeds. In this series AS follows the drag coefficient from Rudi quite close. FH is again generally low, both for C_D and C_L. The lift coefficient at Rudi does a "jump" up to $Sn = 0.317$. This "jump" in C_L is found in LO and CE, but not in the others. The C_L-values are in relative good agreement with the values from Rudi for both CE and LO.

At $\theta = 80°$ (in table 3.6) the obvious jump in C_D-values from $Sn = 0.184$ to $Sn = 0.317$ is basically gone from Rudi, but is still visible to some degree in LO and CE. FH has, as the other methods shown decreasing C_D-values with increasing angle. FH decreases slower, so the C_D-values at $\theta = 80°$ is now closer to Rudi. AS shows a general over prediction relative to Rudi, especially at high solidity, and to a lesser degree at high current velocity. The lift coefficient from FH is very low, and has been rounded off to 0.00. AS gives clearly decreasing C_L-values for increasing current velocity, but more or less constant for change in solidity. Generally very low values, so differences are small, but LO and CE again seems closest to Rudi.

With the net panel normal to the flow direction, at $\theta = 90°$ (see table 3.6), the expected $C_D = 0.04$ is found in LO (see equation 2.4). Calculations of C_D for CE is proportional to $\cos\theta$, so this will be zero. Both FH and AS yields some rather large drag coefficients, which will quite clearly over estimate the drag force if results from Rudi is more realistic. The set closest to Rudi is actually the results from CE. The factor 0.04 in LO seems to large, as Faltinsen (2011) also pointed out. Rudi have some negative results for C_D. This is likely due to error in measurement, and gives an indication to the accuracy of the experiments. The lift force is zero for every method except from AS. It is here generally equal to the AS results from $\theta = 80°$.

Sn	U_∞	Net angle	C_D[N]					C_L[N]				
$[-]$	$[\mathrm{m/s}]$	[deg]	LO	CE	FH	AS	Rudi	LO	CE	FH	AS	Rudi
0.130	0.159	60	0.09	0.11	0.08	0.12	0.11	0.02	0.04	0.01	0.08	0.04
0.144	0.159	60	0.10	0.13	0.08	0.13	0.12	0.03	0.05	0.01	0.08	0.04
0.184	0.159	60	0.15	0.18	0.10	0.16	0.22	0.05	0.07	0.02	0.09	0.07
0.317	0.159	60	0.32	0.40	0.15	0.27	0.32	0.14	0.16	0.02	0.11	0.15
0.130	0.316	60	0.09	0.09	0.08	0.10	0.08	0.02	0.04	0.01	0.03	0.03
0.144	0.316	60	0.10	0.11	0.07	0.11	0.09	0.03	0.05	0.01	0.03	0.03
0.184	0.316	60	0.15	0.16	0.10	0.14	0.14	0.05	0.07	0.02	0.04	0.05
0.317	0.316	60	0.32	0.35	0.15	0.25	0.26	0.14	0.14	0.03	0.06	0.15
0.130	0.966	60	0.09	0.08	0.08	0.10	0.09	0.02	0.03	0.01	0.02	0.03
0.144	0.966	60	0.10	0.09	0.08	0.11	0.10	0.03	0.04	0.01	0.02	0.03
0.184	0.966	60	0.15	0.13	0.10	0.14	0.14	0.05	0.05	0.02	0.02	0.04
0.317	0.966	60	0.32	0.33	0.15	0.25	0.28	0.14	0.12	0.03	0.04	0.11

Table 3.5: Drag and lift coefficient for $\theta = 60°$.

It should be noted that the experiments done by Rudi does not represent "The Truth", i.e. equal to nature. Experiments are also an adaptation of the nature, using a set of simplification and assumptions. Within the given solidity and current velocity range, the experiments should, however give a good indication on what to expect.

To sum up, LO and CE are generally closest to Rudi for both drag and lift coefficients. The drag force in AS shows, as expected from equation 2.45, very little on none current speed dependency. The little there is might be attributed to scatter in the results. AS shows some speed dependency for lift force, but very little for Sn. As predicted, the 0.04 Sn independent C_D-value of AS, looks to large compared to Rudi. FH is consistently low for both C_D and C_L.

Sn	U_∞	Net angle	C_D[N]					C_L[N]				
$[-]$	$[\mathrm{m/s}]$	[deg]	LO	CE	FH	AS	Rudi	LO	CE	FH	AS	Rudi
0.130	0.159	80	0.06	0.04	0.07	0.10	0.08	0.01	0.02	0.00	0.07	0.03
0.144	0.159	80	0.06	0.04	0.08	0.11	0.07	0.01	0.02	0.00	0.07	0.03
0.184	0.159	80	0.08	0.06	0.09	0.13	0.10	0.02	0.03	0.00	0.07	0.03
0.317	0.159	80	0.14	0.14	0.13	0.23	0.11	0.05	0.06	0.00	0.07	0.07
0.130	0.316	80	0.06	0.03	0.07	0.09	0.04	0.01	0.01	0.00	0.02	0.01
0.144	0.316	80	0.06	0.04	0.08	0.10	0.04	0.01	0.02	0.00	0.02	0.02
0.184	0.316	80	0.08	0.06	0.09	0.13	0.06	0.02	0.03	0.00	0.02	0.02
0.317	0.316	80	0.14	0.12	0.13	0.23	0.09	0.05	0.06	0.00	0.02	0.05
0.130	0.966	80	0.06	0.03	0.07	0.09	0.04	0.01	0.01	0.00	0.00	0.01
0.144	0.966	80	0.06	0.03	0.08	0.10	0.04	0.01	0.01	0.00	0.00	0.02
0.184	0.966	80	0.08	0.05	0.09	0.13	0.05	0.02	0.02	0.00	0.00	0.02
0.317	0.966	80	0.14	0.11	0.13	0.22	0.09	0.05	0.05	0.00	0.01	0.04

Table 3.6: Drag and lift coefficient for $\theta = 80°$.

Sn	U_∞	Net angle	C_D[N]					C_L[N]				
$[-]$	$[\mathrm{m/s}]$	[deg]	LO	CE	FH	AS	Rudi	LO	CE	FH	AS	Rudi
0.130	0.159	90	0.04	0	0.07	0.08	0.01	0	0	0.00	0.07	0
0.144	0.159	90	0.04	0	0.08	0.09	0.01	0	0	0.00	0.07	0
0.184	0.159	90	0.04	0	0.09	0.12	0.01	0	0	0.00	0.07	0
0.317	0.159	90	0.04	0	0.13	0.21	0.03	0	0	0.00	0.07	0
0.130	0.316	90	0.04	0	0.07	0.09	−0.01	0	0	0.00	0.02	0
0.144	0.316	90	0.04	0	0.08	0.09	0.00	0	0	0.00	0.02	0
0.184	0.316	90	0.04	0	0.09	0.12	−0.01	0	0	0.00	0.02	0
0.317	0.316	90	0.04	0	0.13	0.22	0.01	0	0	0.00	0.02	0
0.130	0.966	90	0.04	0	0.07	0.08	0.00	0	0	0.00	0.00	0
0.144	0.966	90	0.04	0	0.08	0.09	0.01	0	0	0.00	0.00	0
0.184	0.966	90	0.04	0	0.09	0.12	0.01	0	0	0.00	0.00	0
0.317	0.966	90	0.04	0	0.13	0.22	0.01	0	0	0.00	0.00	0

Table 3.7: Drag and lift coefficient for $\theta = 90°$.

From the results in this chapter, crude predictions can be made about the force on and shape of nets suspended in current. FH has generally low values for both C_D and C_L. This will probably lead to small deformation and low drag force, except at high values of Sn and current velocity. The probably large projected area due to little lift force will give larger drag force. At maximum deformation, the drag coefficients for FH also approaches the other methods.

LO and CE have consistently similar drag and lift force coefficients. This should give similar results for both the deformation and drag force. AS behaves in a different way compared to the other methods, and is more difficult to predict. For the other methods, there is some coherence in between the drag and lift force with respect to where and how much they increase or decrease. This is not seen in AS.

Regarding the catenary equation, the formulas for drag and lift on the net panel with inclination larger than $\theta = 45°$ are more simple to use than those for $\theta < 45°$. If these were used by mistake or as an approximation on net panels with smaller angle then $45°$, the resulting drag and lift force would be changed. The lift coefficients for panels with $\theta < 45°$ would be lower, and the drag coefficients would be higher. This would naturally result in an under prediction of lift, and over prediction of drag force relative to the two-coefficients method. The overall relative difference in the two methods would subside with increasing deformation, as smaller portions would be subjected to the angles where the differences are given.

This "two-coefficients-method" is a major difference from the rigid panel approximation. If the drag force is only proportional to $\cos\theta$, the drag force would be proportional to the projected area.

3.2 Error analysis on the catenary equation solution

To quantify the influence of different error sources an error analysis can be used. Important results which will be affected by different error sources include drag force, F_D, lift force, F_L, max tension within the net structure, T_{max} and the angle between origin and end point on net, α. This thesis compares four different methods for calculating forces and deformations on a net panel. Ideally an error analysis should have been done on all four methods and cases. This was not done due to the need to limit the scope of and time used on the thesis. For some of the methods, the processes would have been very time consuming.

A more detailed presentation is done for the catenary equation. Having insight in the procedure, assumptions and solution method, the solution of the catenary equation was natural choice for an error analysis.

The data used in case 1 was the basis for the analysis. For more info about the basis, see chapter 4.1 and 4.2. The error of F_D, F_L, T_{max} and α on the catenary equation method will be presented as a function of current speed. The following error sources will be considered:

- Buoyancy on sinkers, $\Delta_{w_{sink}}$
  - Difference in results from $W_{sink} = 200\text{N}$ and $W_{sink} = 200\text{N} \cdot 0.90$
- Weight of net in water, $\Delta_{\rho_{net}}$
  - Difference in results from $\rho_{net} = 1125\text{kg/m}^3$ and $\rho_{net} = 925\text{kg/m}^3$.
- Elasticity of net, $\Delta_{E_{net}}$
  - Difference in results from implementing elasticity on the net set to $E_{net} = 1.0 \cdot 10^9\text{MPa}$.
- Change of elasticity of net, $\Delta_{\delta E_{net}}$

  - Difference in results from varying elasticity, $\mathrm{E_{net}} = 1.0 \cdot 10^8 - 2.0 \cdot 10^9$ MPa
- Change in drag coefficient due to twine not being a circular circular, $\Delta_{C_D^{CC}}$
  - Difference in results from varying drag coefficient, $C_D^{CC} \pm 10\%$
- Variations in given solidity ratio, Δ_{Sn}
  - Difference in results from varying solidity, $Sn \pm 10\%$
- Accounting for current force on sinker, $\Delta_{F_D^{sink}}$
  - Difference in results from accounting for current force on a sinker tube along the width of the net ($B = 1\mathrm{m}$). Largest influence (difference from no drag) on results from sinker diameter $D_{sink} = 0.05\mathrm{m}$ or $D_{sink} = 0.10\mathrm{m}$ is chosen.

The total error is found from varying these parameters individually, and mapping the influence this will have on the results. For instance, looking at error sources influence on the resulting drag force: A change in the drag coefficient, C_D^{CC} of some percentage, $\pm p\%$, will affect the total drag force. The change in drag force due to change or uncertainty in drag coefficient is then found as $\Delta_{C_D^{CC}} F_D = F_D(C_{D,max}^{CC}) - F_D(C_{D,min}^{CC})$.

For each current speed the total error in the drag force, Δ_{F_D} is then defined as the quadratic sum over the contributions from every error source:

$$\begin{aligned}(\Delta_{F_D})^2 = (\Delta_{w_{sink}} F_D)^2 + (\Delta_{\rho_{net}} F_D)^2 + (\Delta_{E_{net}} F_D)^2 + \\ (\Delta_{C_D^{CC}} F_D)^2 + (\Delta_{Sn} F_D)^2 + (\Delta_{F_D^{sink}} F_D)^2\end{aligned} \tag{3.1}$$

Likewise for error in lift force Δ_{F_D}, max tension $\Delta_{T_{max}}$, and end point angle Δ_α.

The influence of drag force on the bottom weights was modeled as a sinker tube. Fish farms are normally modeled with point weights with a certain distance in between[1]. In reality a sinker tube is often used to contain the weights, which will be continually distributed along the lower end of the net. The tube goes across the width of the net ($B = 1.0\mathrm{m}$), and two diameters were tested, $D_{sink} = 0.10\mathrm{m}$ and $D_{sink} = 0.05\mathrm{m}$. The assumption was the largest diameter would yield the largest influence, and a smaller was tested in case the larger gave unrealistically high influence. For some reason it varies whether the smaller or larger tube diameter influences drag, lift, tension and end point angle the most. Influence from drag force on the sinker tube is based on the diameter yielding the largest result.

Error analysis on drag force, lift force, max tension (which is equal to the tension at the top) and end point angle is done for four solidity ratios, $Sn = 0.19$, $Sn = 0.20$, $Sn = 0.30$ and $Sn = 0.40$ (see table 3.8). All are done with twine diameter $d = 1.5\mathrm{mm}$ to eliminate variation in Reynolds number within same current speed as an possible error source. This will give some unlikely combinations of d and l_{st} in relation to nets used in aquaculture, but it should also produce consistent error data, which is the goal here. The results for $Sn = 0.19$ are given below (tables 3.9 - 3.12) with some comments. See appendix A.1 - A.3 for results from solidity ratios 0.20, 0.30 and 0.40, and figure 3.1 for a visual summary. It should also be noted that the error values are the complete error range. Any error bars, such as those in figure 3.1, should therefor be plotted (here: for drag force) $F_D \pm \Delta F_D/2$.

The relative error is obtained by dividing the total error with the total force, tension or angle. For $Sn = 0.190$ the values for maximum drag force, lift force and end point angle are found in table 4.2. The tension is indicated in figure 4.2.

[1] Based on experience using AquaSim for dimensioning analysis according to NS9415 during a summer internship.

$Sn[-]$	$d[\mathrm{mm}]$	$l_{st}[\mathrm{mm}]$
0.19	1.50	15.00
0.20	1.50	14.20
0.30	1.50	9.18
0.40	1.50	6.654

Table 3.8: Sn values used in the error analysis.

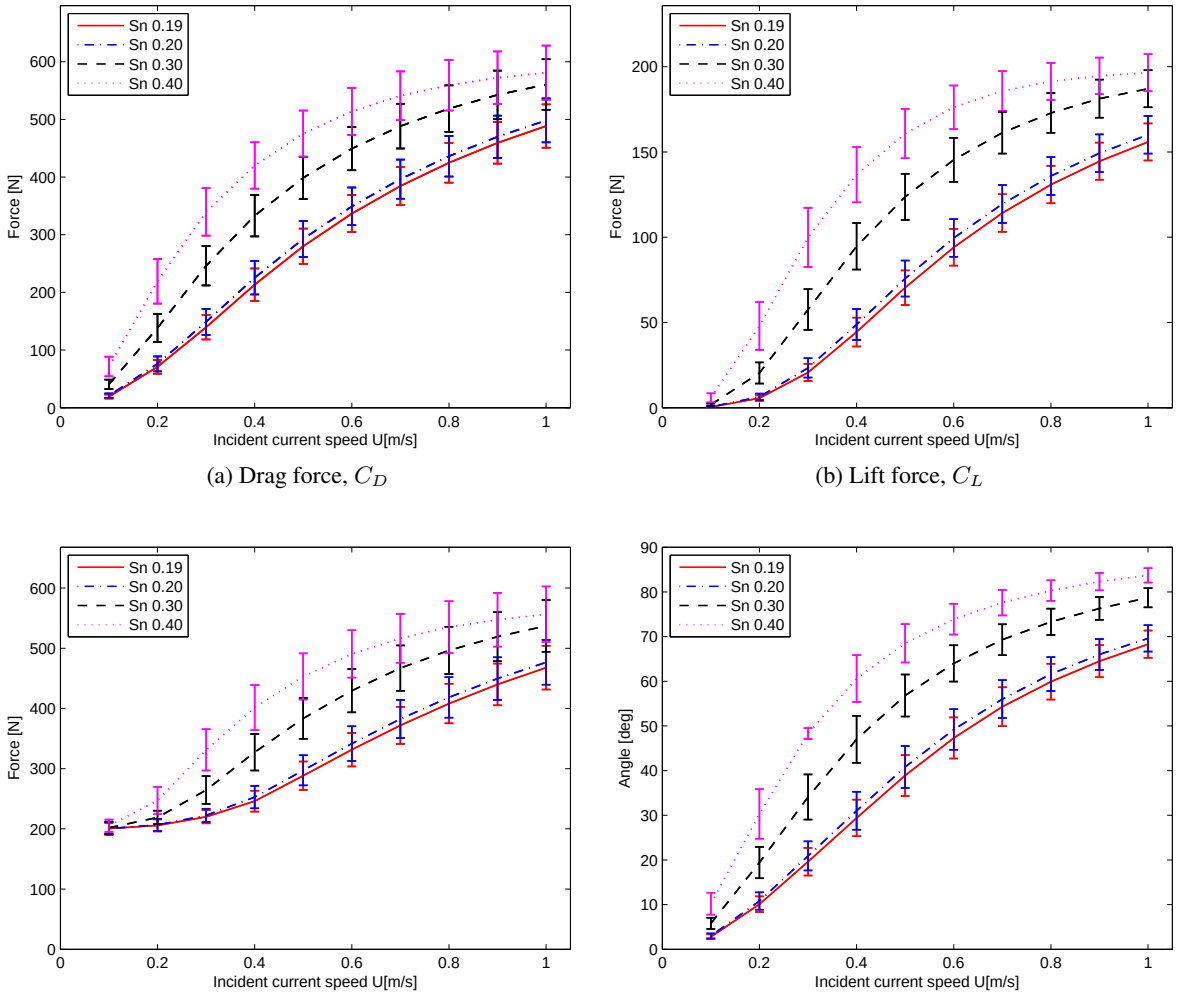

(a) Drag force, C_D

(b) Lift force, C_L

(c) Max tension, T_{max}

(d) End point angle, α

Figure 3.1: Error on drag force, lift force, max tension and endpoint angle for $Sn = 0.19$, $Sn = 0.20$, $Sn = 0.30$ and $Sn = 0.40$

3.2.1 Error on on net with solidity $Sn = 0.190$

For both the drag force, lift force, max tension and end point angle, the largest influences comes from buoyancy on the sinker $\Delta_{W_{sink}}$, variations in solidity Δ_{Sn}, and variations in drag coefficient $\Delta_{C_D^{CC}}$. These are all parameters with a relative high, but realistic degree of uncertainty.

Accounting for buoyancy on the sinker should normally not be a problem, as it is fairly straight forward. But since many sinkers consists of heavy chain contained in a tube it is possible the "normal" chain weight (in air) is used by a mistake. A steel chain will have about 90% of its weight in water relative to air. The tube can be considered neutrally buoyant without this being the case. Some error in the sinker weight may be introduced in this way.

A change of $\pm 10\%$ in the drag coefficient will naturaly have a big impact on the results. This uncertainty is only roughly assumed but can be justified. The twine cross section in the net is not circular. The twine is twisted and or grouped together by several filaments. Different materials can be used in different nets and this, in addition to wear and tear, will give different twines varying coarseness. There will also be some uncertainty around what effect a possible knot will have. The knot is normally not directly accounted for. Some ineraction between the twines is also likely, but it is difficult to find the amount of influence. The twine and knot interaction will also change with varying net panel angle. All this makes it not trivial to precisely quantify the drag coefficient, and the uncertainty in the coefficient. Some indication to the uncertainty can be found by comparing theoretical calculated drag and or lift coefficients with drag and or lift coefficients from experiments. This is done in tables 3.2 - 3.7. The difference between theoretical values of C_D from the catenary equation, and experimental values from Rudi et al. (1988) often came close to and over 20%. In real life applications one must also account for solidity increase due to marine growth. NS9415 (2009) demandes a 50% increase in solidity to account for this. As mentioned, Swift et al. (2006) found the solidity and drag increase, due to marine growth. On an net with original solidity $Sn = 0.121$ the increase was $400 - 670\%$(!). The corresponding increase in drag coefficient relative to a clean net was $6 - 240\%$. The organic shapes are not circular, and will also influence the drag coefficient in a significant way.

As stated previously, there is often some uncertainty associated with the solidity ratio (see section 2.1.3). The definition of Sn vary since there is no obvious way to handle the knot or lack of knot. The twine diameter can be difficult to measure precisely, and is not something the net supplier normally states. The diameter can also vary some within the net. Lien et al. (2009) recommends using a digital camera and software to determine the solidity. Considering the uncertainty with respect to both the twine diameter and what definition of Sn should be used, what choice of $Sn \pm 10\%$ seems well within the expected uncertainty.

The value of the E-modulus is taken from the suggested value from a "standard net" in the Aquastructures package ($E = 1.0 \cdot 10^9 \mathrm{MPa}$). The change is in elasticity, $\Delta_{\delta E_{net}}$, is meant to reflect a wide specter within what can be assumed by an engineer doing a mooring analysis.

Error influence on drag force, $\Delta_{F_D}[\mathrm{N}]$

U [m/s]	0.1	0.2	0.3	0.4	0.5	0.6	0.7	0.8	0.9	1.0
$\Delta_{w_{sink}} F_D$	0.0	0.4	2.0	6.0	11.9	17.8	23.4	28.3	32.8	37.0
$\Delta_{\rho_{net}} F_D$	0.0	0.0	0.0	0.1	0.1	0.4	0.5	0.7	1.0	1.2
$\Delta_{E_{net}} F_D$	0.0	0.0	0.0	0.1	0.2	0.3	0.5	0.6	0.8	1.0
$\Delta_{\delta E_{net}} F_D$	0.0	0.1	0.3	1.0	2.1	3.5	4.9	6.5	7.9	9.5
$\Delta_{C_D^{CC}} F_D$	3.9	13.6	24.4	32.0	35.3	38.2	41.1	44.6	48.5	52.4
$\Delta_{Sn} F_D$	5.7	19.5	34.7	45.3	48.2	48.0	46.3	44.1	41.0	37.6
$\Delta_{F_D^{sink}} F_D$	0.7	2.4	4.4	5.7	5.9	5.6	4.9	3.6	1.9	1.2
Δ_{F_D}	6.9	23.9	42.7	56.1	61.2	64.2	66.6	69.2	71.9	75.0
relative $\Delta_{F_D}[\%]$	36	34	31	26	22	19	17	16	16	15

Table 3.9: Error analysis of drag force, $F_D[\mathrm{N}]$. Sn = 0.19. Relative error is the total error divided by baseline drag force at relevant current velocity.

Error influence on lift force, $\Delta_{F_L}[\mathrm{N}]$

U [m/s]	0.1	0.2	0.3	0.4	0.5	0.6	0.7	0.8	0.9	1.0
$\Delta_{w_{sink}} F_L$	0.1	0.5	1.3	1.2	0.3	2.5	4.7	6.8	8.6	10.4
$\Delta_{\rho_{net}} F_L$	0.0	0.0	0.0	0.0	0.0	0.1	0.2	0.3	0.4	0.5
$\Delta_{E_{net}} F_L$	0.0	0.0	0.1	0.0	0.0	0.1	0.1	0.2	0.2	0.3
$\Delta_{\delta E_{net}} F_L$	0.0	0.1	0.2	0.2	0.1	0.5	1.1	1.8	2.4	3.1
$\Delta_{C_D^{CC}} F_L$	0.1	1.0	2.5	2.7	0.4	2.6	5.3	7.2	8.4	9.2
$\Delta_{Sn} F_L$	0.3	3.0	9.6	16.5	20.2	21.1	20.7	19.5	18.0	16.3
$\Delta_{F_D^{sink}} F_L$	0.0	0.3	1.2	2.0	2.3	2.1	1.6	0.8	0.4	2.1
Δ_{F_L}	0.3	3.2	10.1	16.9	20.3	21.5	22.0	22.0	21.8	21.7
relative $\Delta_{F_L}[\%]$	75	57	49	38	29	23	19	17	15	14

Table 3.10: Error analysis of lift force, $F_L[\mathrm{N}]$. Sn = 0.19. Absolute values. Relative error is the total error divided by baseline lift force at relevant current velocity.

Error influence on max tension, $\Delta_{T_{max}}[\mathrm{N}]$

U [m/s]	0.1	0.2	0.3	0.4	0.5	0.6	0.7	0.8	0.9	1.0
$\Delta_{w_{sink}} T_{max}$	19.9	19.4	19.0	15.8	17.2	20.2	23.9	28.0	31.9	35.6
$\Delta_{\rho_{net}} T_{max}$	2.3	2.3	2.1	2.1	1.7	1.6	1.0	0.7	0.2	0.2
$\Delta_{E_{net}} T_{max}$	0.0	0.0	0.0	0.1	0.0	0.1	0.1	0.3	0.4	0.6
$\Delta_{\delta E_{net}} T_{max}$	0.1	0.1	0.1	0.7	0.5	0.1	1.1	2.2	3.7	5.1
$\Delta_{C_D^{CC}} T_{max}$	0.1	2.1	5.9	18.4	28.0	34.5	39.7	43.9	48.2	52.0
$\Delta_{Sn} T_{max}$	0.3	2.9	8.4	24.5	33.8	38.7	40.3	39.7	38.2	35.7
$\Delta_{F_D^{sink}} T_{max}$	0.1	0.4	1.0	3.1	4.0	4.2	3.8	3.0	1.4	1.5
$\Delta_{T_{max}}$	20.0	19.9	21.7	34.7	47.3	55.8	61.5	65.6	69.4	72.6
relative $\Delta_{T_{max}}[\%]$	10	10	10	14	16	17	17	16	16	16

Table 3.11: Error analysis of max tension, $T_{max}[\mathrm{N}]$. Sn = 0.19. Absolute values. Relative error is the total error divided by baseline max tension at relevant current velocity.

Error influence on end point angle, $\Delta_\alpha[\mathrm{deg}]$

U [m/s]	0.1	0.2	0.3	0.4	0.5	0.6	0.7	0.8	0.9	1.0
$\Delta_{w_{sink}}\alpha$	0.3	1.0	1.8	2.3	2.7	2.6	2.4	2.2	2.0	1.8
$\Delta_{\rho_{net}}\alpha$	0.0	0.0	0.0	0.0	0.0	0.0	0.1	0.1	0.1	0.0
$\Delta_{E_{net}}\alpha$	0.0	0.0	0.1	0.0	0.1	0.1	0.0	0.1	0.1	0.0
$\Delta_{\delta E_{net}}\alpha$	0.0	0.2	0.3	0.4	0.5	0.5	0.5	0.5	0.4	0.5
$\Delta_{C_D^{CC}}\alpha$	0.6	1.9	3.3	4.4	4.7	4.5	4.0	3.4	2.8	2.3
$\Delta_{Sn}\alpha$	0.8	2.7	4.7	6.2	7.1	7.2	6.8	6.3	5.7	5.1
$\Delta_{F_D^{sink}}\alpha$	0.2	0.7	1.3	1.8	2.2	2.5	2.6	2.7	2.7	1.4
Δ_α	1.1	3.5	6.2	8.2	9.2	9.2	8.7	8.0	7.2	6.1
relative $\Delta_\alpha[\%]$	39	35	32	28	24	19	16	13	11	9

Table 3.12: Error analysis of end point angle, $\alpha[deg]$. Sn = 0.19. Absolute values. Relative error is the total error divided by baseline end point angle at relevant current velocity.

Overall, the relative error decreases with increasing current velocity for both drag force, lift force and end point angle. In some cases the relative error is very big for low current speeds. For aquaculture the highest current speeds will be of most importance, as design currents often are around $1.0\mathrm{m/s}$ or even higher. It is positive that the error seems to decrease and or stabilize towards a not to high level at high current speeds.

The error characteristics of maximum tension is fairly similar across all solidity ratios. Generally, the relative error increases with increasing current velocity. There seems to be a max value in the relative error around $0.3 - 0.5\mathrm{m/s}$. This peak becomes more evident at higher solidity. The peak also moves towards lower current speeds for higher solidity.

Increasing solidity resulted in only a very slight increase in the relative error on the drag force. Relative error in lift force decreases with the increasing solidity ratio, but only at quite high current velocity. At low speeds, the absolute force is very low, and the relative error increases with increasing Sn-values. The relative error on end point angle, α decreases with increasing solidity and current velocity.

Chapter 4

Results from the four methods

Many different parameters influence an aquaculture plant, and even the simplified model of a suspended single net panel used in this thesis contains several interacting parameters. Variation in current speed and variation solidity ratio should give some insight in the difference between the four methods. Four sets of simulations will be executed: Case 1, Case 2a, Case 2b and Case 2c.

The first case uses a fixed solidity ratio, and varies the speed from $0.1\mathrm{m/s}$ to $1.0\mathrm{m/s}$ with $0.1\mathrm{m/s}$ increments. The second case varies the solidity ratio from 0.10 to 0.55 with 0.05 increments. This is done for three different current speeds: $U = 0.50, 0.75, 1.00\mathrm{m/s}$. Drag and lift force on the net are logged. The lift force is closely related to the deformation of the net, as is the end point angle, α, which gives the angle between the nets original vertical position and the line from the suspension points to the end of the net, where the bottom weight act. These 3 results, F_D, F_L and α are given for every method in every case. The tension in the net was not possible to extract from the available results files from FhSim. In AquaSim this was time consuming, but possible. The results were however incoherent, and therefor generally not very helpful. The tension as a function of the net length is only given for case 1 and case 2a. Another very important parameter is the bottom weight. If large deformations is experienced, larger bottom weights should be applied. This will increase the net tension, drag force and lift force. A thorough examination of the impact the size of the bottom weight will have in different combinations of solidity ratio and current speed is certainly to be desired, but would have added a new layer of interaction and complexity, and was defined as outside the scope of this thesis. However, a brief comparison between the Løland and catenary equation methods on the impact bottom weight is given later. With hindsight, the size of the standard bottom weight, $W_{sink} = 200\mathrm{N}$ was probably a bit too low. At high solidity and current velocity the net experienced very large deformations. Still, the difference between the four methods did become clear, and this was the main goal.

4.1 Model description and input data

The governing equations for all four methods have been presented in chapter 2. All four methods uses a net length of $L = 10\mathrm{m}$, width of net $B = 1.0\mathrm{m}$ and unless otherwise explicitly stated a bottom weight of $200\mathrm{N}$.

4.1.1 Løland

The Løland method uses the solidity ratio, Sn as input in C_D and C_L, and a large number of elements, $N_{el} = 400$, to ensure sufficiently small elements. A smaller element number would likely yield just as good result. Sea water density is used, $\rho_s = 1025\mathrm{kg/m^3}$, and this methods neglects net weight and elasticity. The solution is two dimensional, taking the width, B only as a constant. Some form of strip theory must be used if it is to be expanded into 3D.

4.1.2 Catenary equation

The solution of the catenary equation uses the twine diameter, d and net mesh size, l_{st} as input values determining the solidity ratio based on this. The coefficients are dependent of Reynolds number. Number of elements is large here as well, $N_{el} = 400$. Other input values; $\rho_s = 1025\mathrm{kg/m^3}$, $g = 9.81\mathrm{m/s^2}$ and $\nu = 1.004 \cdot 10^{-6}\mathrm{m^2/s}$. This method is also two dimensional taking the width only as a constant when calculating the drag and lift coefficient. Calculation can be done with or without taking the weight and elasticity of the net into account. The baseline calculations are done without accounting for elasticity in the net, and without accounting for net weight, which corresponds to a net weight of $\rho_{net} = 1025\mathrm{kg/m^3}$. These simplifications will, according to the error analysis, not affect the results in any significant way.

4.1.3 FhSim

FhSim models in three dimensions, and finds the solution in the time domain. A simulation is run until steady state is achieved, and the end results are exported. The results are sensitive to flutter in the simulation. This was experienced when the net density was equal to the water density. The other methods uses net density equal to seawater, or simply neglects the weight of net in water in the baseline calculations. A better basis for comparison would theoretically be achieved with the same assumption here, but when this was done, the simulation was more unstable, resulting in inconsistent data. The error analysis done for the catenary equation solution shows the difference in net density will have have little impact on the overall results. It was done simulations with net density both $\rho_{net} = 1125\mathrm{kg/m^3}$ and $\rho_{net} = 1025\mathrm{kg/m^3}$. The model is divided into 32 elements of width $1.0\mathrm{m}$ and hight $0.31\mathrm{m}$. Other input values were $g = 9.81\mathrm{m/s^2}$ and kinematic viscosity $\nu = 1.004 \cdot 10^{-6}\mathrm{m^2/s}$.

4.1.4 AquaSim

AquaSim does not give the total reaction force in the bearing points, but rather the maximum tension in ropes, chains and nets. To be able to find the drag and lift forces acting on the net, the model differs slightly from the other models. In each of the two upper end point at the water surface (coordinates $(\pm 0.5, 0, 0)$) the net is hinged, free to rotate. It is also freely supported from translation in the x direction. From these points short, thin, highly inelastic ropes have been modeled a short way in the negative y and positive z direction to be able to measure drag and lift force. The model is divided vertically in 100 elements in the z-direction ($N_{el} = 100$). Only dividing in this direction should minimize any 3 dimensional buckling effects. The bottom weights are vectors, and no hydrodynamic forces act upon them. The net have a Young modules value of $1.0 \cdot 10^9\mathrm{Pa}$ as default.

Mesh size in each direction (local y and z direction), and the twine cross sectional area are used as an input value, $A_{twine} = 0.25 \cdot d^2\pi$. The model is based on summation of forces on single twines, so the

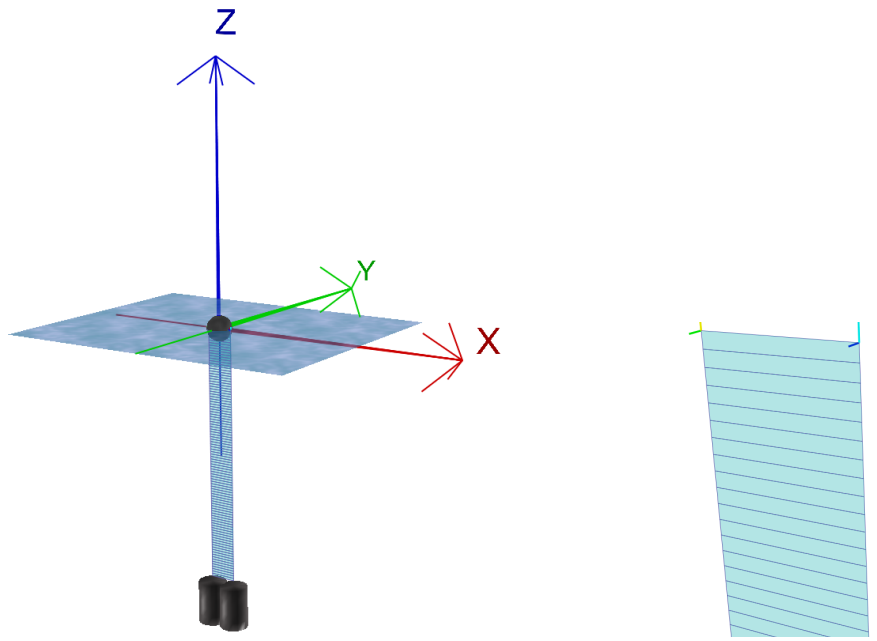

(a) (b)

Figure 4.1: The AquaSim model as shown in AquaBase. (a) with global coordinate system and indicated bottom weight. (b) gives a close up of the suspension system.

solidity ratio should not have a direct impact, but can be found in the result files after the analysis. This ratio is calculated based on the equation Løland (1991) uses [1] (see equation 2.8).

4.2 Case 1: Variation in current velocity

4.2.1 Drag force, lift force and end point angle

Lølands method used drag and lift coefficient not dependent on the current speed, but only on the solidity ratio and net panel angle. The increasing deformation translates into the drag and lift force not increasing with the square of the current speed as it would if the net was vertically for every speed. A larger bottom weight will reduce the deformation, and as a result of the increased projected area, increase the overall drag and lift force. The calculations are done with $Sn = 0.190$, from $d = 1.5\text{mm}$ and $l_{st} = 15\text{mm}$. The results are given in table 4.1.

[1] This is not given in any documentation, but every analysis done gives a solidity ratio equal to one calculated with this formula. It is not clear how a solidity increase will be handled in AquaSim, as the requirement is given as a factor on Sn, and AquaSim uses d in calculations. A 50% increase in d will give a different resulting Sn, than a direct 50% increase in Sn.

$U_\infty[\mathrm{m/s}]$	$F_D[\mathrm{N}]$	$F_L[\mathrm{N}]$	$\alpha[deg]$
0.1	13.6	0.2	1.9
0.2	53.8	3.3	7.7
0.3	116.6	14.9	16.8
0.4	191.3	36.4	27.6
0.5	266.7	62.2	38.2
0.6	337.8	86.6	47.4
0.7	404.4	107.6	54.8
0.8	467.7	125.0	60.8
0.9	528.9	139.3	65.5
1.0	589.2	150.9	69.3

Table 4.1: Calculated drag force, lift force and end point angle at $Sn = 0.190$ from the Løland method

The drag coefficient in the catenary equation method is dependent of the Reynolds number. Low Reynolds number from low current speed and or small twine diameter gives a higher drag coefficient. Compared to the results from the Løland method, the drag and lift forces are higher at low current speed. Results for drag force, lift force and end point angle are given in table 4.2.

$U_\infty[\mathrm{m/s}]$	$F_D[\mathrm{N}]$	$F_L[\mathrm{N}]$	$\alpha[deg]$
0.1	19.4	0.5	2.8
0.2	69.3	6.3	10.1
0.3	129.6	22.1	19.7
0.4	191.4	45.2	29.4
0.5	258.1	71.3	39.0
0.6	314.8	95.3	47.4
0.7	362.6	115.8	54.4
0.8	403.1	133.0	60.1
0.9	437.5	147.2	64.7
1.0	466.7	159.0	68.4

Table 4.2: Calculated drag force, lift force and end point angle at $Sn = 0.190$ from the catenary equation method

As mentioned, there was some flutter in the FhSim results from the zero net weight simulations. The results shows the lift force is generally relative low, and not increasing as much as one would expect for the highest current speeds. The increase in drag force looks consistent, but generally lower then the previous methods up to about $U = 0.8\mathrm{m/s}$, where it "passes" the catenary equation. The net deformations looks a bit low compared to the previous. In table 4.3 the results for drag force, lift force and end point angle are given for both sets ($\rho_{net} = 1125\mathrm{kg/m^3}$ and $\rho_{net} = 1025\mathrm{kg/m^3}$).

U_∞[m/s]	F_D[N]	F_L[N]	$\alpha[deg]$	F_D^0[N]	F_L^0[N]	$\alpha^0[deg]$
0.1	9.4	−0.4	1.3	13.1	−4.6	1.8
0.2	37.4	1.1	5.4	35.7	26.7	6.1
0.3	81.7	6.9	11.9	90.3	−1.8	12.4
0.4	136.5	18.0	19.9	123.4	39.0	20.4
0.5	194.7	31.1	28.8	216.5	19.0	28.8
0.6	258.0	44.7	36.4	286.0	33.0	37.0
0.7	328.1	55.9	43.8	307.5	66.6	44.4
0.8	403.4	63.9	49.9	417.5	58.3	49.8
0.9	487.3	69.9	55.1	496.2	67.5	55.1
1.0	580.4	74.1	59.4	587.5	72.7	59.0

Table 4.3: Calculated drag force, lift force and net angle at $Sn = 0.190$ from FhSim. Superscripted 0 indicates results from model with neutral buoyant net.

Since AquaSim lacked the possibility to give reaction forces in the bearing points, and the model had to be "tweaked" to be able to give the drag and lift force, some extra uncertainty is attached to the results. Both the drag force, lift force and end point angle are within the range from the other methods for relative low current speeds. At higher current speed the drag force deviate. The lift force and end point angle is similar to the results seen in FhSim. See the results in table 4.4.

U_∞[m/s]	F_D[N]	F_L[N]	$\alpha[deg]$
0.1	12.0	0.0	1.8
0.2	47.7	1.8	7.0
0.3	101.4	12.1	15.1
0.4	164.9	27.3	24.8
0.5	234.2	42.2	34.3
0.6	308.8	50.7	42.7
0.7	395.4	58.6	49.5
0.8	494.0	64.7	55.2
0.9	604.3	67.2	59.8
1.0	727.7	70.3	63.6

Table 4.4: Calculated drag force, lift force and net angle at $Sn = 0.190$ from AquaSim.

4.2.2 Tension

Increasing tension over the net length comes from tangential forces acting on the net as it deforms. The change of tension in the net can give some insight into how the net deforms or how much tangential force is incorporated in the different models. As mentioned before, the FhSim result file did not give any information about tension, and AquaSim gave some incoherent data. As expected the maximum tension is at the upper end of the net. At low current speeds the net is very little deformed, resulting in almost no tangential force, especially at the lower parts. The tension comes then almost exclusively from the bottom weight, $T_0 = 200$N. The catenary solution gives the highest tension at low speeds, but at higher current speeds the Løland method "catches up", At $U = 1.00\mathrm{m/s}$ the maximum tension from Lølands method is over 25% higher then the one from the catenary solution. See figure 4.2

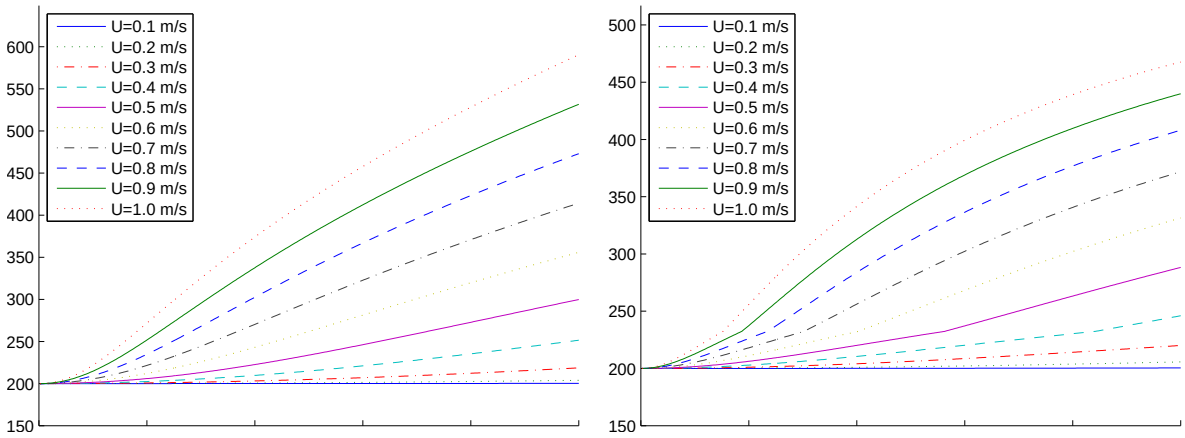

(a) Løland

(b) Catenary equation

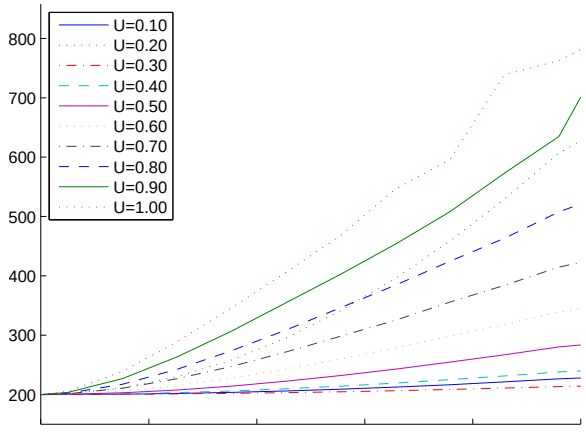

(c) AquaSim

Figure 4.2: Set nr 1: Tension in the net for different current speed. For high resolution see appendix C.

4.2.3 Bottom weight

Due to the need of limiting the time used, the influence of changing the bottom weight was not a primary concern in this thesis. For the Løland and catenary equation method the implementation was easy and fast. A comparison is only done for two methods, and only in this first case. These two gives very similar results for the end point angle. Results are given in table 4.5 and figure 4.3. Looking closer at the influence the bottom weight will have on drag and lift force at high current speed the Løland method will yield much higher drag force at low bottom weights. The end point angles are very similar, so the projected areas are equal. The lift forces are very close to each other. It is likely the lower catenary equation results are more accurate as the Løland method over predicts the drag coefficients at large net deformations.

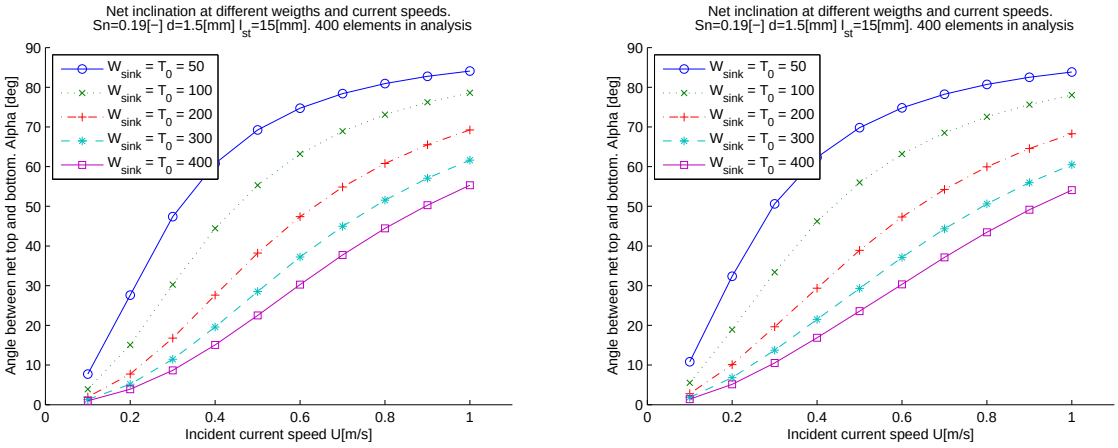

(a) Løland

(b) Catenary equation

Figure 4.3: Set nr 1: End pont angle, α as a function of current speed for different bottom weights. $Sn = 0.190$. For high resolution see appendix C.

W_{sink}	Loland			Cat Eq		
[N]	α	F_D[N]	F_L[N]	α	F_D[N]	F_L[N]
50	84.1	320.8	48.5	83.9	141.7	51.0
100	78.6	423.5	89.8	78.0	268.6	95.1
200	69.3	589.2	150.9	68.3	466.7	159.0
300	61.6	716.8	191.3	60.5	614.1	200.4
400	55.3	817.9	217.9	54.1	727.7	227.3

Table 4.5: Drag and lift force for different bottom weights (W_{sink}) at current speed $U = 1.0\text{m/s}$. $Sn = 0.190$.

4.3 Case 2: Variation in Sn for 3 current speeds

The second major parameter to investigate the influence of changing, is the solidity ratio, Sn. This is done for three current speeds, $U = 0.50\text{m/s}$ (case 2a), $U = 0.75\text{m/s}$ (case 2b) and $U = 1.00\text{m/s}$ (case 2c). Relative high current speeds are the dimensioning factor on aquaculture plants, and in the variation of current speed the differences in the methods became evident at current speed from 0.5m/s and upwards.

High Sn-values may come from marine growth, like hydroids. The required 50% increase in Sn when calculating, as described in NS9415 (2009) means one can reach values of $Sn = 0.55$ from using the solidity ratio definition from Løland (equation 2.8), with $l_{st} = 12\text{mm}$ and $d = 2.1\text{mm}$. Realistically the hydroids will only increase the solidity ratio by increasing d, not l_{st}. This will mean an increase in d from 2.1mm to 3.1mm.

In this case the variation in solidity are done by keeping the twine diameter fixed, and varying the mesh size. The net characteristics can therefore be unrealistic compared to what one might find in the industry, but since the twine diameter affects the methods in different ways it was considered best to keep it fixed.

The end point angle, α gives a value to the expected volume reduction, and the increased solidity ratio. A large end point angle will also demand a large average value on the different net panel angles, θ_i, which will increase the actual deformed solidity ratio (same amount of net twines on a smaller area). Most of this increase will come at the top of the net, near the surface (see figure 5.2 - 5.5), so the actual "perceived" solidity ratio will be lower then the average.

4.3.1 Drag force, lift force and end point angle

For all three current speeds the Løland-method (see table 4.6) seems to plateau when approaching higher solidity. Using the zero moment requirement, the lift force can not exceed the bottom weight, so this is a logical plateau. After passing $Sn = 0.35$, the drag force only increases some small percentage. As mentioned before, the equation calculating C_D and C_L are based on experiments within the solidity ratio $Sn = 0.130 - 0.317$. Outside this area, the coefficient are based on an extrapolated curve without data backing it. Drag force is generally proportional with projected area. The projected area of the circumscribed net (width times the distance down to the bottom weight) is indicated by the end point angle. As the stepwise increase in this angle lessens, so does the increase in drag force.

Method: Løllands equations

	$U = 0.5\text{m/s}$			$U = 0.75\text{m/s}$			$U = 1.0\text{m/s}$		
$Sn[-]$	F_D[N]	F_L[N]	$\alpha[deg]$	F_D[N]	F_L[N]	$\alpha[deg]$	F_D[N]	F_L[N]	$\alpha[deg]$
0.10	116.2	10.7	16.4	240.4	36.0	32.4	382.2	64.2	46.6
0.15	203.2	36.2	28.9	365.4	83.6	48.7	522.5	119.4	61.8
0.20	280.9	68.7	40.4	450.5	123.8	59.9	601.2	156.9	70.7
0.25	341.8	98.9	49.7	504.3	152.4	67.4	641.7	178.8	76.2
0.30	387.6	123.7	56.9	537.3	171.3	72.5	660.8	190.2	79.6
0.35	421.0	142.8	62.3	556.5	183.0	76.0	668.6	195.7	81.9
0.40	445.5	157.1	66.5	567.6	190.1	78.5	671.4	198.2	83.5
0.45	463.2	167.6	69.7	573.9	194.2	80.3	672.3	199.2	84.6
0.50	476.6	175.3	72.1	577.7	196.6	81.7	672.7	199.7	85.3
0.55	486.5	180.8	74.0	580.4	197.9	82.7	673.4	199.9	85.9

Table 4.6: Calculated drag force, lift force and net angle at $U = 0.5, 0.75, 1.0\text{m/s}$ using the Løland method

The solution of the catenary equation (see table 4.7) is sensitive to the twine diameter since this influences the Reynolds number which again determines the drag coefficient of a 2D circular cylinder. In the relevant Reynolds number range ($log_{10}(Re) \approx 2.0 - 3.0$) the drag coefficient decreases with increasing Reynolds number. Since the twine diameter is kept unrealistically low the basis for the results might be lower then expected at a very high solidity ratio. Generally, the catenary equation method behaves very

similar as Løland's method for all three current speeds when it comes to drag and lift force. In contrast to the Løland method, the catenary solution does not have a zero moment requirement on the elements as a part of the solution procedure. The lift force is then dependent on geometry and lift coefficients. In cases of extreme deformation the lift force in then calculated as larger then the maximum value of 200N. This is actually congruent with the coefficients in chapter 3.1, where the lift coefficients from the catenary equations behave very similar as those from Løland, but are consistently just a bit larger. Lift force, can be calculated in a slightly simplified method. If equation 2.29b ($C_L(\theta) = C_L(\pi/4)\sin 2\theta$) is used for every value of θ, the lift coefficients on net panels with smaller inclination than $\theta = 45°$ becomes slightly smaller. In the cases investigated here, this would yield results even closer to the values from Løland.

Method: Solving the catenary equation

	$U = 0.5\mathrm{m/s}$			$U = 0.75\mathrm{m/s}$			$U = 1.0\mathrm{m/s}$		
$Sn[-]$	F_D[N]	F_L[N]	$\alpha[deg]$	F_D[N]	F_L[N]	$\alpha[deg]$	F_D[N]	F_L[N]	$\alpha[deg]$
0.10	138.3	24.8	21.1	243.6	64.2	36.7	337.9	102.3	50.3
0.15	204.2	49.6	31.1	330.8	101.0	49.5	421.1	138.5	62.0
0.20	270.6	76.7	40.8	395.6	130.1	58.9	476.8	163.3	69.6
0.25	327.7	102.2	49.4	445.3	152.8	66.0	515.1	180.4	74.8
0.30	376.5	125.3	56.8	482.6	170.7	71.4	538.7	191.9	78.7
0.35	418.5	145.8	63.1	511.3	184.1	75.7	554.2	199.2	81.5
0.40	453.3	163.6	68.6	529.0	193.7	79.1	559.3	203.6	83.7
0.45	480.3	178.2	73.1	538.9	200.0	81.8	560.3	206.4	85.3
0.50	499.7	189.8	77.1	543.7	203.9	83.9	562.7	208.5	86.6
0.55	508.0	197.7	80.3	541.5	206.4	85.6	557.9	211.6	87.6

Table 4.7: Calculated drag force, lift force and net angle at $U = 0.5, 0.75, 1.00\mathrm{m/s}$ using the catenary solution method.

For FhSim (see table 4.8), it was assumed the relative high current speed ($U \geq 0.50\mathrm{m/s}$) would effectively eliminate the flutter experienced in case 1 with net density $\rho_{net} = 1025\mathrm{kg/m^3}$. This was not the case, and a net density of $\rho_{net} = 1125\mathrm{kg/m^3}$ had to be used. This yielded much more smooth sets of results. At case 2a, $U = 0.50\mathrm{m/s}$, the drag force quickly becomes lower then expected with increasing solidity. At $Sn = 0.20$, it is very close to the value from set 1 at $U = 0.50\mathrm{m/s}$ (and $Sn = 0.19$), which is to be expected, and helps verify the simulations. At the last two steps of the solidity increase, the drag force, lift force and end point angle actually decreases. For higher current speed ($U = 0.75\mathrm{m/s}$ and $U = 1.00\mathrm{m/s}$) the drag force is much higher, and probably more realistic. Still, the drag force decreases after $Sn = 0.45$. The lift force is consistently low, and does not come close to the 200N maximum lift force limit. This is also reflected in the net deformation, as expressed by the end point angle. α is consistently quite low. α also decreases slightly after $Sn = 0.45$. From the validation in chapter 3.1, low drag and lift force was expected, but the decrease was not expected. Why the drag force, lift force and end point angle goes down with increasing solidity is not easy to explain. FhSim does not account for the "speed up" of the water flow as it passes through the net. Neglecting this effect would lead an increasingly larger loss of potential speed with increasing solidity, since the water velocity in reality increases with increasing solidity ($U = U_\infty \cos\theta/(1 - Sn)$). This effect should not, however lead to a drop in drag and lift force. A possible support in the explanation can be as following. If the lift and drag coefficients decreases more with the increasing solidity (and current speed) than what can be countered by the increase in Sn, the forces would decrease.

Method: FhSim

	$U = 0.5\text{m/s}$			$U = 0.75\text{m/s}$			$U = 1.0\text{m/s}$		
$Sn[-]$	F_D[N]	F_L[N]	$\alpha[deg]$	F_D[N]	F_L[N]	$\alpha[deg]$	F_D[N]	F_L[N]	$\alpha[deg]$
0.10	124.6	15.5	18.1	238.9	41.9	34.2	370.7	61.1	47.6
0.15	167.9	25.7	24.5	314.0	54.2	42.5	493.7	70.1	55.5
0.20	202.2	33.8	29.3	376.6	61.3	47.9	600.4	74.7	60.1
0.25	229.8	39.4	32.9	427.7	66.0	51.6	691.7	77.3	63.2
0.30	250.9	43.5	35.6	469.9	68.6	54.1	764.8	79.0	65.1
0.35	266.1	46.1	37.3	499.8	70.4	55.7	818.2	80.0	66.4
0.40	274.4	47.8	38.3	519.2	70.9	56.5	848.6	80.8	67.1
0.45	276.8	47.8	38.5	523.3	71.0	56.7	857.0	80.7	67.2
0.50	269.4	47.6	37.8	510.6	70.5	56.1	837.0	80.2	66.8
0.55	254.1	45.3	36.1	482.3	68.4	54.6	783.3	79.2	65.5

Table 4.8: Calculated drag force, lift force and net angle at $U = 0.5, 0.75, 1.00\text{m/s}$ using FhSim with $\rho_{net} = 1125\text{kg/m}^3$.

The drag force in the AquaSim increases massively with both solidity and current speed. The lift force does not increase in the same manner. The lift force also seems to reach a plateau at the same place for both set 2b (0.75m/s) and set 2c (1.00m/s). Naturally, when the end point angle, α approaches $90°$, the growth of F_L lessens. This is not reflected in the drag force, which continues to grow with almost equal speed. The projected area (as indicated by α) does not seem to influence the drag force. At high values of α, the lift force was expected to be closer to the maximum value of 200N. The value of α is actually very close to the value of F_L for both set 1, set2a, set2b and set 2c, indicating a linear dependency between lift force and net deformation. See table 4.9.

Method: AquaSim

	$U = 0.5\text{m/s}$			$U = 0.75\text{m/s}$			$U = 1.0\text{m/s}$		
$Sn[-]$	F_D[N]	F_L[N]	$\alpha[deg]$	F_D[N]	F_L[N]	$\alpha[deg]$	F_D[N]	F_L[N]	$\alpha[deg]$
0.10	137.7	20.6	20.7	260.7	46.2	37.5	408.8	55.6	50.6
0.15	192.9	33.7	28.8	360.7	54.2	47.1	583.2	62.4	59.1
0.20	244.1	43.9	35.5	464.3	64.2	53.7	764.1	71.2	64.6
0.25	292.1	49.2	41.0	570.6	71.7	58.6	952.6	77.4	68.7
0.30	343.8	57.5	45.5	680.8	75.6	62.6	1129.1	54.7	70.3
0.35	397.9	66.6	49.1	777.6	54.0	64.3	1325.6	55.5	72.5
0.40	450.2	68.3	53.0	907.2	76.5	67.9	1544.3	77.1	75.3
0.45	503.7	71.1	55.8	1025.7	76.0	69.9	1755.3	79.2	76.6
0.50	546.6	54.1	57.2	1151.3	78.8	71.6	1980.8	78.2	77.8
0.55	604.8	54.7	59.4	1282.2	79.6	73.0	2212.0	79.6	78.8

Table 4.9: Calculated drag force, lift force and net angle at $U = 0.5, 0.75, 1.00\text{m/s}$ using AquaSim.

Since the AquaSim drag force looks very high compared to the other methods, the drag coefficients should be compared to those from the validation. It is difficult to compare the results directly, since the net angles changing continually. The end point angle, α will be used as an approximation to the net plane inclination in chapter 3.1, with which the drag coefficients will be compared. Still, since many parameters must be in accordance, very few instances can be checked in this way.

The AquaSim α-value in table 4.9 for $Sn = 0.15$, and $U = 1.0\text{m/s}$, $\alpha^{AS} = 59.1$ is close to the catenary

equation α-value in table 4.7 for $Sn = 0.15$, and $U = 1.0\mathrm{m/s}$, $\alpha^{CE} = 62.0$. Where AS denotes the AquaSim values, and CE the catenary equation value. The drag force and lift force is given as:

$F_D^{CE} = 421.1\mathrm{N}$ and $F_L^{CE} = 138.5\mathrm{N}$

$F_D^{AS} = 583.2\mathrm{N}$ and $F_L^{AS} = 62.4\mathrm{N}$

The parameters above are close to one set of values in table 3.5, with $Sn = 0.144$ and $U = 0.966\mathrm{m/s}$. From table 3.5 the following values are found:

$C_D^{CE} = 0.09$ and $C_L^{CE} = 0.04$

$C_D^{AS} = 0.11$ and $C_L^{AS} = 0.02$

If the difference in the drag and lift coefficients is the reason for the deviation, change of the coefficients should yield a more congruent answer.

$(F_D^{AS}/C_D^{AS})C_D^{CE} = 477\mathrm{N} \approx F_D^{CE}$

$(F_D^{CE}/C_D^{CE})C_D^{AS} = 514\mathrm{N} \approx F_D^{AS}$

$(F_L^{AS}/C_L^{AS})C_L^{CE} = 125\mathrm{N} \approx F_L^{CE}$

$(F_L^{CE}/C_L^{CE})C_D^{AS} = 68\mathrm{N} \approx F_L^{AS}$

The difference in force can be attributed to the rounded values of C_D and C_L.

4.3.2 Tension

The tension is plotted along the length of the net for different solidity ratios at $U = 0.50\mathrm{m/s}$. See figure 4.4. The tension in Løland's method increases almost linear with the length of the net. Max tension for the highest solidity is just under $500\mathrm{N}$. Tension from the catenary equation grows in a more convex shape along the length of the net. Max tension from the catenary solution is just over $500\mathrm{N}$. The AquaSim tension distribution looks wrong. The overall shape and size is probably correct, as it is close to the other tension distribution plots, but some values looks as obvious errors. One error source can be the method used to find and store these values, as it was manual, and time consuming.

Tension plots from set 2b and set 2c is not presented, as the AquaSim tension plot continued to give less than helpful information.

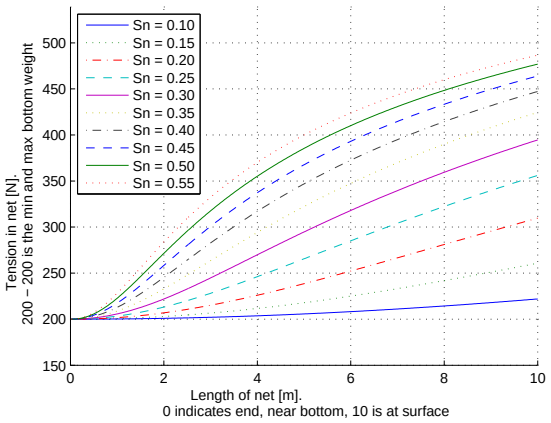

(a) Løland

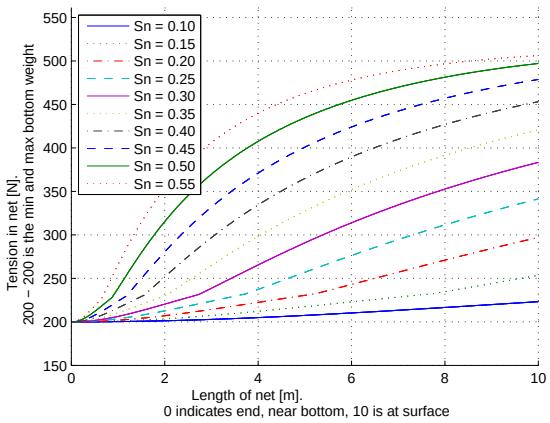

(b) Catenary equation

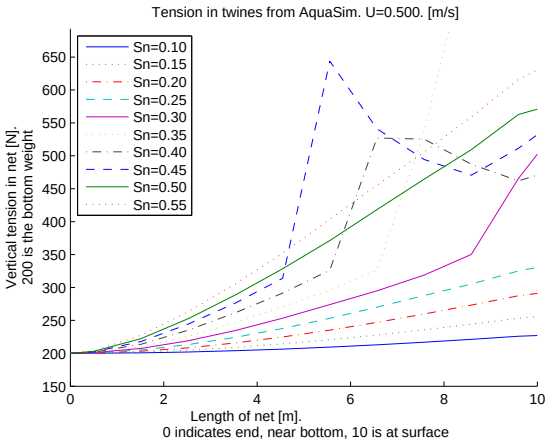

(c) AquaSim

Figure 4.4: Set nr 2a: Tension in the net for different solidity. For high resolution see appendix C.

Chapter 5

Comparison of results from different methods

Analysis of complex structures, such as a net, is based on describing the nature through a set of assumptions and simplifications. Many such assumptions are valid within a certain range. Since the four methods presented here to some degree are based on different assumptions small deviations in the results are always expected. Large variations indicates that some assumptions are wrong ,or some simplifications are no longer valid outside a given range.

In real life, increasing solidity ratio will direct a portion of the flow around the net. This physical phenomena is not considered in the theoretical approaches. The experiments done by Rudi et al. (1988), used a frame and relative low solidity ratio ($Sn \leq 0.317$). This should be enough to keep the effect outside Løvlands formula. The four methods are in this way assumed comparable.

The drag force is arguably the most important result parameter with respect to aquaculture application. Drag force on the net due to current and wave velocity in addition to the inertia force caused by wave motion, will in a fish farm give the dimensioning tension forces in the mooring cables. Under prediction of drag force can cause insufficiently dimensioned fish farms. Over predictions is safer, but can be a competitive disadvantage for a commercial company. Using software based on different assumptions, competitors can offer cheaper solutions and still document the procedure properly. Comparison between numerical measured data, and three accredited companies using different analysis software showed large variation in the force predictions (Olsen & Volent, 2009).

5.1 Drag and lift force

Plot over drag force and lift force for all four methods and all four cases are given in figure 5.1. The first set (with variation of current speed and $Sn = 0.19$) seems, from the information in the subsequent sets, to have been done within the solidity ratio range which would yield small variations between the methods. Generally the difference in drag force seems to be smallest at low speeds and low solidity ratios. This is logical since low speed and, or low solidity will lower the total force, making any difference in drag coefficient less pronounced. As the current speed and solidity increases the AquaSim method stands out with very large drag force values. The drag force for AquaSim seems to increase approximately quadratically in set 1, and linearly in the set 2 plots. Set 1 varies current speed, U, and the drag force is dependent on U^2. Set 2 varies solidity, Sn which drag force is linearly dependent on.

This increase characteristics of AquaSim's drag force is close to what one would expect with very large bottom weight, i.e. not accounting for the change in the projected area as the net deforms.

AquaSim uses summation over single twines to find the drag and lift force. As the net panel angle, θ increases, the drag force on the (originally) vertical threads will subside. The horizontal threads will have the same orientation relative to the current direction independent of the net panel angle. Since AquaSim does not calculate any shielding effect, the horizontal threads will, in fact be independent of the projected area. The drag force on the originally vertical threads will change, and this helps to limit the effect.

The difference in set 2b and 2c may seem extreme. The huge difference between AquaSim and the rest of the methods might be considered somewhat irrelevant as the net is very deformed and most of it is very close to the water surface. In an aquaculture application the bottom weight must be increased, and the deformation lessened to avoid deformation to such a degree. The difference between AquaSim drag force and the methods would most likely be less severe, but still significant if this was done.

In a global system with net of high solidity and large current speeds there will be large sections of the net with similar orientation relative to the current flow as the very deformed panel in set 2c. If sufficiently large bottom weights prohibits the net from deforming to a large degree, side sections and bottom panel will still have the same relative orientation to the current flow as the almost horizontally deformed net panel. The width on these section will usually be smaller than the depth, so the effect will not be quite as big as a vertical net panel perpendicular to the flow direction deformed close to horizontal orientation, but a large influence on the drag force in a complete cage or system nevertheless. Some sort of shielding effect from threads upstream should therefore be considered if a smaller drag force is desired. Since AquaSim can give the mesh size (l_{st}) in both local x and z direction, an "ad hoc" adjustment, may be to manipulate the z distance on the threads. The solidity ratio can be kept, but the effect of drag force contributions independent of the projected are can be minimized.

The lift force seems follow one of two "paths". Lølands method and the solution of the catenary equations gives very similar results for the lift force in virtually every configuration. Only some minor difference in set 1 for the lowest current speeds, and some in set 2 at low solidity. The FhSim and AquaSim methods are also consistently very close. There is some "flutter" resulting in less smooth graphs in some of the results, but generally, the lift force from both methods are very similar for every result. As mentioned before, with high current speed and solidity ratio, portions of the net becomes almost horizontal, and close to the water surface. The catenary equation and Lølands method then gives lift force on the net very close to the maximum lift value (equal to the bottom weight). Due to high values for lift coefficients, the catenary equation gives the lift force to be a bit above the maximum value. This is not the case for FhSim and AquaSim. The relative low lift force is more consistent from FhSim, than from AquaSim since the low lift force in FhSim is in combination with a relative low end point angle, α. AquaSim does not have as high α-value as the Løland and catenary method, but still higher than FhSim.

Both the lift force and the deformation of the net is similar for the Løland method and the catenary solution. The actual averaged lift coefficients must consequently be similar in spite of using very different methods to find them. Lølands formula for the lift coefficient (equation 2.5) is based on curve fitting to the experiments by Rudi et al. (1988). Assuming valid results and good curve fitting, it would imply the lift coefficient found from the catenary solution is close to experimental values. This will only be a valid statement within the parameter range the experiments was conducted, and more experiments should nevertheless be done to be able to fully verify the model.

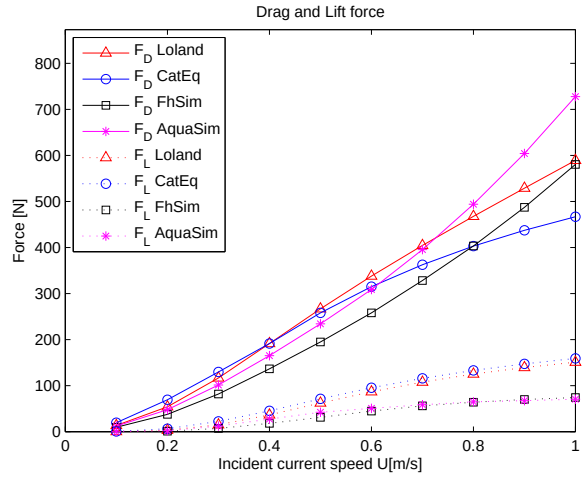

(a) Set 1. $Sn = 0.19$

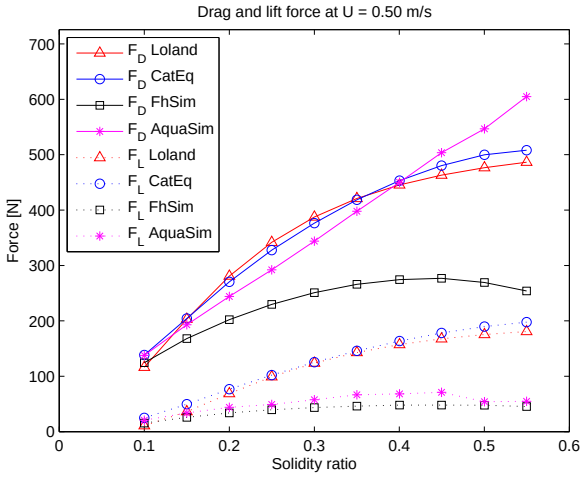

(b) Set 2a. $U = 0.50\mathrm{m/s}$

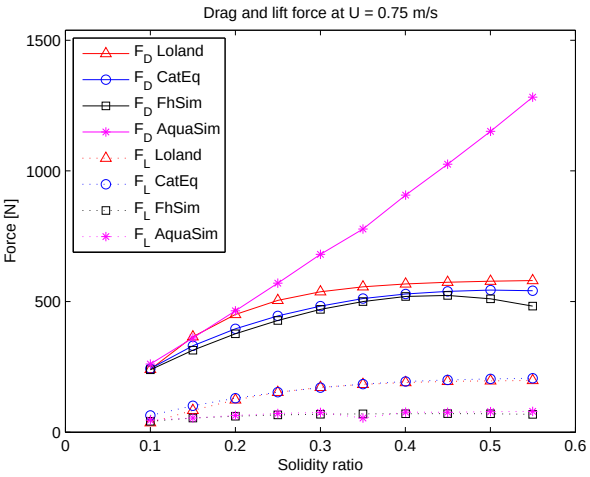

(c) Set 2b. $U = 0.75\mathrm{m/s}$

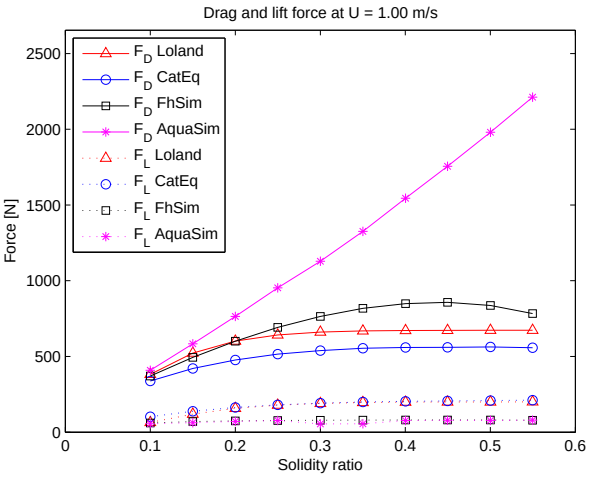

(d) Set 2c. $U = 1.00\mathrm{m/s}$

Figure 5.1: Drag and Lift forces on the net in. All four methods. Four different cases. For high resolution images, see appendix C.

5.2 Net shape

Deformation decrease the available volume in a cage. If the volume is reduced to much, this may have a negative effect on the fish. Smaller volume will mean less available water depth, and can cause problems in waves, as the fish normally will settle at deeper water to avoid the wave motion.

The end point angle can not alone give the total projected area of the deformed net, but will give a good indication of how much the net has been deformed, which in a global system may be related to the volume reduction. α-values for every method and both cases are given in tables 5.1 and 5.2.

U_∞	Case 1, $\alpha[deg]$			
[m/s]	LO	CE	FH	AS
0.1	1.9	2.8	1.3	1.8
0.2	7.7	10.1	5.4	7.0
0.3	16.8	19.7	11.9	15.1
0.4	27.6	29.4	19.9	24.8
0.5	38.2	39.0	28.8	34.3
0.6	47.4	47.4	36.4	42.7
0.7	54.8	54.4	43.8	49.5
0.8	60.8	60.1	49.9	55.2
0.9	65.5	64.7	55.1	59.8
1.0	69.3	68.4	59.4	63.6

Table 5.1: End point angle, case 1

Sn	Case 2a, $\alpha[deg]$				Case 2b, $\alpha[deg]$				Case 2c, $\alpha[deg]$			
[−]	LO	CE	FH	AS	LO	CE	FH	AS	LO	CE	FH	AS
0.10	16.4	21.1	18.1	20.7	32.4	36.7	34.2	37.5	46.6	50.3	47.6	50.6
0.15	28.9	31.1	24.5	28.8	48.7	49.5	42.5	47.1	61.8	62.0	55.5	59.1
0.20	40.4	40.8	29.3	35.5	59.9	58.9	47.9	53.7	70.7	69.6	60.1	64.6
0.25	49.7	49.4	32.9	41.0	67.4	66.0	51.6	58.6	76.2	74.8	63.2	68.7
0.30	56.9	56.8	35.6	45.5	72.5	71.4	54.1	62.6	79.6	78.7	65.1	70.3
0.35	62.3	63.1	37.3	49.1	76.0	75.7	55.7	64.3	81.9	81.5	66.4	72.5
0.40	66.5	68.6	38.3	53.0	78.5	79.1	56.5	67.9	83.5	83.7	67.1	75.3
0.45	69.7	73.1	38.5	55.8	80.3	81.8	56.7	69.9	84.6	85.3	67.2	76.6
0.50	72.1	77.1	37.8	57.2	81.7	83.9	56.1	71.6	85.3	86.6	66.8	77.8
0.55	74.0	80.3	36.1	59.4	82.7	85.6	54.6	73.0	85.9	87.6	65.5	78.8

Table 5.2: End point angle, case 2

The net deformation according to the Løland method and the catenary equation method are very congruent. Lølands formula were based on experiments, and especially within the solidity ratio range the experiments were done ($Sn = 0.130 - 0.317$), the results are close. At high current speed and solidity ratio both nets experiences large deformation, with portions of the net almost horizontal and parallel with the surface. As mentioned before, these extreme cases might not be the most directly applicable to aquaculture and fish farms since extreme net deformation is unwanted. However, being consistent they provide useful insight in force distribution on a complete cage, where large portions of the net is more or less tangential to the flow direction.

Considering α and the deformation plots in figure 5.2 - 5.5, the deformation according to AquaSim is less then from Løland's and the catenary equation methods for relative high current speeds and or

solidity ratios. Based on the coefficients in section 3.1 and the actual lift force on the net from AquaSim, the lift coefficients in AquaSim are likely unrealistically low for high solidity and current speeds. If the lift coefficients in AquaSim are increased, the lift force will increase, and the deformation will likely also increase. The resulting smaller projected net area will likely reduce the drag force to some degree. Since large deformation is undesirable, this increase can lead to the need for larger bottom weights. This will naturally undo the possible drag force reduction. The increase in the lift coefficient should only be done if some plausible argument to the under prediction of deformation is presented. One such argument could be if volume reduction on net cages seldom or never are a problem in analysis, and this is backed by data from actual locations. The limited dependency of the projected area, will limit the efficiency of this approach.

The net deformation according to FhSim does not look logical. In set 2, the lift force and end point angle are very little influenced by the increase in solidity beyond about $Sn = 0.25$. The drag force continues to increase a bit, but lift force and end point angle quickly plateaus long before the logical limit of max lift force (200N) and deformation. The same "plateau level" in lift force is reached for both set 2b and 2c. These obervations are backed up by the consistently low C_D and C_L values for net inclinations less then 60° in chapter 3.1.

The deformed net shape figures contains informations from six of the ten plots for each of the cases 1, 2a, 2b and 2c. This was done to keep the report manageable and fairly well arranged. See appendix C for high resolution, electronic copies for every speed and solidity.

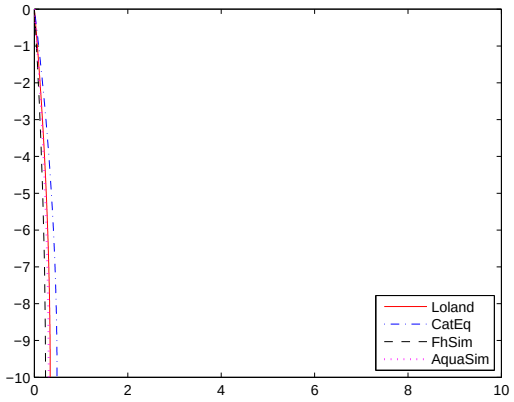

(a) $U = 0.1\mathrm{m/s}$

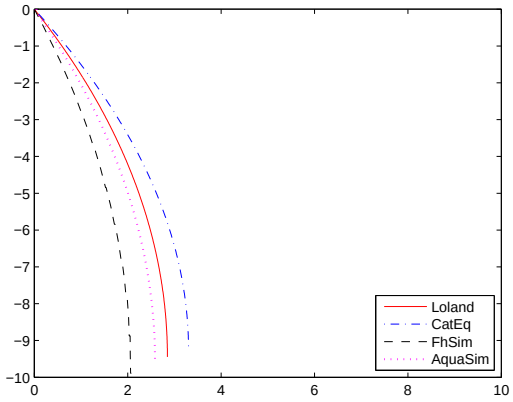

(b) $U = 0.3\mathrm{m/s}$

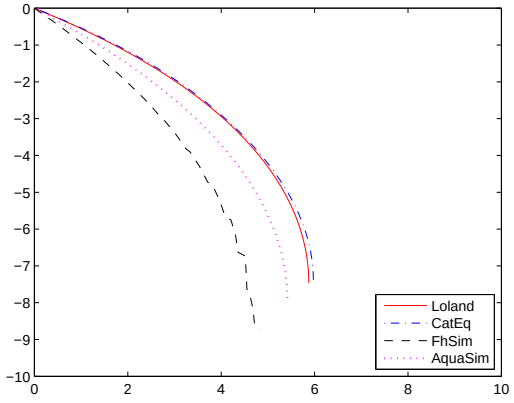

(c) $U = 0.5\mathrm{m/s}$

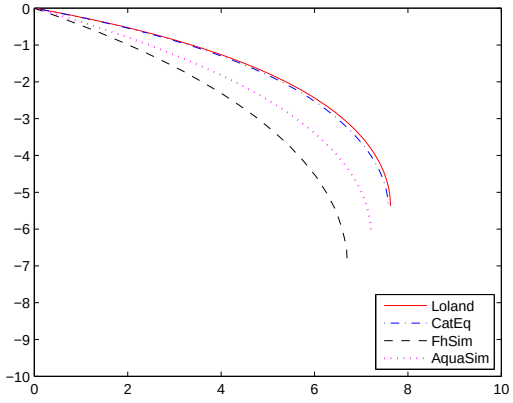

(d) $U = 0.7\mathrm{m/s}$

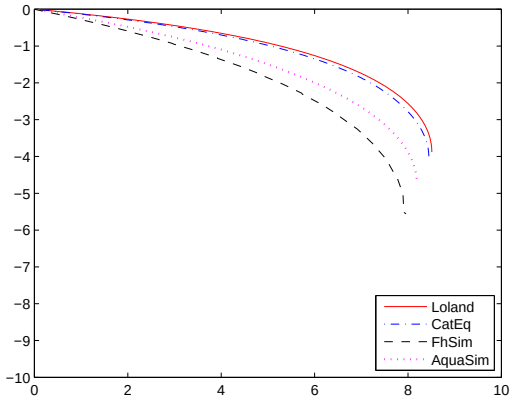

(e) $U = 0.9\mathrm{m/s}$

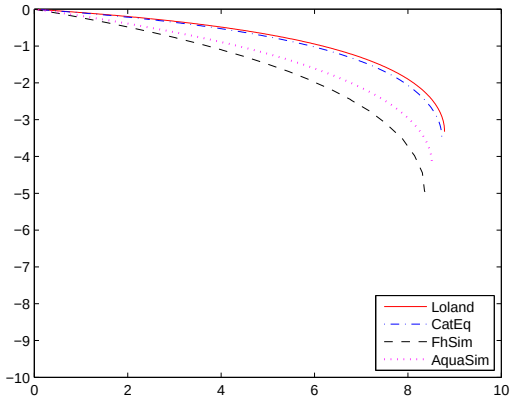

(f) $U = 1.0\mathrm{m/s}$

Figure 5.2: Net shape in current. $Sn = 0.19$

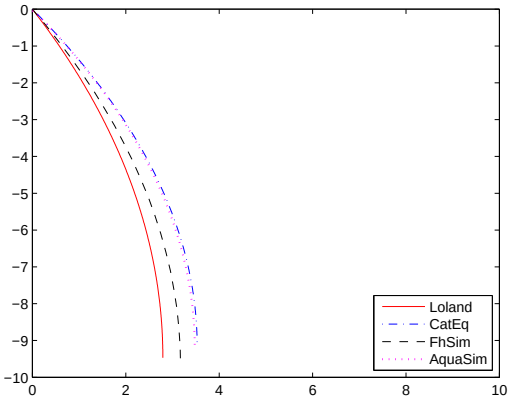

(a) $Sn = 0.10$

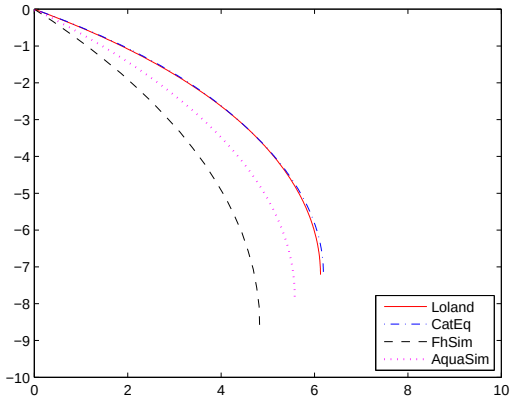

(b) $Sn = 0.20$

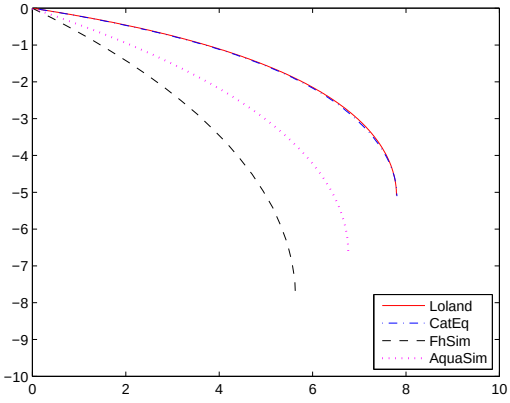

(c) $Sn = 0.30$

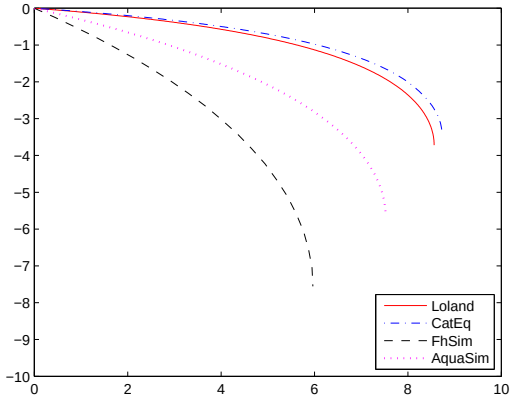

(d) $Sn = 0.40$

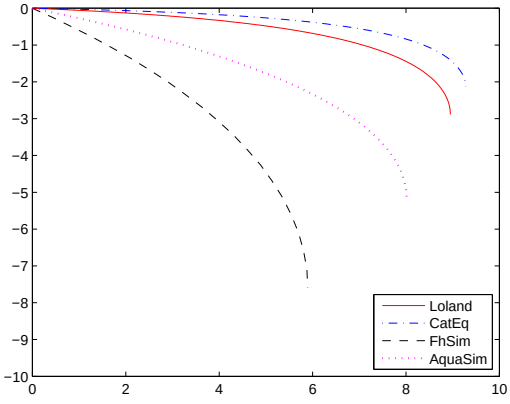

(e) $Sn = 0.50$

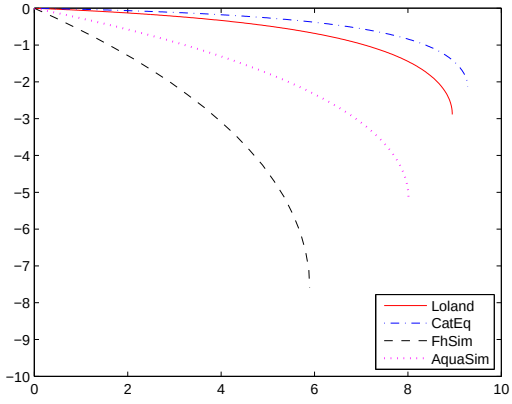

(f) $Sn = 0.55$

Figure 5.3: Net shape in current. $U = 0.50\mathrm{m/s}$

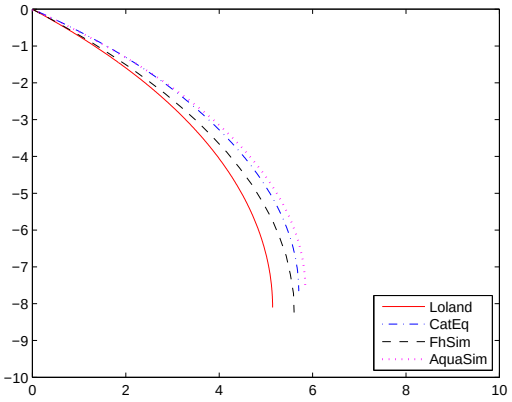

(a) $Sn = 0.10$

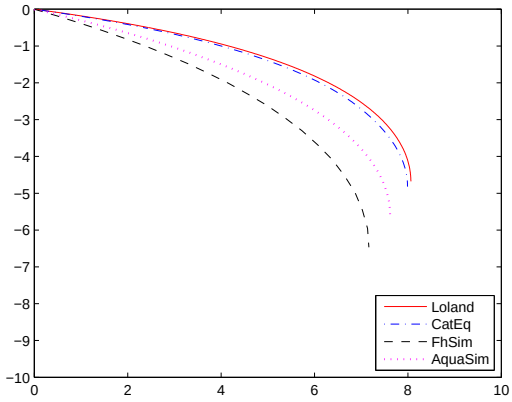

(b) $Sn = 0.20$

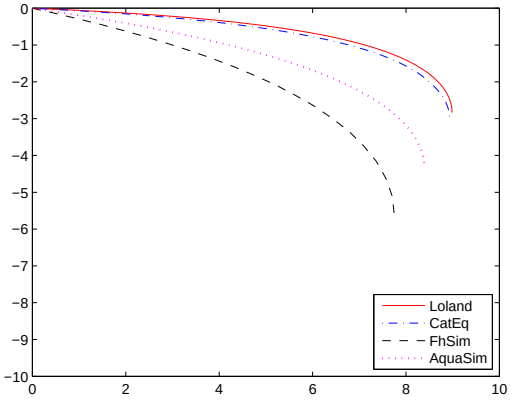

(c) $Sn = 0.30$

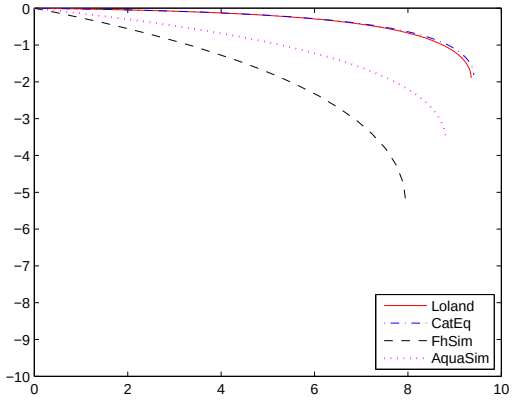

(d) $Sn = 0.40$

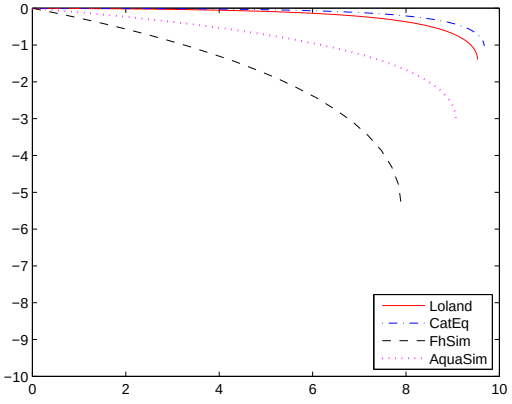

(e) $Sn = 0.50$

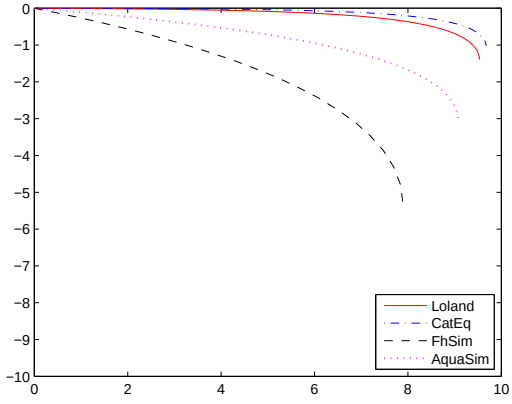

(f) $Sn = 0.55$

Figure 5.4: Net shape in current. $U = 0.75\mathrm{m/s}$

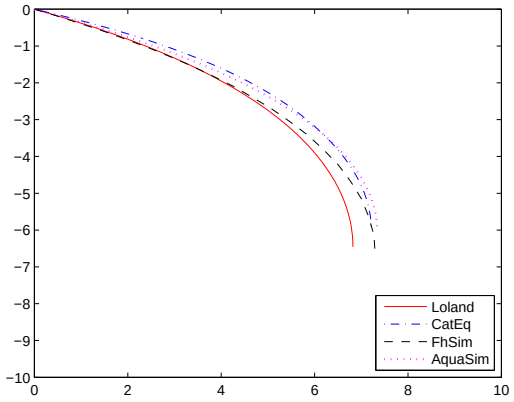

(a) $Sn = 0.10$

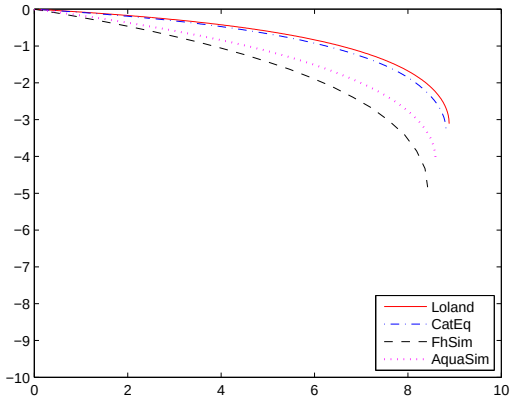

(b) $Sn = 0.20$

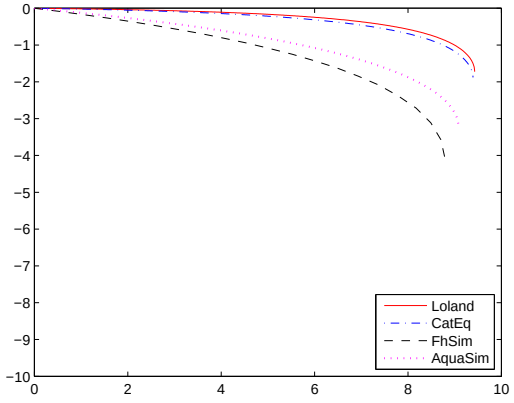

(c) $Sn = 0.30$

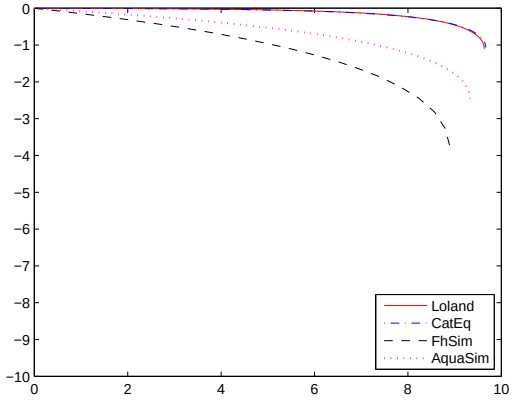

(d) $Sn = 0.40$

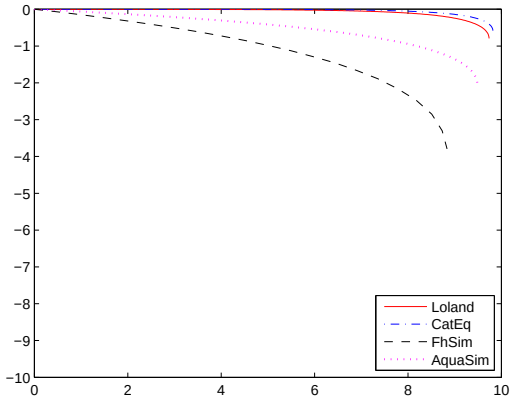

(e) $Sn = 0.50$

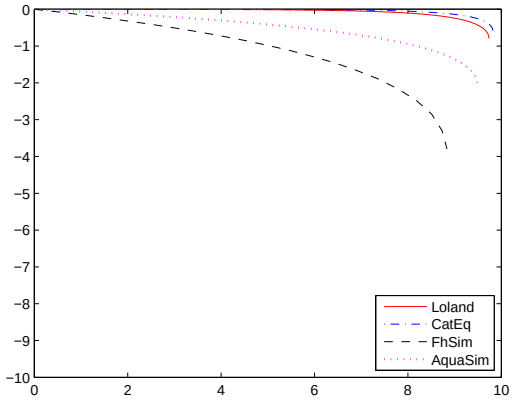

(f) $Sn = 0.55$

Figure 5.5: Net shape in current. $U = 1.00\mathrm{m/s}$

Chapter 6

Conclusion

6.1 Recommendations

In this thesis it has been shown there can be large differences between methods for calculation of forces on and deformation of nets in uniform current.

Since only the drag and lift coefficients are compared to experimental data within a limited range of solidity and current velocity, some of the results will have limited formal validity. However, the results will likely be a good indication on principle trends.

The drag coefficients as expressed for FhSim are believed to be too low for net panels with inclination less then $60°$. The lift coefficients are also low, especially for net panels with angles above $45°$. The resulting low lift force will lead to a relative small deformation on the net. The large projected area will increase the drag force at higher current velocity and solidity ratio.

The drag coefficient formula from Løland contains a constant independent of solidity and net panel inclination. This value (0.04) is likely to large, and should be reduced or neglected.

The drag force according to AquaSim is very likely significantly overpredicted at relative high current velocity and solidity, i.e. at large deformation. The drag force is based on contributions from single twines. The horizontal twines in the mesh will not be influenced by the net panel angle. Some sort of shielding effect from threads upstream should therefore be considered if a smaller drag force is desired. Since AquaSim can give the mesh size (l_{st}) in local x and z direction, an "ad hoc" adjustment, can be to manipulate the z distance on the threads. The solidity ratio can be kept, but the effect of drag force contributions independent of the projected area may be minimized.

The lift coefficients from AquaSim are likely low for high solidity and current velocity. At lower solidity and current values, the coefficients are likely too high. If the relevant lift coefficients are increased, the deformation of the net will increase. This will result in smaller projected net area, and thus reduce the drag force to some degree. Since large deformations are also undesirable, the increase in lift coefficient values may lead to the need for larger bottom weights. This will naturally undo the possible drag force reduction. The increase in the lift coefficient should only be done if some plausible argument to the underestimation of deformation is presented. One such argument could be if volume reduction on net cages seldom or never is a problem in analysis. This should be backed by data from actual locations. The limited dependency of the projected area, will limit the efficiency of this approach.

FhSim and AquaSim use a very simplified method for determining the value of the lift coefficients. Both methods also perform poorly when the lift coefficients are compared to experimental data. Since the lift

force will influence the drag force by way of projected area, the importance of lift force should not be underestimated in aquaculture applications. This also shows the importance of good and documented simplifications and assumptions in all instances.

The input data for the catenary equation should be fairly good to avoid large errors. At current speeds above $0.6\mathrm{m/s}$, drag force, lift force and end point angle will all give a error of 16% or less. The relative error of maximim tension increases, in contrast to the drag, lift and end point angle, with increasing current velocity. Considering the uncertainty in the input parameters, the total error is not unacceptable.

The drag and lift coefficients from Løland and the catenary equations shows consistently the best congruency with experimental data. Outside the range of the experimental data, Løland and the catenary equation continues to give similar results for both drag force, lift force and net deformation. To further validate these methods, comparisons with other experiments should be done.

The solution of the catenary equation seems to be a viable method for aquaculture applications. The lift coefficients from the catenary equation are likely a bit too high, but this is only visible at extreme deformations.

There is definitively flow speed dependency in the drag and lift coefficients, which should be taken into consideration. However, these influences will be largest at low current speed. The dimensioning current speeds for aquaculture applications will be quite high. Taking a practical approach, other factors will likely have a more significant impact on the calculations.

6.2 Further work

The work with analysis of fish farms is very complex, and much work remains before a complete picture is obtained.

There are some gaps more obvious than others related to the problems presented in this thesis. Calculations are only done for incoming current normal to the undisturbed net. The catenary equation method should be expanded to three dimensions.

The calculated net deformations are, for the most part, not compared with actual deformation from experiments. Since the parameters are so interdependent, it should be verified that all important parameters are correct for the same set up.

The error analysis is only done for the catenary equation. It is not known is the error sensitivity of the other methods are similar to that of the catenary equation.

As new and updated versions of FhSim and or AquaSim are released, the work obviously becomes outdated with respect to those methods.

With hindsight, the standard bottom weight of $200\mathrm{N}$ was probably small. For aquaculture applications, the current variation could go from $0.5\mathrm{m/s}$ to $1.5\mathrm{m/s}$. The deformations should be kept within the acceptable range for fish farming. This should be noted as areas of possible improvement for similar assignments.

Some theory for flow reduction with higher solidity should also be developed. As the solidity increase, a larger part of the flow will be directed outside the cage. This is not considered in any of the theoretical approaches.

References

Aarsnes, J. V., & Løland, G. (1990). Current forces on cage, net deflection. *Engineering for Offshote Fish Farming*, (pp. 137–152).

Ådnanes, H. (2010). Current measurment and forces on aquaculture plants. TMR4520 Specialization Project in Marine Hydrodynamics.

Almås, K. A. (2010). 1 million tonn laks i 2010. Presentation at Tekmar 2010, Trondheim.

Berstad, A. J. (2011). e-mail. dated 27.04.2011.

Berstad, A. J., & Tronstad, H. (2005). Response from current and regular/irregular waves on a typical polyethylene fish farm. Tech. rep., Aquastructures.

E24.no (2010). Enorme fortjenester i lakseoppdrett. NTB 03.06.2010 (via www.e24.no).

Edvardsen, T. (2010). Kan norsk oppdrettsindustri bidra til europas rolle som global matprodusent? Presentation at Tekmar 2010, Trondheim.

Ersdal, S., & Faltinsen, O. (2006). Normal forces on cylinders in near-axial flow. *Journal of Fluids and Structures*, *22*(8), 1057 – 1077.

Faltinsen, O. M. (1990). *Sea Loads on Ships and Offshore Structures*. Cambridge University Press.

Faltinsen, O. M. (2011). Wave response fish farms with circular floater (preliminary).

Føre, M. (2011). Documentation of FhSim NetCage. Relvante equations and prosedure; some documentation of FhSim NetCage.

Fredheim, A., Heide, M., & Jensen, Ø. (2010). Sluttrapport - utvikling av sikre oppdrettsanlegg. Tech. rep., SINTEF Fiskeri og havbruk.

Kristiansen, D. (2010). *Wave induced effects on floaters of aquaculture plants*. Ph.D. thesis, Norwegian University og Science and Technology.

Lader, P. F., & Enerhaug, B. (2005). Experimental investigation of forces and geometry of a net cage in uniform flow. *IEEE Journal of Oceanic Engineering*, *30*(1), 79–84.

Lader, P. F., Olsen, A., Jensen, A., Sveen, J. K., Fredheim, A., & Enerhaug, B. (2007). Experimental investigation of interaction between waves and net structures - damping mechanism. *Aquacultural Engineering*, *37*, 100–114.

Lien, E., Moe, H., & Maroni, K. (2009). Hvordan bestemme soliditet og trådtykkelse til notlin. Notat, SINTEF Fiskeri og havbruk and FHL and FHF.

Løland, G. (1991). *Current Force On and Flow Through Fish Farms*. Ph.D. thesis, The Norwegian Institute of Technology.

NS9415 (2009). *Norsk Standard 9415:2009 - Flytende oppdrettsanlegg Krav til lokalitetsundersøkelse, risikoanalyse, utforming, dimensjonering, utførelse og drift*. Standard Norge, www.standard.no.

Olsen, A., & Volent, Z. (2009). Utvikling av sikre oppdrettsanlegg fase 1. Sammenligning av måledata og numerisk analyse for lokalitet Farmansøy. Tech. Rep. SFH80 A096051, SINTEF Fiskeri og havbruk.

Rudi, H., Aarsnes, J. V., & Dahle, L. A. (1988). Environmental forces on a floating cage system, mooring considerations. *Rugby : Institution of Chemical Engineers*, *I: Aquaculture engineering technologies for the future.*, S. 97–122 : ill.

Schubauer, G., Klebanoff, P., & Spangenberg, W. (1950). Aerodynamic characteristics of damping screens. *NACA, National Advisory Committee for Aeronautics*, *NACA NT 2001*, 39.

Swift, M. R., Fredriksson, D. W., Unrein, A., Fullerton, B., Patursson, O., & Baldwin, K. (2006). Drag force acting on biofouled net panels. *Aquacultural Engineering*, *35*, 292–299.

Tronstad, H. (2000). *Nonlinear hydroelastic analysis and design of cable net structures like fishing gear based on the finite element method*. Ph.D. thesis, NTNU Trondheim.

Vikestad, K., & Lien, E. (2005). A non-dimensional weight-velocity parameter for estimating drag force and net deformation of gravity fish cages. vol. 2, (pp. 905–909).

Appendix A

Error sources

A.1 Error calculation for Sn = 0.20

U [m/s]	0.1	0.2	0.3	0.4	0.5	0.6	0.7	0.8	0.9	1.0
$\Delta_{w_{sink}} F_D$	0.0	0.4	2.3	7.0	13.2	19.3	24.9	29.7	34.5	38.7
$\Delta_{\rho_{net}} F_D$	0.0	0.0	0.1	0.1	0.2	0.4	0.6	0.9	1.2	1.4
$\Delta_{E_{net}} F_D$	0.0	0.0	0.0	0.1	0.2	0.3	0.5	0.6	1.1	1.4
$\Delta_{\delta E_{net}} F_D$	0.0	0.0	0.3	1.0	2.3	3.6	5.0	6.4	8.1	9.7
$\Delta_{C_D^{CC}} F_D$	4.2	14.6	25.6	32.7	35.9	38.8	42.0	45.7	49.8	53.6
$\Delta_{Sn} F_D$	6.2	21.2	37.1	46.9	49.2	48.6	46.4	43.7	40.4	36.7
$\Delta_{F_D^{sink}} F_D$	0.7	2.4	4.3	5.3	5.4	5.0	4.3	3.2	1.2	1.5
Δ_{F_D}	7.5	25.9	45.3	57.9	62.6	65.4	67.7	70.2	73.3	76.3
relative Δ_{F_D}[%]	36	34	30	26	21	19	17	16	16	15

Table A.1: Error analysis of drag force, F_D[N]. Sn = 0.20. Absolute values. Relative error is the total error divided by baseline drag force at relevant current speed

U [m/s]	0.1	0.2	0.3	0.4	0.5	0.6	0.7	0.8	0.9	1.0
$\Delta_{w_{sink}} F_L$	0.0	0.6	1.3	1.1	0.7	3.0	5.3	7.4	9.4	11.1
$\Delta_{\rho_{net}} F_L$	0.0	0.0	0.0	0.0	0.1	0.1	0.2	0.4	0.4	0.6
$\Delta_{E_{net}} F_L$	0.0	0.0	0.0	0.1	0.1	0.0	0.1	0.2	0.3	0.4
$\Delta_{\delta E_{net}} F_L$	0.0	0.1	0.2	0.1	0.2	0.7	1.3	1.8	2.5	3.2
$\Delta_{C_D^{CC}} F_L$	0.1	1.1	2.6	2.5	0.2	3.3	5.9	7.7	8.8	9.4
$\Delta_{Sn} F_L$	0.3	3.6	10.8	17.8	21.0	21.6	20.8	19.4	17.8	16.0
$\Delta_{F_D^{sink}} F_L$	0.0	0.4	1.2	2.0	2.1	1.9	1.4	0.7	0.2	2.3
Δ_{F_L}	0.3	3.8	11.3	18.1	21.1	22.1	22.3	22.2	22.1	22.0
relative Δ_{F_L}[%]	60	59	48	37	28	22	19	16	15	14

Table A.2: Error analysis of lift force, F_L[N]. Sn = 0.20. Absolute values.

U [m/s]	0.1	0.2	0.3	0.4	0.5	0.6	0.7	0.8	0.9	1.0
$\Delta_{w_{sink}} T_{max}$	19.9	19.5	18.9	15.9	17.6	21.0	25.1	29.3	33.1	36.7
$\Delta_{\rho_{net}} T_{max}$	2.4	2.3	2.3	2.1	1.7	1.3	0.9	0.5	0.0	0.4
$\Delta_{E_{net}} T_{max}$	0.0	0.0	0.1	0.1	0.0	0.0	0.2	0.3	0.1	0.1
$\Delta_{\delta E_{net}} T_{max}$	0.0	0.0	0.2	0.6	0.5	0.2	1.3	2.7	3.9	5.3
$\Delta_{C_D^{CC}} T_{max}$	0.2	2.4	6.3	20.2	29.6	35.9	40.9	45.4	49.6	54.0
$\Delta_{Sn} T_{max}$	0.3	3.4	9.2	26.9	35.8	39.8	41.0	40.0	38.0	35.0
$\Delta_{F_D^{sink}} T_{max}$	0.1	0.3	1.1	3.1	4.0	4.1	3.4	2.3	1.3	2.1
$\Delta_{T_{max}}$	20.0	20.1	22.1	37.4	49.9	57.7	63.2	67.3	70.8	74.3
relative $\Delta_{T_{max}}$[%]	10	10	10	15	17	17	17	16	16	16

Table A.3: Error analysis of max tension, T_{max}[N]. Sn = 0.20. Absolute values.

U [m/s]	0.1	0.2	0.3	0.4	0.5	0.6	0.7	0.8	0.9	1.0
$\Delta_{w_{sink}} \alpha$	0.3	1.2	1.8	2.5	2.6	2.5	2.4	2.1	1.9	1.7
$\Delta_{\rho_{net}} \alpha$	0.0	0.0	0.0	0.0	0.0	0.1	0.1	0.1	0.0	0.0
$\Delta_{E_{net}} \alpha$	0.0	0.0	0.0	0.1	0.0	0.0	0.1	0.0	0.0	0.0
$\Delta_{\delta E_{net}} \alpha$	0.1	0.2	0.3	0.4	0.5	0.5	0.4	0.4	0.5	0.4
$\Delta_{C_D^{CC}} \alpha$	0.6	2.0	3.5	4.5	4.7	4.4	3.8	3.2	2.6	2.2
$\Delta_{Sn} \alpha$	0.9	3.0	5.0	6.5	7.4	7.2	6.8	6.1	5.6	5.0
$\Delta_{F_D^{sink}} \alpha$	0.2	0.7	1.2	1.8	2.1	2.3	2.5	2.4	2.5	1.3
Δ_{α}	1.1	3.9	6.5	8.5	9.4	9.1	8.5	7.6	6.9	5.9
relative Δ_{α}[%]	37	36	31	27	23	18	15	12	10	8

Table A.4: Error analysis of end point angle, $\alpha[deg]$. Sn = 0.20. Absolute values.

A.2 Error calculation for Sn = 0.30

U [m/s]	0.1	0.2	0.3	0.4	0.5	0.6	0.7	0.8	0.9	1.0
$\Delta_{w_{sink}} F_D$	0.1	2.0	8.8	17.8	25.5	32.3	37.8	42.7	47.3	50.6
$\Delta_{\rho_{net}} F_D$	0.0	0.0	0.1	0.5	0.9	1.5	2.1	2.8	3.4	4.0
$\Delta_{E_{net}} F_D$	0.0	0.1	0.1	0.2	0.3	0.5	0.7	0.7	0.9	1.0
$\Delta_{\delta E_{net}} F_D$	0.0	0.2	0.9	2.1	3.4	4.7	5.8	7.1	9.0	9.6
$\Delta_{C_D^{CC}} F_D$	8.0	24.2	33.7	37.6	41.9	46.8	52.1	57.5	62.2	66.8
$\Delta_{Sn} F_D$	14.6	43.1	58.4	58.5	54.5	48.6	42.7	36.2	29.4	22.8
$\Delta_{F_D^{sink}} F_D$	0.7	2.0	2.9	2.8	2.4	1.6	0.7	0.3	0.9	4.3
Δ_{F_D}	16.7	49.5	68.1	71.9	73.4	75.0	77.5	80.6	84.1	87.6
relative Δ_{F_D}[%]	41	36	28	22	18	17	16	16	16	16

Table A.5: Error analysis of drag force, F_D[N]. Sn = 0.30. Absolute values.

U [m/s]	0.1	0.2	0.3	0.4	0.5	0.6	0.7	0.8	0.9	1.0
$\Delta_{w_{sink}} F_L$	0.2	1.3	0.7	2.5	5.8	8.8	11.1	13.2	15.0	16.30
$\Delta_{\rho_{net}} F_L$	0.0	0.0	0.0	0.1	0.4	0.7	0.9	1.2	1.5	1.70
$\Delta_{E_{net}} F_L$	0.0	0.1	0.0	0.1	0.1	0.2	0.2	0.3	0.3	0.30
$\Delta_{\delta E_{net}} F_L$	0.1	0.2	0.1	0.4	0.9	1.5	2.0	2.6	3.2	3.60
$\Delta_{C_D^{CC}} F_L$	0.3	2.5	1.8	2.6	6.3	8.5	9.6	9.8	9.7	9.10
$\Delta_{Sn} F_L$	1.3	12.1	23.9	27.0	25.7	22.8	19.5	16.2	12.9	9.90
$\Delta_{F_D^{sink}} F_L$	0.1	0.6	1.1	1.2	0.9	0.4	0.2	0.1	0.7	3.50
Δ_{F_L}	1.4	12.4	24.0	27.3	27.1	25.9	24.5	23.3	22.3	21.8
relative $\Delta_{F_L}[\%]$	78	61	42	29	22	18	15	13	12	12

Table A.6: Error analysis of lift force, $F_L[\mathrm{N}]$. Sn = 0.30. Absolute values.

U [m/s]	0.1	0.2	0.3	0.4	0.5	0.6	0.7	0.8	0.9	1.0
$\Delta_{w_{sink}} T_{max}$	19.8	19.0	16.2	19.9	25.5	30.9	36.6	41.2	44.5	48.1
$\Delta_{\rho_{net}} T_{max}$	3.7	3.5	3.1	2.2	1.4	0.5	0.5	1.3	2.2	3.0
$\Delta_{E_{net}} T_{max}$	0.0	0.0	0.0	0.1	0.2	0.2	0.4	0.5	0.7	0.8
$\Delta_{\delta E_{net}} T_{max}$	0.1	0.1	0.5	0.0	1.0	2.0	3.5	4.8	5.2	7.1
$\Delta_{C_D^{CC}} T_{max}$	0.7	5.5	23.3	33.9	40.7	46.6	52.1	57.3	61.7	67.1
$\Delta_{Sn} T_{max}$	1.3	9.8	36.1	46.2	47.7	45.3	40.2	34.0	28.0	22.4
$\Delta_{F_D^{sink}} T_{max}$	0.1	0.4	1.8	2.2	2.0	1.5	0.4	0.3	0.2	4.2
$\Delta_{T_{max}}$	20.2	22.4	46.1	60.7	67.7	72.0	75.4	78.5	81.3	86.0
relative $\Delta_{T_{max}}[\%]$	10	10	17	19	18	17	16	16	16	16

Table A.7: Error analysis of max tension, $T_{max}[\mathrm{N}]$. Sn = 0.30. Absolute values.

U [m/s]	0.1	0.2	0.3	0.4	0.5	0.6	0.7	0.8	0.9	1.0
$\Delta_{w_{sink}} \alpha$	0.6	1.8	2.5	2.6	2.4	2.0	1.7	1.4	1.3	1.0
$\Delta_{\rho_{net}} \alpha$	0.0	0.0	0.1	0.0	0.0	0.1	0.0	0.1	0.1	0.1
$\Delta_{E_{net}} \alpha$	0.0	0.1	0.0	0.0	0.0	0.0	0.0	0.0	0.0	0.0
$\Delta_{\delta E_{net}} \alpha$	0.1	0.1	0.2	0.3	0.3	0.3	0.3	0.2	0.3	0.2
$\Delta_{C_D^{CC}} \alpha$	1.2	3.2	4.7	4.5	3.7	2.9	2.2	1.6	1.3	1.0
$\Delta_{Sn} \alpha$	2.1	5.9	8.5	9.0	8.2	7.2	6.2	5.3	4.6	4.0
$\Delta_{F_D^{sink}} \alpha$	0.2	0.7	1.0	1.2	1.3	1.3	1.3	1.3	1.3	0.6
Δ_{α}	2.5	7.0	10.1	10.5	9.4	8.1	6.9	5.9	5.1	4.3
relative $\Delta_{\alpha}[\%]$	43	36	30	22	17	13	10	8	7	5

Table A.8: Error analysis of end point angle, $\alpha[deg]$. Sn = 0.30. Absolute values.

A.3 Error calculation for Sn = 0.40

U [m/s]	0.1	0.2	0.3	0.4	0.5	0.6	0.7	0.8	0.9	1.0
$\Delta_{w_{sink}} F_D$	0.3	6.6	18.7	28.7	36.8	43.5	48.6	51.8	54.7	56.1
$\Delta_{\rho_{net}} F_D$	0.0	0.2	0.7	1.6	2.8	4.0	5.1	6.1	7.2	8.0
$\Delta_{E_{net}} F_D$	0.0	0.0	0.2	0.3	0.4	0.5	0.6	0.8	0.9	0.9
$\Delta_{\delta E_{net}} F_D$	0.0	0.5	1.6	3.0	4.4	5.7	6.9	7.4	8.1	8.6
$\Delta_{C_D^{CC}} F_D$	13.7	32.1	37.7	43.4	50.3	56.6	62.9	67.5	71.5	74.2
$\Delta_{Sn} F_D$	31.3	70.1	70.2	60.8	49.7	38.3	27.6	18.1	11.1	5.9
$\Delta_{F_D^{sink}} F_D$	0.7	1.6	1.6	1.3	0.7	0.1	0.3	1.0	1.7	5.2
Δ_{F_D}	34.2	77.4	81.9	80.1	79.9	81.3	84.6	87.5	91.4	94.1
relative Δ_{F_D}[%]	48	35	24	19	17	16	16	16	16	16

Table A.9: Error analysis of drag force, F_D[N]. Sn = 0.40. Absolute values.

U [m/s]	0.1	0.2	0.3	0.4	0.5	0.6	0.7	0.8	0.9	1.0
$\Delta_{w_{sink}} F_L$	0.5	1.2	3.0	7.4	11.0	13.9	16.0	17.3	18.4	19.0
$\Delta_{\rho_{net}} F_L$	0.0	0.0	0.2	0.7	1.3	1.8	2.3	2.8	3.2	3.5
$\Delta_{E_{net}} F_L$	0.0	0.0	0.1	0.0	0.1	0.2	0.3	0.3	0.4	0.4
$\Delta_{\delta E_{net}} F_L$	0.0	0.1	0.3	0.9	1.5	2.1	2.5	2.9	3.1	3.3
$\Delta_{C_D^{CC}} F_L$	1.0	2.6	3.2	7.7	9.6	10.1	9.5	8.9	8.2	7.7
$\Delta_{Sn} F_L$	5.2	27.9	34.4	30.7	25.0	18.9	13.5	8.8	5.6	3.3
$\Delta_{F_D^{sink}} F_L$	0.1	0.6	0.7	0.6	0.2	0.0	0.3	0.6	1.0	4.0
Δ_{F_L}	5.3	28.1	34.7	32.5	29.0	25.7	23.2	21.7	21.4	21.7
relative Δ_{F_L}[%]	91	59	35	24	18	15	12	11	11	11

Table A.10: Error analysis of lift force, F_L[N]. Sn = 0.40. Absolute values.

U [m/s]	0.1	0.2	0.3	0.4	0.5	0.6	0.7	0.8	0.9	1.0
$\Delta_{w_{sink}} T_{max}$	19.5	15.7	20.4	28.0	35.2	40.8	45.3	50.4	52.2	55.5
$\Delta_{\rho_{net}} T_{max}$	5.1	4.4	3.0	1.3	0.4	2.1	3.6	4.9	6.1	7.1
$\Delta_{E_{net}} T_{max}$	0.0	0.0	0.0	0.1	0.3	0.4	0.5	0.6	0.7	0.8
$\Delta_{\delta E_{net}} T_{max}$	0.0	0.3	0.1	1.0	1.9	2.9	3.7	5.6	6.3	6.8
$\Delta_{C_D^{CC}} T_{max}$	1.8	18.8	34.1	42.8	49.7	56.4	61.7	67.1	71.3	73.1
$\Delta_{Sn} T_{max}$	4.1	37.8	56.0	54.7	46.7	36.5	26.2	17.4	9.1	3.0
$\Delta_{F_D^{sink}} T_{max}$	0.1	0.9	1.3	1.2	0.6	0.1	0.2	0.8	1.4	5.7
$\Delta_{T_{max}}$	20.6	45.3	68.7	74.9	76.8	78.7	81.1	86.0	89.3	92.5
relative $\Delta_{T_{max}}$[%]	10	18	21	19	17	16	16	16	16	17

Table A.11: Error analysis of max tension, T_{max}[N]. Sn = 0.40. Absolute values.

U [m/s]	0.1	0.2	0.3	0.4	0.5	0.6	0.7	0.8	0.9	1.0
$\Delta_{w_{sink}}\alpha$	1.1	2.4	2.7	2.2	1.8	1.5	1.2	0.9	0.7	0.6
$\Delta_{\rho_{net}}\alpha$	0.0	0.0	0.1	0.1	0.1	0.1	0.1	0.1	0.1	0.0
$\Delta_{E_{net}}\alpha$	0.0	0.0	0.0	0.0	0.1	0.0	0.1	0.0	0.0	0.0
$\Delta_{\delta E_{net}}\alpha$	0.1	0.2	0.2	0.2	0.2	0.2	0.2	0.1	0.1	0.1
$\Delta_{C_D^{CC}}\alpha$	1.9	4.5	4.5	3.3	2.3	1.7	1.2	0.9	0.6	0.5
$\Delta_{Sn}\alpha$	4.4	9.9	11.2	9.7	8.0	6.5	5.4	4.4	3.7	3.1
$\Delta_{F_D^{sink}}\alpha$	0.2	0.5	0.7	0.7	0.8	0.7	0.7	0.7	0.6	0.4
Δ_α	4.9	11.11	2.4	10.5	8.6	6.9	5.7	4.6	3.9	3.2
relative $\Delta_\alpha[\%]$	48	37	5	17	13	9	7	6	5	4

Table A.12: Error analysis of end point angle, $\alpha[deg]$. Sn = 0.40. Absolute values.

Appendix B

Matlab

B.1 main.m

```
%%%%%%%%%%%%%%%%%%%%%%%%%%%%%%%%%%%%%%%%%%%%%%%%%%%%%%%%%%%%%%%%%%%%%%%%%%%%%%%
%
% MAIN
%
% Calculate forces in and deformation of a 2D net panel (with width)
% Uses the solution of the catenary equation
%
% Part of Hakon Adnanes Master Thesis.
%
%%%%%%%%%%%%%%%%%%%%%%%%%%%%%%%%%%%%%%%%%%%%%%%%%%%%%%%%%%%%%%%%%%%%%%%%%%%%%%%

%% INPUT and CONSTANTS
clc;
clear;

%% Static input
rhos = 1025;     % density of seawater [kg/m^3]
g = 9.81;        % gravity [kg/s^2]
nu = 1.004e-6;   % kinematic viscocity at 20 deg C [m^2/s]
Nel = 400;       % number of elements to be used in analysis

L = 10;          % length of net panel [m]
B = 1;           % width of net panel [m]
%Wsinkdyn = [50 100 200 300 400]; % total weight of sinkers [N]
Wsinkdyn = 200;


rhonet = 1025;  % density of net [kg/m^3]
EmodNet = 1.0E9; % E mod to the net [Pa] (Nylon: E=2-4GPa )

useElast =0; % account for elastisity and weight in water? 0=no, 1=yes
Dsink = 0.0; % diametre of sinker. [m]

BouySink = 0.25*pi*g*rhos*B*Dsink^2;

% if weight on winker should be based on
% the buoyancy of the sinker tube:
% Wsinkdyn = Wsinkdyn - BouySink;
%% Dynamic input
```

```
% Udyn = [0.159 0.316 0.966]; % initial current velocity [m/s] - any size
% lstdyn = [27.2 18.45 10.655 10.545]/1000; %Loland test set
% ddyn = [1.83 1.38 1.03 1.83]/1000; % Loland test set

% case 1
ddyn = 1.5/1000;   % Error Sn=0.19
lstdyn = 15/1000;  % Error Sn=0.19
Udyn = 0.1:0.1:1.0;

% case 2a
% Udyn = 0.5;
% lstdyn = [29.23 19.22 14.21 11.20 9.18 7.74 6.65 5.81 5.12 4.56]/1000;
% ddyn = (ones(1,size(lstdyn,2))+0.5)/1000;

% case 2b
% Udyn = 0.75;
% lstdyn = [29.23 19.22 14.21 11.20 9.18 7.74 6.65 5.81 5.12 4.56]/1000;
% ddyn = (ones(1,size(lstdyn,2))+0.5)/1000;

% case 2c
% Udyn = 1;
% lstdyn = [29.23 19.22 14.21 11.20 9.18 7.74 6.65 5.81 5.12 4.56]/1000;
% ddyn = (ones(1,size(lstdyn,2))+0.5)/1000;

% w sink test
% ddyn = [1.5 1.5 1.5 1.5 1.5]/1000;   % Error Sn=0.19
% lstdyn = [15 15 15 15 15]/1000;  % Error Sn=0.19
% Wsinkdyn = [50 100 200 300 400]
% Udyn = 1;

%ddyn = [1.5 1.5 1.5 1.5 1.5 1.5 1.5 1.5 1.5 1.5 1.5 1.5 1.5]/1000; % diameter
    of net tread [m] - any size
%lstdyn = [5 6 7 8 10 12 14 16 18 20 23 27 30]/1000; % length between twines [m]
     - same size as d
%ddyn =[3.3 2.5 2.145 1.875 1.5 1.25 1.07 0.94 0.835 0.75 0.65 0.555 0.5]/1000;
%lstdyn = [10 10 10 10 10 10 10 10 10 10 10 10 10]/1000;


NumRound = size(Udyn,2)*size(ddyn,2);

%% START VALUES

NumRound= size(Udyn,2)*size(ddyn,2);
theta   = zeros(1,Nel+1);
T       = zeros(NumRound,Nel+1);
alphaTot= zeros(size(Wsinkdyn,2),size(Udyn,2));
yzpos   = zeros(2,Nel+1);
LOyzpos = zeros(2,Nel+1);
dtheta  = zeros(1,Nel);
alpha   = zeros(1,Nel);
dT      = zeros(1,Nel);
Cn      = zeros(1,Nel);
Ct      = zeros(1,Nel);
thetaM  = zeros(1,Nel);
dy      = zeros(1,Nel);
dz      = zeros(1,Nel);
CEypos  = zeros(Nel+1,size(Udyn,2));
CEzpos  = zeros(Nel+1,size(Udyn,2));
LOypos  = zeros(Nel+1,size(Udyn,2));
LOzpos  = zeros(Nel+1,size(Udyn,2));
FdTot   = zeros(size(Wsinkdyn,2),size(Udyn,2));
```

```
99  FlTot    = zeros(size(Wsinkdyn,2),size(Udyn,2));
100 FdTot2   = zeros(size(Wsinkdyn,2),size(Udyn,2));
101 FlTot2   = zeros(size(Wsinkdyn,2),size(Udyn,2));
102 loFd     = zeros(size(Wsinkdyn,2),size(Udyn,2));
103 loFl     = zeros(size(Wsinkdyn,2),size(Udyn,2));
104 ReNom    = zeros(1,NumRound);
105 m=0;
106
107
108 %% Start calculation
109
110 if size(Wsinkdyn,2)<size(ddyn,2)
111    Wsinkdyn(1,size(Wsinkdyn,2):size(ddyn,2))=Wsinkdyn(end);
112 end
113
114
115 for k = 1:size(Udyn,2)
116     Uini = Udyn(k);
117     for j = 1:size(ddyn,2)
118         m=m+1;
119         d = ddyn(j);
120         lst = lstdyn(j);
121
122 ds = L/Nel;
123 Sn = (2*d)/lst - power((d/lst),2); % solidity ratio
124 Sn = Sn * 1.0;
125 SnSave(m) = Sn;
126 Anet = (B/lst)*0.25*pi*d^2;
127 wnet = (rhos-rhonet)*Anet*g;
128 WnetTot = (rhos-rhonet)*Anet*L*g;
129
130 % function: find Nominel and Average Reynolds number
131 ReNom(m) = Uini*d/nu;
132 ReAv = Uini*d/(nu*(1-Sn));
133 ReAvPi4 = Uini*cos(pi/4)*d/(nu*(1-Sn));
134
135 Umin_nom = 20*nu/d;
136 Umin_av = 20*nu*(1-Sn)/d;
137
138 % Uses a seventh order polinominal of log_10 Re
139 CdCirCyl = DragCoefCirc(ReAv);
140
141 Wsink    = Wsinkdyn(j);
142 FdSink   = 0.5*DragCoefCirc(ReNom(m))*Dsink*B*rhos*Uini^2;
143 theta(1)= atan(FdSink/Wsink);
144 T(1)     = sqrt(Wsink^2 + FdSink^2);
145
146 FD = FdSink; % Start values.
147 FD2= FdSink; % Start values.
148 FL = 0; % Start values.
149 FL2= 0; % Start values.
150
151     % Cd0 = Cn(0)
152     Cd0 = CdCirCyl *(Sn/(power(1-Sn,2)));
153
154     % Clpi4 based on iteration C_L from Cn and Ct
155     Clpi4 = LiftCoefPi4(ReAvPi4,Sn);
156
157 %% test seksjon
158 % find Cd and Cl for comparing with LO CE FH AS and Rudi
159 [CatEqTheta0 TabLow TabHi loTheta0 loThetaLow loThethaHi] = ClCd;
```

```
160
161 %% Main program
162 for i = 1:Nel
163     % from the bottom up.
164
165 % function: find Cn(theta(i))
166     Cn(i) = CoefNorm(theta(i),Sn,CdCirCyl,Cd0,Clpi4);
167 % function: find Ct(theta(i))
168     Ct(i) = CoefTang(theta(i),Cn(i),Cd0,Clpi4);
169 % function: find dTi(Ct(theta(i)))
170     dTi = ΔTension(rhos,Uini,Ct(i),B,ds,Anet,wnet,theta(i),T(m,i),EmodNet,g,
        useElast);
171 % function: update T(i) = T(i-1)+dTi
172     T(m,i) = updateTension(dTi,T(m,:),i,Wsink);
173 % function: find alpha
174     alpha(i) = findAlpha(CdCirCyl,Clpi4,Cd0,Sn,theta(i));
175 % function: find dTheta(i)
176     dtheta(i) = findDtheta(rhos,Uini,B,ds,T(m,i),dTi,Cn(i),alpha(i),g,Anet,wnet,
        theta(i),EmodNet,useElast);
177 % update theta(i+1)
178     theta(i+1) = theta(i) + dtheta(i);
179 % function: update the position value changes
180     [thetaM(i) dy(i) dz(i)] = updatePosition(i,theta,ds);
181 % function: integrate the Lift and Drag force
182     [FD FL] = intForces2(FD,FL,rhos,Uini,B,Cd0,Clpi4,thetaM(i),ds,Cn(i),Ct(i));
183 end
184
185 FdTot(j,k)=FD; % Stores the total drag force
186 FlTot(j,k)=FL; % Stores the total lift force
187 thetaMdeg = thetaM*(180/pi); % angles in midle of element [deg]
188 thetaE = thetaM(Nel); % angle at top of net
189
190 for i=1:Nel
191     % from the top down finds the deformation
192     yzpos(1,i+1) = yzpos(1,i) - dy(Nel+1-i);
193     yzpos(2,i+1) = yzpos(2,i) - dz(Nel+1-i);
194 end
195
196    CEypos(:,k) = yzpos(1,:); % Make variable for comparison script
197    CEzpos(:,k) = yzpos(2,:); % U variation - set 1
198
199  % CEypos(:,j) = yzpos(1,:); % Make variable for comparison script
200  % CEzpos(:,j) = yzpos(2,:); % Sn variations - set 2
201
202 % approximation of Fl according to on CL. NOT USED.
203 FlTestInt = 0.5*rhos*power(Uini,2)*B*Clpi4*(ds*trapz(sin(2*theta)));
204
205 % approximation of Fd according to on CD. NOT USED.
206 FdTestZbot = -0.5*rhos*power(Uini,2)*B*Cd0*(yzpos(2,end));
207 FdTestInt = -0.5*rhos*power(Uini,2)*B*Cd0*(-ds*trapz(cos(theta)));
208
209 alphaTot(j,k) = atan(yzpos(1,Nel+1)/(-yzpos(2,Nel+1)))*180/pi;
210
211 %%%%%%%%%%%%%%%%%%%%%%%%%%%%%%%%%%%%%%%%%%%%%%%%%%%%%%%%%%%%%%%%%%%%%%%%%%%%
212 %% Using Loland (1991) method directly
213 %%%%%%%%%%%%%%%%%%%%%%%%%%%%%%%%%%%%%%%%%%%%%%%%%%%%%%%%%%%%%%%%%%%%%%%%%%%%
214
215 [loFd(j,k) loFl(j,k) LOdy LOdz loCd(j,k) loT(m,:)] = lolandMet(Sn,L,B,rhos,Uini,
    Nel,Wsink);
216     for i=1:Nel
217         % from the top down
```

```
218          LOyzpos(1,i+1) = LOyzpos(1,i) - LOdy(Nel+1-i);
219          LOyzpos(2,i+1) = LOyzpos(2,i) - LOdz(Nel+1-i);
220      end
221           LOypos(:,k) = LOyzpos(1,:); % Make variable for comparison script
222           LOzpos(:,k) = LOyzpos(2,:); % U variation - set 1
223
224          % LOypos(:,j) = LOyzpos(1,:); % Make variable for comparison script
225          % LOzpos(:,j) = LOyzpos(2,:); % Sn variation - set 2
226
227  LOalpha(j,k) = atan(LOyzpos(1,Nel+1)/(-LOyzpos(2,Nel+1)))*180/pi;
228
229  %% PLOT
230  % function: plots the deformed net shape, prints FD anf FL
231       % plotShape(m,yzpos,L,Uini,Wsink,d,lst,Sn,FD,FL,Nel,Dsink);
232       % loland
233       % plotShape(m+10,LOyzpos,L,Uini,Wsink,d,lst,Sn,loFd(j,k),loFl(j,k),Nel,
             Dsink);
234
235      end
236  end
237
238  %% PLOT part II
239  % function: plot net tension as function of length, ds
240     %plotTension(L,B,Udyn,Uini,Wsinkdyn,Nel,ds,NumRound,T,ReNom,rhos,SnSave,m+11)
          ;
241     %plotTension(L,B,Udyn,Uini,Wsinkdyn,Nel,ds,NumRound,loT,ReNom,rhos,SnSave,m
          +13);
242  % funcion: plot alpha.
243  % use same Sn, differ Wsink
244      %plotAlpha(Udyn,Wsinkdyn,d,lst,Sn,Nel,ds,NumRound,alphaTot,nu,m+15)
245      %plotAlpha(Udyn,Wsinkdyn,d,lst,Sn,Nel,ds,NumRound,LOalpha,nu,m+17)
```

B.2 DragCoefCirc.m

```
1  function CdCC = DragCoefCirc(Re)
2
3  % Uses curve fitted experimental values from Goldstein(1965)
4  % Uses a seventh order polinominal of log_10 Re
5  % Procedure from Faltinsen(2011)
6  % valid from Re = 31.6 to 10 000
7
8  A=-78.46675;
9  B1=254.73873;
10 B2=-327.8864;
11 B3=223.64577;
12 B4=-87.92234;
13 B5=20.00769;
14 B6=-2.44894;
15 B7=0.12479;
16 X = log10(Re);
17
18 CdCC = A + B1*X + B2*(power(X,2)) + B3*(power(X,3)) + B4*(power(X,4)) + B5*(
       power(X,5)) + B6*(power(X,6)) + B7*(power(X,7));
19
20 end
```

B.3 LiftCoefPi4.m

```
function ClPi4 = LiftCoefPi4(Re,Sn)

% finds the lift coefficient, Cl, for the given reynolds number for
% theta=pi/4.
CdCC = DragCoefCirc(Re);
Cn = CdCC * 0.5 * Sn/(power((1-Sn),2));
Ct = pi*Cn/(8+Cn);
ClPi4 = Cn*sin(pi/4) - Ct*cos(pi/4);

end
```

B.4 CoefNorm.m

```
function Cn = CoefNorm(theta,Sn,CdCirCyl,Cd0,Clpi4)

% finds Cn as function of theta. Above and below 45 deg
if theta ≤ pi/4
    Cn = CdCirCyl * power((cos(theta)),2)*(Sn/(power(1-Sn,2)));
elseif theta ≤ pi/2
    Cn = Cd0 * power(cos(theta),2) + Clpi4 *sin(2*theta)*sin(theta);
else
    Cn = 100.0;
end
end
```

B.5 CoefTang.m

```
function Ct = CoefTang(theta,Cn,Cd0,Clpi4)

% finds Ct as function of theta. Above and below 45 deg
if theta ≤ pi/4
    Ct = theta * ((4*Cn) / (8+Cn));
elseif theta ≤ pi/2
    Ct = 0.5 * Cd0 *sin(2*theta) - Clpi4 *cos(theta) *sin(2*theta);
else
    Ct = 100.0;
end
end
```

B.6 deltaTension.m

```
function dTi = ΔTension(rho,Uini,Ct,B,ds,A,w,theta,Ti,E,g,useElast)

% finds the change in Tension with and without elast and weight of net
if useElast == 1
```

```
5       dTi = ((w*cos(theta)) + (0.5*rho*Uini^2*Ct*B*(1+(Ti/(A*E)))))*ds;
6   else
7       dTi = 0.5*rho*power(Uini,2)*Ct*B*ds;
8   end
9   end
```

B.7 findAlpha.m

```
1   function alpha = findAlpha(CdCC,Clpi4,Cd0,Sn,theta)
2
3   % alpha is the partial deritive of Cn evaluated at theta_i
4   if theta ≤ pi/4
5       alpha = -2*CdCC *((Sn)/(power(1-Sn,2)))*cos(theta)*sin(theta);
6   elseif theta ≤ pi/2
7       alpha = -2*Cd0 *cos(theta)*sin(theta) + 0.5*Clpi4*(3*sin(3*theta)-sin(theta)
            );
8   else
9       alpha = 10000;
10  end
11  end
```

B.8 findDtheta.m

```
1   function dtheta = findDtheta(rhos,Uini,B,ds,Ti,dTi,Cn,alpha,g,A,w,theta,E,
        useElast)
2
3   % finds the change in theta with and without elast and weight of net
4   if useElast == 1
5       tempUp = w*sin(theta)*ds + 0.5*rhos*(Uini^2)*Cn*B*(1+(Ti/(A*E)))*ds;
6       tempDown = Ti +0.5*dTi - 0.25*rhos*(Uini^2)*alpha*B*(1+(Ti/(A*E)))*ds;
7       dtheta = tempUp/tempDown;
8   else
9       kappa = (0.5*rhos*power(Uini,2)*B*ds) / (Ti + 0.5*dTi);
10      dtheta = (kappa*Cn)/(1 - 0.5*kappa*alpha);
11  end
12  end
```

B.9 updatePosition.m

```
1   function [thetaM dy dz]= updatePosition(i,theta,ds)
2
3   % finds the value of theta_m
4   % Updates the change in position
5   thetaM = 0.5*(theta(i)+theta(i+1));
6   dy = -sin(thetaM)*ds;
7   dz = cos(thetaM)*ds;
8   end
```

B.10 intForces2.m

```
function [FD FL] = intForces2(FD,FL,rhos,Uini,B,Cd0,Clpi4,t,ds,Cn,Ct)

% sums the drag anf lift forces on the net elements.
% Checks the net panel inclination and adjust the coefficients accordingly
if t ≤ pi/4
    Cd = ((Cn*(1-power(sin(t),2)))/cos(t) ) + Ct*sin(t);
    Cl = Cn*sin(t) - Ct*cos(t);
elseif t ≤ pi/2
    Cd = Cd0*cos(t);
    Cl = Clpi4*sin(2*t);
end

FD = FD + 0.5*rhos*power(Uini,2)*B*Cd*ds;
FL = FL + 0.5*rhos*power(Uini,2)*B*Cl*ds;

end
```

B.11 plotShape.m

```
function [] = plotShape(m,xzpos,L,Uini,Wsink,d,lst,Sn,FD,FL,Nel,Dsink)

% Plots the complete net deformation. Can take force on bottom ring into
% account.

figure(m)
% subplot(3,4,m)
plot(xzpos(1,:),xzpos(2,:),'-')
axis([0 L -L 0])
grid on
prcs_title=sprintf('Net shape at U=%g[m/s] and T_0=%g[N] d=%g[mm] l_{st}=%g[mm]
    Sn=%1.3f \n F_D=%1.3g[N] F_L=%1.3g[N]. %g elements in analysis',Uini,Wsink,d
    *1000,lst*1000,Sn,FD,FL,Nel);
% title(prcs_title);
% text(-xzpos(1,Nel),-xzpos(2,Nel),'\leftarrow sin(-\pi\div4)','
    HorizontalAlignment','left')
prcs_text=sprintf('End point at (%1.3g,%1.3g)',xzpos(1,Nel+1),xzpos(2,Nel+1));
Sntext=sprintf('Sn=%2.2f',Sn);
text(L*0.98,-L*0.96,Sntext,'HorizontalAlignment','right','BackgroundColor',[1.0
    1.0 1.0]);
if Dsink ≠ 0
% rectangle('Position',[xzpos(1,Nel+1)-Dsink/2,xzpos(2,Nel+1)-Dsink/2,Dsink,
    Dsink],'Curvature',[1,1],'LineWidth',1,'LineStyle','-')
rectangle('Position',[xzpos(1,Nel+1)-Dsink/2,xzpos(2,Nel+1)-Dsink/2,Dsink,Dsink
    ],'Curvature',[1,1],'LineWidth',1,'LineStyle','-')
else
end
```

B.12 plotTension.m

```
function [] = plotTension(L,B,Udyn,Uini,Wsink,Nel,ds,NumRound,T,ReNom,rho,SnSave
    ,k)

% Plots tension across the lengt of several nets. One net gets one line.

s = zeros(1,Nel);
for j=1:Nel
    s(1,j) = ds*j;
end

linestyles = cellstr(char('-',':','-.','--','-',':','-.','--','-',':','-.','--',
    ...
                         '-',':','-.','--','-',':','-.','--','-',':','-.','--',
                            ...
                         '-',':','-.','--','-',':','-.','--','-',':','-.','--',
                            ...
                         '-',':','-.','--','-',':','-.','--','-',':','-.','--')
                            );
MarkerEdgeColors=lines(NumRound);

    hleg = zeros(1,NumRound);
    figure(k)
       hold on
       %grid on
       axis([0 L Wsink(1)/2*1.5 round(max(max(T())/10))*10*1.1])
       printXlabel = sprintf('Length of net [m].\n 0 indicates end, near bottom,
            %g is at surface',L);
       xlabel(printXlabel);
       printYlabel = sprintf('Tension in net [N].\n %g - %g is the min and max
           bottom weight',Wsink(1),Wsink(end));
       ylabel(printYlabel);
    for m=1:NumRound
       hleg(m) = plot(s,T(m,1:Nel),[linestyles{m}],'Color',MarkerEdgeColors(m,:)
           );
       if size(Udyn,2)>1
        printLeg{m} = sprintf('U=%2.1f m/s',Udyn(m));
       else
        printLeg{m} = sprintf('Sn = %2.2f',SnSave(m));
       end
    end
       numleg = [1:1:NumRound];
       legend(hleg(numleg),printLeg{numleg},'Location','NorthWest');

%% Test dimensionless figure
% By dividing Tension on 0.5*rho*power(Uini,2)*B*L
% and s on L

    hleg = zeros(1,NumRound);
    figure(k+1)
       hold on
       grid on
       axis([0 1 0 round(max(max(T())/10))*10*1.1/(0.5*rho*power(Uini,2)*B*L)])
       %printXlabel = sprintf('Length of net [-].\n 0 indicates end, near bottom
           , Dimensionless');
       ylabel('Dimensionless tension in net [-] T / $\frac{1}{2} \rho U_{ini}^2
           B L $','Interpreter','LaTex')
       printXlabel = sprintf('Length of net [-]. s/L');
       xlabel(printXlabel);
    for m=1:NumRound
```

```
51          hleg(m) = plot(s/L,T(m,1:Nel)/(0.5*rho*power(Uini,2)*B*L),[linestyles{m
                }],'Color',MarkerEdgeColors(m,:));
52          printLeg{m} = sprintf('Re=%6.0f',ReNom(m));
53      end
54          numleg = [1:1:NumRound];
55          legend(hleg(numleg),printLeg{numleg},'Location','NorthWest');
56  end
```

B.13 plotAlpha.m

```
1   function [] = plotAlpha(U,Wsink,d,lst,Sn,Nel,ds,NumRound,alpha,nu,kk)
2
3   % Plot the end point angle, alpha for current speed. Different bottom
4   % weights will give multiple lines in the figure.
5   s = zeros(1,Nel);
6   for j=1:Nel
7       s(1,j) = ds*j;
8   end
9
10  linestyles = cellstr(char('-',':','-.','--','-',':','-.','--','-',':','-.','--',
        ...
11                           '-',':','-.','--','-',':','-.','--','-',':','-.','--',
                                 ...
12                           '-',':','-.','--','-',':','-.','--','-',':','-.','--',
                                 ...
13                           '-',':','-.','--','-',':','-.','--','-',':','-.','--',
                                 ...
14                           '-',':','-.','--','-',':','-.','--','-',':','-.','--')
                                   );
15  MarkerEdgeColors=lines(NumRound);
16  Markers=['o','x','+','*','s','d','v','^','<','>','p','h','.',...
17  '+','*','o','x','^','<','h','.','>','p','s','d','v',...
18  'o','x','+','*','s','d','v','^','<','>','p','h','.'];
19
20      hleg = zeros(1,5);
21      figure(kk)
22      hold on
23          axis([0 max(U)*1.1 0 90])
24          printTitle=sprintf('Net inclination at different weigths and current
                speeds. \n Sn=%1.2g[-] d=%g[mm] l_{st}=%g[mm]. %g elements in analysis
                ',Sn,d*1000,lst*1000,Nel);
25          title(printTitle);
26          printXlabel = sprintf('Incident current speed U[m/s]');
27          xlabel(printXlabel);
28          printYlabel = sprintf('Angle between net top and bottom. Alpha [deg]');
29          ylabel(printYlabel);
30      for m=1:size(Wsink,2)
31          hleg(m) = plot(U,alpha(m,:),[linestyles{m} Markers(m)],'Color',
                MarkerEdgeColors(m,:));
32          % plot(X(i,:), Y(i,:),[linestyles{i} Markers(i)],'Color',MarkerEdgeColors
                (i,:));
33          %hleg = plot(U,alpha);
34          printLeg{m} = sprintf('W_{sink} = T_0 = %g',Wsink(m));
35      end
36          numleg = [1:1:size(Wsink,2)];
37          legend(hleg(numleg),printLeg{numleg},'Location','NorthWest');
38
```

```
%% Dimensionless as a test. NOT USED in thesis.

    hleg = zeros(1,5);
    figure(kk+1)
    hold on
       axis([0 max(U)*d*1.1/nu 0 90])
       printTitle=sprintf('Net inclination at different weigths and Reynolds
           number. \n Sn=%1.2f[-] d=%g[mm] l_{st}=%g[mm]. %g elements in analysis
           ',Sn,d*1000,lst*1000,Nel);
       title(printTitle);
       printXlabel = sprintf('Incident current speed expressed as Re[-]');
       xlabel(printXlabel);
       printYlabel = sprintf('Angle between net top and bottom. Alpha [deg]');
       ylabel(printYlabel);
   for m=1:size(Wsink,2)
       hleg(m) = plot(U*d/nu,alpha(m,:),[linestyles{m} Markers(m)],'Color',
           MarkerEdgeColors(m,:));
       % plot(X(i,:), Y(i,:),[linestyles{i} Markers(i)],'Color',MarkerEdgeColors
           (i,:));
       %hleg = plot(U,alpha);
       printLeg{m} = sprintf('W_{sink} = T_0 = %g',Wsink(m));
   end
       numleg = [1:1:size(Wsink,2)];
       legend(hleg(numleg),printLeg{numleg},'Location','NorthWest');


end
```

B.14 lolandMet.m

```
function [Fd Fl dy dz CD T] = lolandMet(Sn,L,B,rhos,U,Nel,Wsink)

% Complete Loland method.
% finds deformation and forces on a net by iterating the net angle for each
% net element.

% Takes in soliduty, geometry (L B), current, number of elements, and
% weight of sikers.
% Gives out Total drag and lift force and displacement for each element

Fy = zeros(1,Nel);
Fz = zeros(1,Nel);
dy = zeros(1,Nel);
dz = zeros(1,Nel);
ds = L/Nel;
Fy(1)=0;
Fz(1)=Wsink;
m=0;

for i = 1:Nel
alpha = 0;
alphaTemp = pi/2;

% iterating to the correct angle
while abs(alpha-alphaTemp)>0.00001
    alphaTemp = alpha;
```

```
27      CdLO = 0.04 + (-0.04 + 0.33*Sn + 6.54*power(Sn,2) - 4.88*power(Sn,3))*cos(
            alphaTemp);
28      ClLO = (-0.05*Sn + 2.3*power(Sn,2) - 1.76*power(Sn,3))*sin(2*alphaTemp);
29
30      dFd = 0.5*rhos*CdLO*power(U,2)*B*ds;
31      dFl = 0.5*rhos*ClLO*power(U,2)*B*ds;
32
33      alpha = atan(-((dFd + 2*Fy(i)) / (dFl +2*Fz(i))));
34      m=m+1; %counts number of iterations
35  end
36
37      Fy(i+1) = dFd + Fy(i);
38      Fz(i+1) = dFl + Fz(i);
39      dy(i) = ds*sin(alpha);
40      dz(i) = ds*cos(alpha);
41
42  end
43
44  Fd = Fy(end);
45  CD = Fd / (0.5 * rhos *L*B *U*U);
46  Fl = Wsink - Fz(end);
47  T = sqrt(Fy.^2 + Fz.^2);
48
49  end
```

B.15 ClCd.m

```
1   function [CatEqTheta0 TabLow TabHi loTheta0 loThetaLow loThethaHi] = ClCd()
2
3   % Calculates and compares the drag and lift coefficients from Loland and
4   % the catenary equation.
5   % For angles 0, 30, 45, 60, 80 and 90 deg.
6
7   %% Input
8   U = [0.159 0.316 0.966];
9   d = [1.83 1.38 1.08 1.83]/1000;
10  Sn = [0.13 0.144 0.184 0.317];
11  nu = 1.004e-6;
12  j=1;
13
14
15  %% Cd based on CatEq for theta = 0
16  theta = 0;
17  Cl = zeros(4,3);
18  Cd = zeros(4,5);
19  for n=1:4
20          for k=1:3
21              ReAv = U(k)*cos(theta)*d(n)/(nu*(1-Sn(n)));
22              CdCirCyl = DragCoefCirc(ReAv);
23
24              Cn = CdCirCyl * power(cos(theta),2)*Sn(n) / power(1-Sn(n),2);
25              Ct = theta*4*Cn/(8+Cn);
26
27              Cl(j,k) = Cn*sin(theta) - Ct*cos(theta);
28              Cd(j,k) = (Cn*(1-(power(sin(theta),2))))/(cos(theta)) + Ct*sin(theta
                    );
29              Cd(j,4) = Sn(n);
```

```
            Cd(j,5) = theta*180/pi;
        end
        j=j+1;
end
CatEqTheta0=[Cd(:,4) Cd(:,5) Cd(:,1) Cl(:,1) Cd(:,2) Cl(:,2) Cd(:,3) Cl(:,3)];
CatEqTheta0=(round(CatEqTheta0*100))/100;


%% Cd and Cl based on CatEq for theta up to pi/4
theta = [pi/6 pi/4];
Cl = zeros(8,3);
Cd = zeros(8,5);
j=1;
for n=1:4
    for m=1:2
        for k=1:3
            ReAv = U(k)*cos(theta(m))*d(n)/(nu*(1-Sn(n)));
            CdCirCyl = DragCoefCirc(ReAv);

            Cn = CdCirCyl * power(cos(theta(m)),2)*Sn(n) / power(1-Sn(n),2);
            Ct = theta(m)*4*Cn/(8+Cn);

            Cl(j,k) = Cn*sin(theta(m)) - Ct*cos(theta(m));
            Cd(j,k) = (Cn*cos(theta(m)) + Ct*sin(theta(m)));
            Cd(j,4) = Sn(n);
            Cd(j,5) = theta(m)*180/pi;
        end
        j=j+1;
    end
end
TabLow=[Cd(:,4) Cd(:,5) Cd(:,1) Cl(:,1) Cd(:,2) Cl(:,2) Cd(:,3) Cl(:,3)];
TabLow=(round(TabLow*100))/100;

%% Cd and Cl based on CatEq for theta from pi/4 to pi/2
theta = [pi/3 4*pi/9 pi/2];
Cl = zeros(12,3);
Cd = zeros(12,5);
j=1;
for n=1:4
    for m=1:3
        for k=1:3
            ReAv = U(k)*cos(theta(m))*d(n)/(nu*(1-Sn(n)));
            ReAv0 = U(k)*cos(0)*d(n)/(nu*(1-Sn(n)));
            ReAvPi4 = U(k)*cos(pi/4)*d(n)/(nu*(1-Sn(n)));
            CdCirCyl = DragCoefCirc(ReAv);
            CdCirCyl0 = DragCoefCirc(ReAv0);
            CdCirCylpi4 = DragCoefCirc(ReAvPi4);

            Cd0 = CdCirCyl0 * Sn(n) / power(1-Sn(n),2);
            %Cd0 = 0.1718;

            Cnpi4 = 0.5*CdCirCylpi4 *Sn(n) / power((1-Sn(n)),2);
            Ctpi4 = pi*Cnpi4/(8+Cnpi4);
            Clpi4 = Cnpi4*sin(pi/4) - Ctpi4*cos(pi/4);

            Cd(j,k) = Cd0*cos(theta(m));
            Cl(j,k) = Clpi4 * sin(2*theta(m));
            Cd(j,4) = Sn(n);
            Cd(j,5) = theta(m)*180/pi;
            %Cn = Cd0 *power(cos(theta(m)),2) + Clpi4*sin(2*theta(m))*sin(theta(
                m));
```

```
90              %Ct = 0.5*Cd0*sin(2*theta(m)) - Clpi4*sin(2*theta(m))*cos(theta(m));
91
92          end
93          j=j+1;
94      end
95  end
96
97  TabHi=[Cd(:,4) Cd(:,5) Cd(:,1) Cl(:,1) Cd(:,2) Cl(:,2) Cd(:,3) Cl(:,3)];
98  TabHi=(round(TabHi*100))/100;
99
100 %% Cd based on Loland for theta = 0
101 Cl = zeros(4,3);
102 Cd = zeros(4,5);
103 j=1;
104 for n=1:4
105     for k=1:3
106      theta=0;
107      Cd(j,k) = 0.04 + (-0.04 + 0.33*Sn(n) + 6.54*power(Sn(n),2) - 4.88*power(Sn(n
             ),3))*cos(theta);
108      Cl(j,k) = (-0.05*Sn(n) + 2.3*power(Sn(n),2) - 1.76*power(Sn(n),3))*sin(2*
             theta);
109      Cd(j,4) = Sn(n);
110      Cd(j,5) = theta*180/pi;
111     end
112    j=j+1;
113 end
114 loTheta0=[Cd(:,4) Cd(:,5) Cd(:,1) Cl(:,1) Cd(:,2) Cl(:,2) Cd(:,3) Cl(:,3)];
115
116
117 %% Cd based on Loland for theta up to pi/4
118 Cl = zeros(4,3);
119 Cd = zeros(4,5);
120 theta = [pi/6 pi/4];
121 j=1;
122 for n=1:4
123   for m=1:2
124     for k=1:3
125      Cd(j,k) = 0.04 + (-0.04 + 0.33*Sn(n) + 6.54*power(Sn(n),2) - 4.88*power(Sn(n
             ),3))*cos(theta(m));
126      Cl(j,k) = (-0.05*Sn(n) + 2.3*power(Sn(n),2) - 1.76*power(Sn(n),3))*sin(2*
             theta(m));
127      Cd(j,4) = Sn(n);
128      Cd(j,5) = theta(m)*180/pi;
129     end
130    j=j+1;
131   end
132 end
133 loThetaLow=[Cd(:,4) Cd(:,5) Cd(:,1) Cl(:,1) Cd(:,2) Cl(:,2) Cd(:,3) Cl(:,3)];
134
135
136 %% Cd based on Loland for theta from pi/4 to pi/2
137 Cl = zeros(4,3);
138 Cd = zeros(4,5);
139 theta = [pi/3 4*pi/9 pi/2];
140 j=1;
141 for n=1:4
142   for m=1:3
143     for k=1:3
144      Cd(j,k) = 0.04 + (-0.04 + 0.33*Sn(n) + 6.54*power(Sn(n),2) - 4.88*power(Sn(n
             ),3))*cos(theta(m));
```

```
145      Cl(j,k) = (-0.05*Sn(n) + 2.3*power(Sn(n),2) - 1.76*power(Sn(n),3))*sin(2*
             theta(m));
146      Cd(j,4) = Sn(n);
147      Cd(j,5) = theta(m)*180/pi;
148     end
149    j=j+1;
150   end
151 end
152 loThethaHi=[Cd(:,4) Cd(:,5) Cd(:,1) Cl(:,1) Cd(:,2) Cl(:,2) Cd(:,3) Cl(:,3)];
153
154
155
156 end
```

Appendix C

Electronic: CD

- Matlab code
- Figures and plots
- The result files from FhSim (matlab\data)
- The rest of data from AquaSim and FhSim in “CompScript.m”